National Library
of Canada

Acquisitions and
Bibliographic Services Branch

395 Wellington Street
Ottawa, Ontario
K1A 0N4

Bibliothèque nationale
du Canada

Direction des acquisitions et
des services bibliographiques

395, rue Wellington
Ottawa (Ontario)
K1A 0N4

Your file   Votre référence

Our file   Notre référence

NOTICE

The quality of this microform is heavily dependent upon the quality of the original thesis submitted for microfilming. Every effort has been made to ensure the highest quality of reproduction possible.

If pages are missing, contact the university which granted the degree.

Some pages may have indistinct print especially if the original pages were typed with a poor typewriter ribbon or if the university sent us an inferior photocopy.

Reproduction in full or in part of this microform is governed by the Canadian Copyright Act, R.S.C. 1970, c. C-30, and subsequent amendments.

AVIS

La qualité de cette microforme dépend grandement de la qualité de la thèse soumise au microfilmage. Nous avons tout fait pour assurer une qualité supérieure de reproduction.

S'il manque des pages, veuillez communiquer avec l'université qui a conféré le grade.

La qualité d'impression de certaines pages peut laisser à désirer, surtout si les pages originales ont été dactylographiées à l'aide d'un ruban usé ou si l'université nous a fait parvenir une photocopie de qualité inférieure.

La reproduction, même partielle, de cette microforme est soumise à la Loi canadienne sur le droit d'auteur, SRC 1970, c. C-30, et ses amendements subséquents.

Canada

UNIVERSITY OF ALBERTA

SYNTHESIS AND CHARACTERIZATION OF CYCLOHEPTATRIENYL BRIDGED BIMETALLIC COMPLEXES.

BY

WENYI FU

©

A thesis submitted to the Faculty of Graduate Studies and Research in partial fulfillment of the requirements for the degree of Doctor of Philosophy.

DEPARTMENT OF CHEMISTRY

Edmonton, Alberta

Fall, 1993

National Library
of Canada

Acquisitions and
Bibliographic Services Branch

395 Wellington Street
Ottawa, Ontario
K1A 0N4

Bibliothèque nationale
du Canada

Direction des acquisitions et
des services bibliographiques

395, rue Wellington
Ottawa (Ontario)
K1A 0N4

Your file Votre référence

Our file Notre référence

The author has granted an irrevocable non-exclusive licence allowing the National Library of Canada to reproduce, loan, distribute or sell copies of his/her thesis by any means and in any form or format, making this thesis available to interested persons.

L'auteur a accordé une licence irrévocable et non exclusive permettant à la Bibliothèque nationale du Canada de reproduire, prêter, distribuer ou vendre des copies de sa thèse de quelque manière et sous quelque forme que ce soit pour mettre des exemplaires de cette thèse à la disposition des personnes intéressées.

The author retains ownership of the copyright in his/her thesis. Neither the thesis nor substantial extracts from it may be printed or otherwise reproduced without his/her permission.

L'auteur conserve la propriété du droit d'auteur qui protège sa thèse. Ni la thèse ni des extraits substantiels de celle-ci ne doivent être imprimés ou autrement reproduits sans son autorisation.

ISBN 0-315-88292-1

Canada

UNIVERSITY OF ALBERTA

RELEASE FORM

NAME OF AUTHOR:	WENYI FU
TITLE OF THESIS:	SYNTHESIS AND CHARACTERIZATION OF CYCLOHEPTATRIENYL BRIDGED BIMETALLIC COMPLEXES
DEGREE:	Ph. D.
YEAR THIS DEGREE GRANTED:	1993

Permission is hereby granted to the University of Alberta Library to reproduce single copies of this thesis and to lend or sell such copies for private, scholarly or scientific research purposes only.

The author reserves all other publication and other rights in association with the copyright in the thesis, and except as herein before provided neither the thesis nor any substantial portion thereof may be printed or otherwise reproduced in any material form whatever without the author's prior written permission.

Permanent Address:
Room 206, No 19, Building 5,
Shu Guang Xin Cun, Shu Guang Road
Hangzhou, Zhejiang
P. R. China

Sept. 30 1993

UNIVERSITY OF ALBERTA

FACULTY OF GRADUATE STUDIES AND RESEARCH

The undersigned certify that they have read, and recommend to the Faculty of Graduate Studies and Research for acceptance, a thesis entitled SYNTHESIS AND CHARACTERIZATION OF CYLCLOHEPTATRIENYL BRIDGED BIMETALLIC COMPLEXES submitted by WENYI FU in partial fulfillment of the requirements for the degree of Doctor of Philosophy.

Josef Takats
Supervisor: Dr. J. Takats

RGCavell
Dr. R. G. Cavell

WAGGraham
Dr. W. A. G. Graham

Karel R. Kopecky
Dr. K. R. Kopecky

S.E. Wanke
Dr. S. E. Wanke

Derek Sutton
External Examiner: Dr. D. Sutton

Date September 23, 1993

To My parents, Lei and Chao

Abstract

Reactions of ambident organometallic nucleophiles, $(\eta^3\text{-}C_7H_7)M(CO)_3^-$ (M=Fe, Ru, Os) with different transition metal electrophiles to form cycloheptatrienyl bridged bimetallic compounds have been studied.

Thus, $(\eta^3\text{-}C_7H_7)M(CO)_3^-$ (M=Ru, Os) reacted with $[M'(CO)_4X]_2$ (M'=Mn, Re; X=Br, Cl) to give cis-$(\mu\text{-}\eta^3,\eta^4\text{-}C_7H_7)M(CO)_3M'(CO)_3$ where two metal moieties occupy same face of the C_7H_7 ring with concurrent formation of a metal-metal bond. These results mirror previous work where reactions of $(\eta^3\text{-}C_7H_7)Fe(CO)_3^-$ with the same Mn/Re electrophiles afforded cis type products as well. Interestingly, the reaction of $[Ph_4As][(\eta^3\text{-}C_7H_7)Os(CO)_3]$ with $[Re(CO)_4Br]_2$ afforded an unusual cis-$(\mu\text{-}\eta^3,\eta^2\text{-}C_7H_7)Os(CO)_3Re(CO)_4$ compound with an uncoordinated double bond in the C_7H_7 ring.

The metal-dependent nucleophilicity of anions, $(\eta^3\text{-}C_7H_7)M(CO)_3^-$ (M=Fe, Ru) was observed in their reactions with $[Pd(\eta^3\text{-}C_3H_5)Cl]_2$. The iron anion gave the normal, cycloheptatrienyl bridged cis type complex, cis-$(\mu\text{-}\eta^3,\eta^4\text{-}C_7H_7)Fe(CO)_3Pd(\eta^3\text{-}C_3H_5)$. But in the Ru reaction allyl transfer occured and $(\eta^3\text{-}C_7H_7)Ru(CO)_2(\eta^3\text{-}C_3H_5)$ and $(\mu\text{-}C_7H_7)Ru(CO)_3Ru(CO)(\eta^3\text{-}C_3H_5)$ were isolated. No Ru-Pd product was obtained in this reaction.

Both ambident nucleophilicity and subtle electrophilic discrimination were observed in the reactions of $(\eta^3\text{-}C_7H_7)M(CO)_3^-$ (M=Fe, Ru, Os) with $[Mo(CO)_2(CH_3CN)_2(L)]^+$ (L=$\eta^5\text{-}C_9H_7$, $\eta^5\text{-}C_5H_5$). The Fe and Ru reactions resulted in the exclusive formation of trans-$(\mu\text{-}\eta^4,\eta^3\text{-}C_7H_7)M(CO)_3Mo(CO)_2(L)$ (M=Fe, Ru; L=$\eta^5\text{-}C_9H_7$, $\eta^5\text{-}C_5H_5$). But, the Os reactions afforded two types of products, the trans OsMo compounds and unusual cis compounds without a metal-metal bond, cis-(μ-η^4,η^3-C_7H_7)M(CO)$_3$Mo(CO)$_2$(L). These complexes are fluxional, but the rates of metal migration around the C_7 ring were slower in the trans compounds than in the normal cis compounds and the rates decrease as the metal triad is descended. The metal migration in the trans complexes was shown to proceed by a series of 1,2-shifts.

The preparation and characterization of the formyl substituted cycloheptatrienyl anion, $[(CHOC_7H_6)Fe(CO)_3]^-$, were carried out. In the solid state the C_7H_6CHO ligand is bonded to the $Fe(CO)_3$ moiety in an η^3 fashion. In solution, however, an equilibrium between two isomeric species was deduced. The substituted anion also displays versatile reactivities towards organic electrophiles. The reaction with methyl iodide gave two ring substituted products, but with trimethylsilyl chloride only trimethylsilyloxy substituted fulvene compounds were obtained.

Acknowledgements

There are many people to whom I wish to express sincere appreciation and gratitude. Without their friendly contribution and help this work have been impossible to complete.

In particular I would like to express my sincere gratitude to Professor Josef Takats for his enthusiastic and kind guidance, patience and encouragement in all my studying time and also kindly care of my family.

Special thanks are due to Dr. Gong Kiel and Dr. Stephen T. Astley for their help and discussion.

The author wishes to thank members of the Takats' research group and his other friends in this department who prcvided assistance when necessary, and an enjoyable environment. They are Melinda Burn, Mark Sandercock, John Washington, Juergen Jacke, Ken Hoffman, Yimin Sun, Xingwang Zhang, Torsten Funk, Jason Cooke, Tianfu Mao, Jinliang Xiao, Jin Chen, Liang Tang, Weimin Jiang, Lisheng Wang, Dr. James Hoyano, Michael D. Mikoluk, Dusan Ristic-Petrovic, Shaun Duhaime.

I would also like to thank:

Professor McClung and Gerdy Aarts for the multisite magnetization transfer experiments and helpful discussions.

Dr. Bernie Satarsiero and Dr. Bob McDonald for providing the X-ray structure determinations and for helpful discussions.

The members of the NMR laboratory, Dr. Tom T. Nakashima, Glenn Bigam, Tom Brisbane, Gerdy Aarts and Lai Kong for their dedication and patience. Andrew Jodhan for obtaining mass spectra. Darlene Mahlow and Andrea Dunn for accurate elemental analysis.

Professors Cavell, Graham, Kopecky, Sutton and Wanke for providing helpful advices and prompt, efficient reading of this thesis. Especially, I would like to thank professor Cavell for the many enjoyable and beneficial talks.

Mrs. Jackie Jorgensen for her help in the preparation of this thesis.

The University of Alberta and NSERC for providing the funds which were necessary for completing this research.

Finally, all the members of my family and friends back in China for their assistance and encouragement.

Table of Contents

Abstract

Acknowledgements

List of Tables

List of Figures

List of Schemes

List of Abbreviations

Chapter One - Introduction.

1.1. Development of Heterobinuclear Transition Metal Complexes. 1

1.2. Cycloheptatrienyl (C_7H_7) and Cycloheptatriene (C_7H_8) Ligands. 4

1.2.1. Complexes with an η^1-C_7H_7 Ligand. 5

1.2.2. Complexes with an η^2-C_7H_8 Ligand. 6

1.2.3. Complexes with an η^3-C_7H_7 Ligand. 9

1.2.4. Complexes with an η^4-C_7H_8 Ligand. 12

1.2.5. Complexes with an η^5-C_7H_7 Ligand. 17

1.2.6. Complexes with an η^6-C_7H_8 Ligand. 18

1.2.7. Complexes with an η^7-C_7H_7 Ligand. 21

1.3. Cycloheptatrienyl Bridged Heterobimetallic Complexes. 24

1.4. Further Reactions of the Anionic Complexes $(\eta^3$-$C_7H_7)M(CO)_3^-$ (M=Fe, Ru, Os) with Electrophiles: Scope of the Thesis. 29

1.5. References. 31

Chapter 2 - Synthesis and Spectroscopic Characterization of cis-(μ-C_7H_7)$M(CO)_3M'(CO)_3$ (M=Ru, Os; M'=Mn, Re).

2.1. Introduction. 38

2.2. Results and Discussion. 41

2.2.1. Reactions of (η^3-C_7H_7)$M(CO)_3^-$ (M=Ru, Os) with $[M'(CO)_4X]_2$ (M'=Mn, Re; X=Br, Cl). 41

2.2.2. Reaction of $[Ph_4As][(\eta^3\text{-}C_7H_7)Os(CO)_3]$ with $[Re(CO)_4Br]_2$. 44

2.3. Conclusion. 50

2.4. Experimental. 51

2.5. References. 60

Chapter 3 - Reactions of (η^3-C_7H_7)$M(CO)_3^-$ (M=Fe, Ru) with $[(\eta^3\text{-}C_3H_5)PdCl]_2$: Unexpected Allyl Ligand Transfer between Ru and Pd Complexes.

3.1. Introduction. 61

3.2. Results and Discussion. 62

3.2.1. Synthesis and Fluxionality of (μ-C_7H_7)$Fe(CO)_3Pd$(η^3-C_3H_5). 62

3.2.2. Reaction of (η^3-C_7H_7)$Ru(CO)_3^-$ with $[(\eta^3\text{-}C_3H_5)PdCl]_2$. 67

3.2.3. Possible Reaction Route of Forming Allyl Transfer Products. 81

3.2.4. Conclusion. 83

3.3. Experimental. 83

3.4. References. 90

Chapter 4 - Synthesis and Characterization of Cycloheptatrienyl Bridged Heterobimetallic Complexes $(\mu\text{-}C_7H_7)M(CO)_3Mo(CO)_2(L)$ (M=Fe, Ru, Os) $(L=\eta^5\text{-}C_9H_7,\ \eta^5\text{-}C_5H_5)$.

4.1. Introduction. 92

4.2. Results and Discussion. 94

4.2.1. Preparation and Characterization of $\mu\text{-}(\eta^4,\eta^3\text{-}C_7H_7)M(CO)_3Mo(CO)_2(\eta^5\text{-}C_9H_7)$ (M=Fe, Ru, Os). 94

4.2.2. Solid State Structures of $(\mu\text{-}C_7H_7)M(CO)_3Mo(CO)_2(\eta^5\text{-}C_9H_7)$ (M=Fe, Os). 102

4.2.3. Fluxional Behavior of trans-$(\mu\text{–}C_7H_7)M(CO)_3Mo(CO)_2(\eta^5\text{-}C_9H_7)$ (M=Fe, Ru, Os). 107

4.2.4. Characterization of the Byproduct, $(\eta^3\text{-}C_7H_7)Mo(CO)_2(\eta^5\text{-}C_9H_7)$ from Decomposition of $(\mu\text{–}C_7H_7)Ru(CO)_3Mo(CO)_2(\eta^5\text{-}C_9H_7)$ on the Silica Gel Column. 112

4.2.5. Characterization of the Minor Product from the Reaction of $(\eta^3\text{-}C_7H_7)Os(CO)_3^-$ with $[(\eta^5\text{-}C_9H_7)Mo(CO)_2(CH_3CN)_2]^+$. 115

4.2.6. Reactions of $(\eta^3\text{-}C_7H_7)M(CO)_3^-$ (M=Fe, Ru, Os) with $[(\eta^5\text{-}C_5H_5)Mo(CO)_2(CH_3CN)_2]^+$. 122

4.3. Conclusion. 123

4.4. Experimental. 125

4.5. References. 139

Chapter 5 - Synthesis, Characterization and Reactivity of (Formylcycloheptatrienyl)tricarbonyliron Anion $[(CHOC_7H_6)Fe(CO)_3]^-$.

5.1. Introduction. 141

5.2. Results and Discussion. 142

5.2.1. Preparation and Characterization of $[(CHOC_7H_6)Fe(CO)_3]^-$. 142

5.2.2. Reaction of $[(CHOC_7H_6)Fe(CO)_3]^-$ with CH_3I. 151

5.2.3. Reaction of $[(CHOC_7H_6)Fe(CO)_3]^-$ with Me_3SiCl. 154

5.3. Conclusion. 157

5.4. Experimental. 158

5.5. References. 162

List of Tables

1.1 ^{1}H NMR data of free C_7H_8 and $(\eta^4\text{-}C_7H_8)M(CO)_3$ (**20**) (M=Fe **a**, Ru **b**, Os **c**). 15

2.1 Drying agents used in the distillation of solvents. 52

3.1 Selected bond distances of $(\mu\text{-}C_7H_7)Ru(CO)_3Ru(CO)(\eta^3\text{-}C_3H_5)$ (**4**). 79

3.2 Crystallographic data of $(\mu\text{-}C_7H_7)Ru(CO)_3Ru(CO)(\eta^3\text{-}C_3H_5)$ (**4**). 88

3.3 Fractional coordinates and equivalent isotropic thermal parameters of $(\mu\text{-}C_7H_7)Ru(CO)_3Ru(CO)(\eta^3\text{-}C_3H_5)$ (**4**). 89

4.1 IR, ^{1}H and ^{13}C NMR data of trans-$(\mu\text{–}C_7H_7)M(CO)_3Mo(CO)_2(\eta^5\text{-}C_9H_7)$ (**3**) (M=Fe **a**, Ru **b**, Os **c**) and cis-$(\mu\text{–}C_7H_7)Os(CO)_3Mo(CO)_2(\eta^5\text{-}C_9H_7)$ (**5c**). 99

4.2 Selected bond distances of $(\mu\text{–}C_7H_7)M(CO)_3Mo(CO)_2(\eta^5\text{-}C_9H_7)$ (**3**) (M=Fe **a**, Os **c**) and $(\mu\text{–}C_7H_7)Fe(CO)_3Mo(CO)_2(\eta^5\text{-}C_5H_5)$. 105

4.3 Selected bond angles of $(\mu\text{–}C_7H_7)M(CO)_3Mo(CO)_2(\eta^5\text{-}C_9H_7)$ (**3**) (M=Fe **a**, Os **c**) and $(\mu\text{–}C_7H_7)Fe(CO)_3Mo(CO)_2(\eta^5\text{-}C_5H_5)$. 106

4.4 Rate constants of metal migration in $(\mu\text{–}C_7H_7)M(CO)_3Mo(CO)_2(\eta^5\text{-}C_9H_7)$ (**3**) (M=Fe **a**, Ru **b**, Os **c**). 111

4.5 Activation parameters of metal migration in $(\mu\text{–}C_7H_7)M(CO)_3Mo(CO)_2(\eta^5\text{-}C_9H_7)$ (**3**) (M=Fe **a**, Ru **b**, Os **c**). 112

4.6 Crystallographic data of $(\mu\text{-}C_7H_7)Fe(CO)_3Mo(CO)_2(\eta^5\text{-}C_9H_7)$ (**3a**). 135

4.7 Fractional coordinates and equivalent isotropic thermal parameters for trans-$(\mu\text{-}C_7H_7)Fe(CO)_3Mo(CO)_2(\eta^5\text{-}C_9H_7)$ (**3a**). 136

4.8 Crystallographic data of $(\mu\text{-}C_7H_7)Os(CO)_3Mo(CO)_2(\eta^5\text{-}C_9H_7)$ (**3c**). 137

4.9 Fractional coordinates and equivalent isotropic thermal parameters for $(\mu\text{-}C_7H_7)Os(CO)_3Mo(CO)_2(\eta^5\text{-}C_9H_7)$ (**3c**). 138

5.1 ^1H and ^{13}C NMR data of $[\eta^4\text{-}C_7H_6(CHO)(CH_3)]Fe(CO)_3$ (**5**-**6**) and $[\eta^4\text{-}C_7H_6CHOSi(CH_3)_3]Fe(CO)_3$ (**7**). 153

List of Figures

1.1 Molecular structure of $(\eta^3\text{-}C_7H_7)Mo(CO)_2(\eta^5\text{-}C_5H_5)$ (**19**). 10

1.2 Molecular structures of $(\eta^3\text{-}C_7H_7)M(CO)_3^-$ (**20**) (M=Ru **b**, Os **c**). 13

1.3 Molecular structure of $(\eta^6\text{-}C_7H_8)Mo(CO)_3$ (**27b**). 20

1.4 Molecular structure of $[(\eta^7\text{-}C_7H_7)Mo(CO)_3][BF_4]$ (**33b**). 22

1.5 ORTEP drawing of $(\mu\text{-}\eta^3,\eta^2\text{-}C_7H_7)Fe(CO)_3Pd(\eta^5\text{-}C_5H_5)$ (**46**). 28

2.1 IR spectra of cis-$(\mu\text{-}C_7H_7)Os(CO)_3Re(CO)_3$ (**5**) and cis-$(\mu\text{-}C_7H_7)Os(CO)_3Re(CO)_4$ (**8**). 47

2.2 Variable temperature ^1H NMR spectra (400 MHz) of cis-$(\mu\text{-}C_7H_7)Os(CO)_3Re(CO)_3$ (**5**) and cis-$(\mu\text{-}C_7H_7)Os(CO)_3Re(CO)_4$ (**8**). 48

2.3 IR spectra of $[Ph_4As][(\eta^3\text{-}C_7H_7)Os(CO)_3]$ and $K[(\eta^3\text{-}C_7H_7)Os(CO)_3]$ in THF. 57

3.1 Variable temperature ^1H NMR spectra (360 MHz) of $(\mu\text{-}C_7H_7)Fe(CO)_3Pd(\eta^3\text{-}C_3H_5)$ (**2**). 64

3.2 Experimental and simulated mass spectra of $(\mu\text{-}C_7H_7)Ru(CO)_3Ru(CO)(\eta^3\text{-}C_3H_5)$ (**4**). 68

3.3 Variable temperature ^1H NMR spectra (360 MHz) of $(\eta^3\text{-}C_7H_7)Ru(CO)_2(\eta^3\text{-}C_3H_5)$ (**3**). 71

3.4 Variable temperature ^1H NMR spectra (400 MHz) of $(\mu\text{-}C_7H_7)Ru(CO)_3Ru(CO)(\eta^3\text{-}C_3H_5)$ (**4**). 75

3.5 ORTEP diagram of $(\mu\text{-}C_7H_7)Ru(CO)_3Ru(CO)(\eta^3\text{-}C_3H_5)$ (**4**). 78

4.1 Variable temperature ^1H NMR spectra (360 MHz) of $(\mu\text{-}C_7H_7)Fe(CO)_3Mo(CO)_2(\eta^5\text{-}C_9H_7)$ (**3a**) in toluene-d_8. 100

4.2 Perspective views of $(\mu\text{-}C_7H_7)M(CO)_3Mo(CO)_2(\eta^5\text{-}C_9H_7)$ (**3**) (M=Fe **a**, Os **c**). 103

4.3 Perspective views of trans-(μ-C_7H_7)Fe(CO)$_3$Mo(CO)$_2$(η^5-C_9H_7) (**3a**) and trans-(μ-C_7H_7)Fe(CO)$_3$Mo(CO)$_2$(η^5-C_5H_5). 104

4.4 ^{1}H NMR spectra (360 MHz) of (η^5-C_9H_7)Mo(CO)$_2$(η^3-C_7H_7) (**7**). 114

4.5 Infrared spectra of **3c** and **5c**. 116

4.6 ^{1}H NMR spectra (400 MHz) of **3c** and **5c**. 118

4.7 Perspective view of cis-(μ-C_7H_7)Os(CO)$_3$Mo(CO)$_2$(η^5-C_9H_7) (**5c**). 121

5.1 Variable temperature ^{1}H NMR spectra (200 MHz) of (C_7H_6CHO)Fe(CO)$_3^-$ (**3a**) in THF-d_8. 145

5.2 Perspective views of (η^3-C_7H_7)Fe(CO)$_3^-$ and (C_7H_6CHO)Fe(CO)$_3^-$ (**3a**). 148

5.3 Perspective views of (η^4-$C_7H_6CH_2$)Fe(CO)$_3$ and (C_7H_6CHO)Fe(CO)$_3^-$ (**3a**). 149

5.4 ^{1}H NMR spectra (200 MHz) of (8-phenyl-8-acetoxyheptafulvene)Fe(CO)$_3$ and (400 MHz) (8-trimethylsiloxyheptafulvene)Fe(CO)$_3$ (**7**). 156

List of Schemes.

1.1 A possible mechanism of the Fischer-Tropsch process. 3

1.2 Different bonding modes of cycloheptatrienyl (C_7H_7) and cycloheptatriene (C_7H_8) ligands. 5

1.3 Preparation of $(\eta^1\text{-}C_7H_7)Re(CO)_5$. 6

1.4 Preparation of $[(1,2\text{-}\eta^2\text{-}C_7H_8)Re(CO)(NO)(\eta^5\text{-}C_5H_5)][BF_4]$. 8

1.5 Preparation of an η^2-tropyne complex. 8

1.6 Reactivity of an η^2-tropyne complex. 9

1.7 Equilibrium of *exo* - and *endo*-$(\eta^3\text{-}C_7H_7)Mo(CO)_2(\eta^5\text{-}C_5H_5)$. 11

1.8 Possible bonding modes of $(C_7H_7)M(CO)_3^-$ (M=Fe, Ru, Os). 12

1.9 Reaction of n-BuLi with $(\eta^4\text{-}C_7H_8)Os(CO)_3$. 17

1.10 Formation of $(\eta^5\text{-}C_7H_7)Mn(CO)_3$. 17

1.11 Preparation of $[(\eta^5\text{-}C_7H_7)Fe(CO)_3][BF_4]$. 18

1.12 Synthesis of $(\eta^6\text{-}C_7H_8)M(CO)_3$ (M=Cr, Mo, W). 19

1.13 Thermal 1,5 hydrogen shifts of 7-substituted $(\eta^6\text{-}C_7H_7R)M(CO)_3$. 20

1.14 Substitution of a carbonyl group with another neutral ligand in $(\eta^7\text{-}C_7H_7)Mo(CO)_3^+$. 23

1.15 Nucleophilic attack of PR_3 on $(\eta^7\text{-}C_7H_7)M(CO)_3^+$ (M=Cr, Mo, W). 23

1.16 Nucleophilic attack of anions on $(\eta^7\text{-}C_7H_7)M(CO)_3^+$ (M=Cr, Mo, W). 24

1.17 Preparation of $(\mu\text{-}C_7H_7)Fe(CO)_3Fe(CO)_3$. 25

1.18 Preparation of $[(\mu\text{-}C_7H_7)Rh(\eta^5\text{-}C_5H_5)Rh(\eta^5\text{-}C_5H_5)]^+$ by hydride abstraction from a coordinated cycloheptatriene ligand. 25

1.19 Preparation of trans-$(\mu\text{-}\eta^4,\eta^3\text{-}C_7H_7)Fe(CO)_3Mo(CO)_2(\eta^5\text{-}C_5H_5)$. 26

1.20 Preparation of $(\mu\text{-}C_7H_7)Fe(CO)_3Rh(CO)_2$. 27

1.21 Reactions of $(\eta^3\text{-}C_7H_7)M(CO)_3^-$ (M=Fe, Ru, Os) with $[M''(COD)Cl]_2$ (M"=Rh, Ir). 28

1.22 Preparation of $(\mu\text{-}\eta^6,\eta^1\text{-}C_7H_7)Mo(CO)_3M(L)$ (L=$Ru(CO)_2(\eta^5\text{-}C_5Me_5)$, $Re(CO)_5$). 29

2.1 Reactions of $(\eta^3\text{-}C_7H_7)M(CO)_3^-$ (M=Fe, Ru, Os) with $[M''(COD)Cl]_2$ (M"=Rh, Ir). 39

2.2 Possible bonding modes of $(C_7H_7)M(CO)_3^-$ (M=Fe, Ru, Os). 39

2.3 Formation of two possible products, cis-$(\mu\text{-}C_7H_7)M(CO)_3M'(CO)_3$ and trans-$(\mu\text{-}C_7H_7)M(CO)_3M'(CO)_4$ (M=Ru, Os; M'=Mn, Re). 42

2.4 Structures of cis-$(\mu\text{-}\eta^3,\eta^4\text{-}C_7H_7)Os(CO)_3Re(CO)_3$ and cis-$(\mu\text{-}\eta^3,\eta^2\text{-}C_7H_7)Os(CO)_3Re(CO)_4$. 49

2.5 Possible reaction route for the formation of cis-$(\mu\text{-}\eta^3,\eta^4\text{-}C_7H_7)Os(CO)_3Re(CO)_3$ and cis-$(\mu\text{-}\eta^3,\eta^2\text{-}C_7H_7)Os(CO)_3Re(CO)_4$. 51

3.1 Formation of $(\mu\text{-}C_7H_7)Fe(CO)_3Pd(\eta^3\text{-}C_3H_5)$. 63

3.2 Rotation of the allyl group in $(\mu\text{-}C_7H_7)Fe(CO)_3Pd(\eta^3\text{-}C_3H_5)$. 66

3.3 Allylic rearrangement proceeding via an $\eta^3\text{-}\eta^1\text{-}\eta^3$ route. 66

3.4 Different orientations of the allyl group and the C_7H_7 ring in $(\eta^3\text{-}C_7H_7)Ru(CO)_2(\eta^3\text{-}C_3H_5)$. 72

3.5 Ray-Dutt and Bailar twist mechanisms for $(\eta^3\text{-}C_7H_7)Ru(CO)_2(\eta^3\text{-}C_3H_5)$. 74

3.6 Proposed mechanism for the formation of the allyl transfer product, $(\eta^3\text{-}C_3H_5)Co(CO)_3$. 81

3.7 Proposed mechanism for the formation of $(\eta^3\text{-}C_7H_7)Ru(CO)_2(\eta^3\text{-}C_3H_5)$ and $(\mu\text{-}C_7H_7)Ru(CO)_3Ru(CO)(\eta^3\text{-}C_3H_5)$. 82

4.1 Ambident reactivity of $(\eta^3\text{-}C_7H_7)M(CO)_3^-$ (M=Fe, Ru, Os) 93

4.2 Reactions of $[(\eta^5\text{-}C_9H_7)Mo(CO)_2(CH_3CN)_2]^+$ with $(\eta^3\text{-}C_7H_7)M(CO)_3^-$ (M=Fe, Ru, Os). 96

4.3 *exo* -$(\eta^3\text{-}C_3H_5)Mo(CO)_2(\eta^5\text{-}C_9H_7)$ and $(\mu\text{-}C_7H_7)M(CO)_3Mo(CO)_2(\eta^5\text{-}C_9H_7)$ (M=Fe, Ru, Os). 101

4.4 Possible 1,2-shift process of the metal moieties in $(\mu\text{-}C_7H_7)M(CO)_3Mo(CO)_2(\eta^5\text{-}C_9H_7)$ (M=Fe, Ru, Os). 110

4.5 Equilibrium of *exo* - and *endo*-$(\eta^3\text{-}C_7H_7)Mo(CO)_2(\eta^5\text{-}C_5H_5)$. 115

4.6 Relationship between IR peak intensity and bond angles. 117

4.7 Two orientations of the C_7H_7 ring in $(\mu\text{-}C_7H_7)Os(CO)_3Mo(CO)_2(\eta^5\text{-}C_9H_7)$. 117

4.8 Two conformations of the C_7H_7 ring in $(\mu\text{-}C_7H_7)Os(CO)_3Mo(CO)_2(\eta^5\text{-}C_9H_7)$. 120

4.9 Possible bonding modes of $(C_7H_7)M(CO)_3^-$. 123

4.10 A possible route for the formation of trans- and cis-$(\mu\text{-}C_7H_7)Os(CO)_3Mo(CO)_2(\eta^5\text{-}C_9H_7)$. 124

5.1 Reactions of $(\eta^3\text{-}C_7H_7)Fe(CO)_3^-$ with organic electrophiles. 142

5.2 Preparation of $[(C_7H_6CHO)Fe(CO)_3]^-$. 143

5.3 Possible structures of $[(C_7H_6CHO)Fe(CO)_3]^-$. 146

5.4 Isomerization of acylcycloheptatriene Fe complexes. 151

5.5 Reaction of $[(C_7H_6CHO)Fe(CO)_3]^-$ with CH_3I. 154

5.6 Reaction of $[(C_7H_6CHO)Fe(CO)_3]^-$ with $(CH_3)_3SiCl$. 157

List of Abbreviations

BDA	benzylideneacetone, ($C_6H_5CH{=}CHCOCH_3$)
br	broad
n-Bu	butyl, (C_4H_9)
t-Bu	tertiarybutyl, [$C(CH_3)_3$]
CHT	cycloheptatriene, (C_7H_8)
COD	1,5-cyclooctadiene, (C_8H_{12})
Cp	cyclopentadienyl, (C_5H_5)
COT	cyclooctatetraene, (C_8H_8)
d	doublet
diglyme	bis(2-methoxyethyl) ether
Et	Ethyl, (CH_3CH_2)
IR	infrared
LDA	lithium diisopropylamide, ($LiN(C_3H_7)_2$)
m	medium (with reference to IR spectra)
m	multiplet (with reference to NMR spectra)
m.p.	melting point
Me	Methyl, (CH_3)
MMT	multisite magnetization transfer
MS	mass spectrometry
NMR	nuclear magnetic resonance
NOE	nuclear Overhauser effect
Ph	phenyl, (C_6H_5)

ppm	parts per million
sh	shoulder
s	singlet (with reference to NMR spectra)
s	strong (with reference to IR spectra)
SST	spin saturation transfer
THF	tetrahydrofuran, (C_4H_8O)
TMS	tetramethylsilane, [$(CH_3)_4Si$]
t	triplet (with reference to NMR spectra)
v	very (with reference to IR spectra)
w	weak (with reference to IR spectra)

Chapter 1

Introduction.

1.1. Development of Heterobinuclear Transition Metal Complexes.

One of the most important developments in the field of heterogeneous catalysis was the discovery of superior catalytic properties of certain mixed metal species. These heterometallic catalysts appear much more active, more selective and more stable than their pure metal components.[1-6] It is believed that the interactions between different metals in these systems play an important role in the alteration of their catalytic properties.[7] That is the reason why today major research efforts are being directed toward understanding these metal-metal interactions and their relationship with the unusual behavior of heterometallic compounds.

The catalytic phenomenon has been recognized for a long time since Davy first reported the flameless combustion of coal gas in the presence of a platinum wire in 1817.[8] However, until now, the detailed understanding of many catalytic processes is still very limited. A major reason for this is that most industrial processes are heterogeneous, i.e. the reactants are present in a phase which is different from the phase of catalysts.[9] Most catalysts in these processes are supported metal salts or metal oxides which are insoluble in most common solvents. Thus it is not easy to apply classical spectroscopic techniques (such as IR or NMR) to monitor the progress of the reaction or to detect possible intermediates.

In order to circumvent these difficulties, chemists have turned to homogeneous model systems, often cluster compounds, to uncover the mechanisms of heterogenous catalytic reactions and also to study possible metal-metal interactions in these systems.[10] It is argued that the metal-metal bonded framework of these clusters resembles the structural characteristics of heterogeneous multimetallic catalysts, meanwhile the good solubility of these clusters in common solvents allows a ready access to most classical spectroscopic methods. In addition, some of the novel clusters may act as unique catalysts themselves. A most recent example is the cluster compound, $Pt_3Ru_6(CO)_{20}(\mu_3\text{-}PhC_2Ph)(\mu_3\text{-}H)(\mu\text{-}H)$ (**1**).[11] The compound behaves as an unusually active catalyst for the selective hydrogenation of diphenylacetylene to (Z)-stilbene (Equation 1.1). The catalytic activity of **1** is both significantly higher and more selective than that of either pure ruthenium or platinum catalysts.

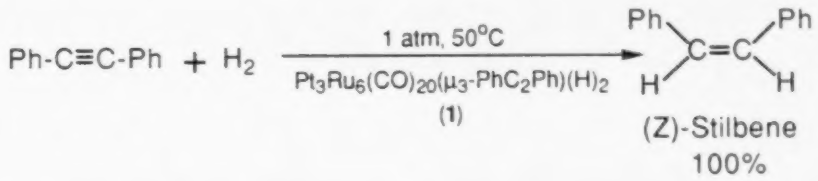

(1.1)

At the other end of the spectrum, the chemistry of simple mononuclear complexes has attracted the attention of organometallic chemists for over three generations. The central role of some mononuclear compounds in homogeneous catalysis has been well recognized.[12] In order to relate the mononuclear compounds to multinuclear clusters, it is noted that dinuclear complexes can be perfect candidates due to their mid positions between mononuclear compounds and multinuclear clusters.[10d,13] It is hoped that fundamental studies of these dinuclear complexes may link the two areas of mononuclear complexes and multinuclear clusters and therefore provide a smooth and logical progression in the studies of metal mediated catalysis. Based on this idea thousands of binuclear compounds have been prepared and studied.

One of the fundamental and well developed strategies for the preparation of binuclear complexes is to link two metal centers via a bridging ligand.[13] A major advantage of these bridged binuclear compounds is that by choosing a specific ligand system, it is possible to build model compounds that resemble postulated intermediates in catalytic processes. For example, the carbon chain growth in the heterogeneous Fischer-Tropsch process has been postulated to occur through the combination of a surface-bound methylene moiety with a surface-bound alkyl group (Scheme 1.1).[14] As a result of these postulates, extensive series of hydrocarbon bridged binuclear complexes have been prepared and the chemistry of bridging hydrocarbon fragments has been thoroughly investigated.[13a,b]

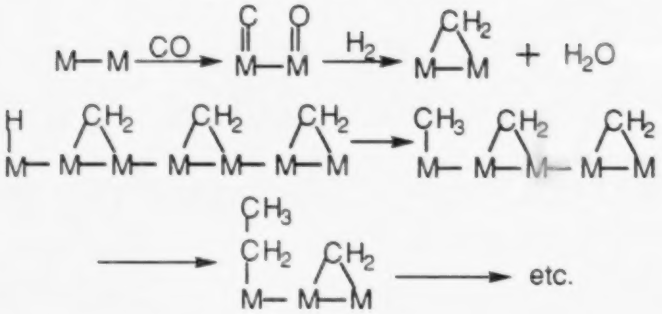

(Scheme 1.1)

In the past 20 years thousands of different binuclear complexes with a broad range of bridging ligand systems have been prepared.[10d,13] Among them binuclear compounds with cycloheptatrienyl (C_7H_7) or cycloheptatriene (C_7H_8) as bridging ligands have emerged as interesting series of compounds and they have been a long standing research interest of the Takats' research group.

1.2. Cycloheptatrienyl (C_7H_7) and Cycloheptatriene (C_7H_8) Ligands.

The choice of selecting cycloheptatrienyl (C_7H_7) or cycloheptatriene (C_7H_8) as a special bridging group is based on the fact that these ligands are very versatile. They can bond to transition metals in several different ways, utilizing one to seven carbon atoms. This variable bonding capability has been clearly demonstrated in mononuclear systems and also promises ready access to different metal combinations in the same molecule. The potential of rich derivative chemistry for these binuclear compounds is apparent.[15]

A schematic representation of the different bonding modes for cycloheptatrienyl (C_7H_7) or cycloheptatriene (C_7H_8) ligands in mononuclear compounds is shown below (Scheme 1.2), utilizing the hapto (η) designation, a nomenclature first introduced by Cotton.[16] What follows is a brief review of the different bonding modes for cycloheptatrienyl (C_7H_7) and cycloheptatriene (C_7H_8) ligands. This review is not intended to be exhaustive but to provide only a brief overview of the preparation, some structural characteristics and reactivity trends of different coordination modes for the cycloheptatrienyl (C_7H_7) and cycloheptatriene (C_7H_8) complexes.

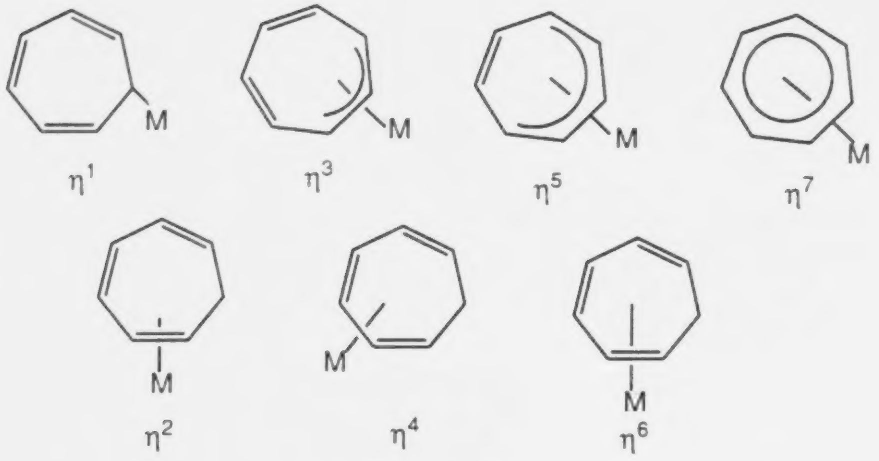

(Scheme 1.2)

1.2.1. Complexes with an η^1-C_7H_7 Ligand.

The most obvious route to a compound containing an η^1-C_7H_7 ligand is the reaction of a tropylium cation with a nucleophilic transition metal center. However, due to the mild oxidizing nature of the tropylium cation, these reactions normally result in oxidized transition metal anions and ditropyl, $(C_7H_7)_2$ (Equation. 1.2-1.4).[17-19]

$$2\ \underset{\mathbf{2}}{Na[(\eta^5\text{-}C_5H_5)Cr(CO)_3]} \xrightarrow{2\ C_7H_7Br} \underset{\mathbf{3}}{[(\eta^5\text{-}C_5H_5)Cr(CO)_3]_2} + (C_7H_7)_2 \qquad (1.2)$$

$$2\ \underset{\mathbf{4}}{Na[Mn(CO)_5]} + 2\ C_7H_7Br \longrightarrow \underset{\mathbf{5}}{Mn_2(CO)_{10}} + (C_7H_7)_2 \qquad (1.3)$$

$$2\ \underset{\mathbf{6}}{[Na(diglyme)_2]V(CO)_6} \xrightarrow{2\ [C_7H_7]BF_4} 2\ \underset{\mathbf{7}}{V(CO)_6} + (C_7H_7)_2 \qquad (1.4)$$

The failure to isolate η^1-cycloheptatrienyl complexes had been attributed to a combination of ready electron transfer from the anionic complexes to tropylium, followed by immediate coupling of tropyl radicals to give ditropyl, and to the weakness of the metal-carbon σ bond in these monohapto-cycloheptatrienyl complexes. Thus, for a long time no η^1-cycloheptatrienyl transition metal complex had been reported.[20]

In 1979, Heinekey and Graham first reported a series of stable η^1-cycloheptatrienyl complexes.[21-23] Initially, in order to avoid possible electron transfer, the acyl complex, $(\eta^1\text{-}C_7H_7CO)Re(CO)_5$ (**8**) was prepared. Photochemical decarbonylation of **8** successfully afforded the monohapto cycloheptatrienyl rhenium complex, $(\eta^1\text{-}C_7H_7)Re(CO)_5$ (**9**) (Scheme 1.3). Surprisingly, it was later discovered that the reaction of $Na[Re(CO)_5]$ (**10**) with $[C_7H_7][BF_4]$ also directly yields the same η^1-complex in 90% isolated yield. Complex **9** is fluxional and the metal moiety migrates rapidly around the C_7H_7 ring. Spin-saturation-transfer (SST) experiments have confirmed that the metal migration occurs via a series of 1,2-shifts.[22]

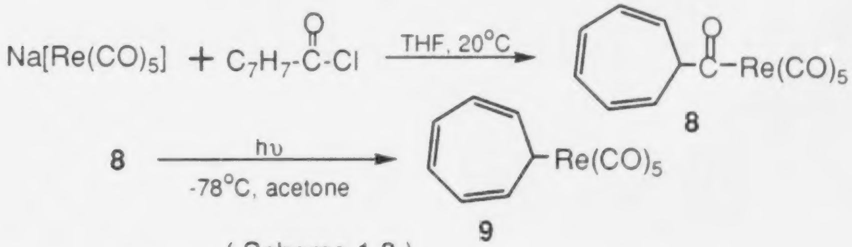

(Scheme 1.3)

1.2.2. Complexes with an η^2-C_7H_8 Ligand.

Only a few η^2-cycloheptatriene complexes are known. Pauson and coworkers first detected an η^2-cycloheptatriene intermediate by infrared spectroscopy in the synthesis of $(\eta^6\text{-}C_7H_8)Mn(\eta^5\text{-}C_5H_5)$ (**11**).[24] Later, the

η^2-complex, $(\eta^2\text{-}C_7H_8)Mn(CO)_2(\eta^5\text{-}C_5H_5)$ (**12**) was isolated as a yellow crystalline solid from the reaction of $[(\eta^5\text{-}C_5H_5)Mn(CO)_2(THF)]$ with cycloheptatriene (Equation 1.5).[25] Its ^{13}C NMR spectrum indicated that the cycloheptatriene ligand was coordinated through a double bond adjacent to the ring methylene carbon.

$$(\eta^5\text{-}C_5H_5)Mn(CO)_3 \xrightarrow[\text{THF}]{h\upsilon,\ -CO} [(\eta^5\text{-}C_5H_5)Mn(CO)_2(THF)]$$

$$[(\eta^5\text{-}C_5H_5)Mn(CO)_2(THF)] \xrightarrow[\text{-THF}]{h\upsilon,\ C_7H_8} \underset{\mathbf{12}}{(\eta^2\text{-}C_7H_8)Mn(CO)_2(\eta^5\text{-}C_5H_5)} \qquad (1.5)$$

More recently cationic η^2-cycloheptatriene complexes of Fe and Re were prepared but by two rather different routes. The "classical" halide abstraction method was used by Reger et al..[26] Treatment of $[(\eta^5\text{-}C_5H_5)Fe(CO)_2][BF_4]$ (**13**) with C_7H_8 afforded the cationic η^2-olefin complex, $[(\eta^5\text{-}C_5H_5)Fe(CO)_2(\eta^2\text{-}C_7H_8)][BF_4]$ (**14**) (Equation. 1.6).

$$(\eta^5\text{-}C_5H_5)Fe(CO)_2I \xrightarrow[CH_2Cl_2]{AgBF_4} \underset{\mathbf{13}}{[(\eta^5\text{-}C_5H_5)Fe(CO)_2][BF_4]} \qquad (1.6)$$

$$\mathbf{13} \xrightarrow{C_7H_8} \underset{\mathbf{14}}{[(\eta^2\text{-}C_7H_8)Fe(CO)_2(\eta^5\text{-}C_5H_5)][BF_4]}$$

On the other hand, the unusual reaction, insertion of the electrophilic tropylium ion into a metal-hydride bond to give the stable complex, $[(\eta^2\text{-}C_7H_8)Re(CO)(NO)(\eta^5\text{-}C_5H_5)][BF_4]$ (**15**) was reported by Sweet and Graham (Scheme 1.4).[27]

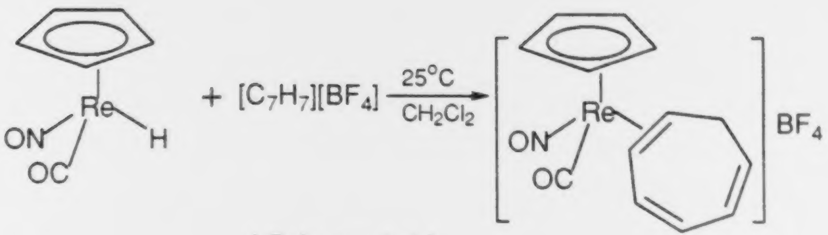
Re
ON
OC
H
+ $[C_7H_7][BF_4]$
25°C
CH_2Cl_2
BF$_4$

(Scheme 1.4)

15

Although not strictly following the definition of this section, it is still worthwhile to mention an interesting recent example where the η^2-cycloheptadienyne and the η^2-tropyne ligands are stabilized by a Pt center.[28] Reaction of a mixture 1-, 2- and 3-bromocycloheptatrienes with $Pt(PPh_3)_3$ in the presence of LDA led to the cycloheptadienyne complexes **16** and **17** in a ratio of 8:1. Hydride abstraction from the mixture of **16** and **17** with $[Ph_3C][BF_4]$ gave the tropyne complex **18** as red, air stable crystals (Scheme 1.5). As shown in scheme 1.6, the tropyne complex **18** is relatively inert to most of shown reagents.[28]

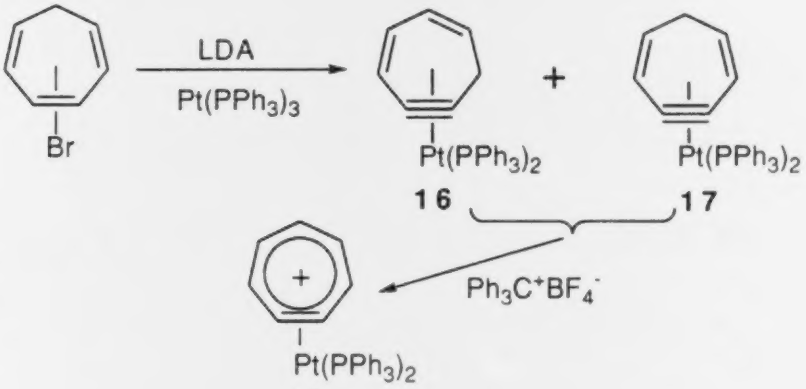
Br
LDA
$Pt(PPh_3)_3$
+
$Pt(PPh_3)_2$
16
$Pt(PPh_3)_2$
17
+
$Ph_3C^+BF_4^-$
$Pt(PPh_3)_2$

18

(Scheme 1.5)

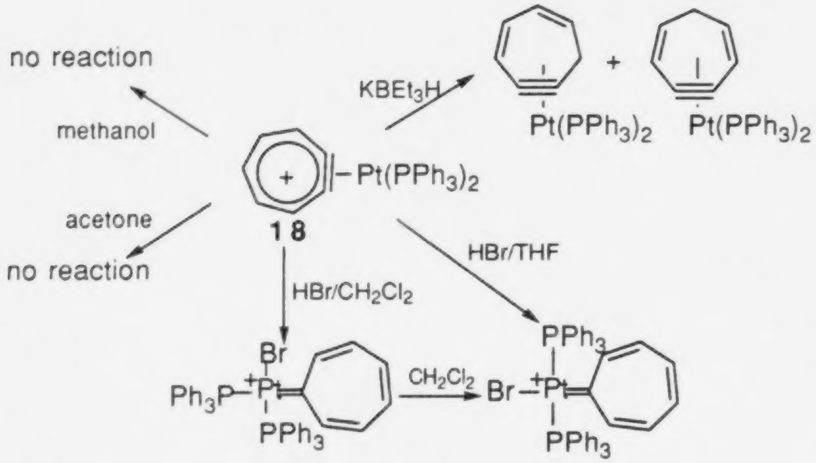
no reaction
methanol
KBEt$_3$H
+
Pt(PPh$_3$)$_2$
Pt(PPh$_3$)$_2$
+
Pt(PPh$_3$)$_2$
acetone
no reaction
18
HBr/THF
HBr/CH$_2$Cl$_2$
PPh$_3$
Br
Ph$_3$P
Pt
PPh$_3$
CH$_2$Cl$_2$
Br
Pt
PPh$_3$

(Scheme 1.6)

1.2.3. Complexes with an η^3-C_7H_7 Ligand.

A series of η^3-C_7H_7 complexes has been prepared.[29] The common characteristic of these complexes is that the cycloheptatrienyl ligand bonds to a metal center via an allyl moiety and leaves the diene part uncoordinated, which can be further utilized to bond to another metal center.[30] The typical geometry of an η^3-cycloheptatrienyl ligand is demonstrated by the solid state structure of $(\eta^3\text{-}C_7H_7)Mo(CO)_2(\eta^5\text{-}C_5H_5)$ (**19**) (Figure 1.1).[31] In this structure the seven membered ring is not planar but folded, the dihedral angle between the allyl and diene parts is 143°.

Another interesting feature of these η^3-C_7H_7 complexes is the highly fluxional C_7H_7 ring.[32,33] Thus, at room temperature, the metal moiety rapidly rearranges on the C_7H_7 ring of $(\eta^3\text{-}C_7H_7)Mo(CO)_2(\eta^5\text{-}C_5H_5)$ (**19**) and its ^1H NMR spectrum shows a single, time averaged signal for the C_7H_7 ring. The ring whizzing can be stopped at -110°C and gives four well-separated peaks in a ratio of 2:2:2:1. This is consistent with the above solid state structure which has C_s symmetry with a mirror plane through the C_7H_7 ring (Figure 1.1). Line shape analysis of the variable temperature ^1H NMR spectra suggested that the principle pathway for metal migration in **19** is the 1,2 shift.[33]

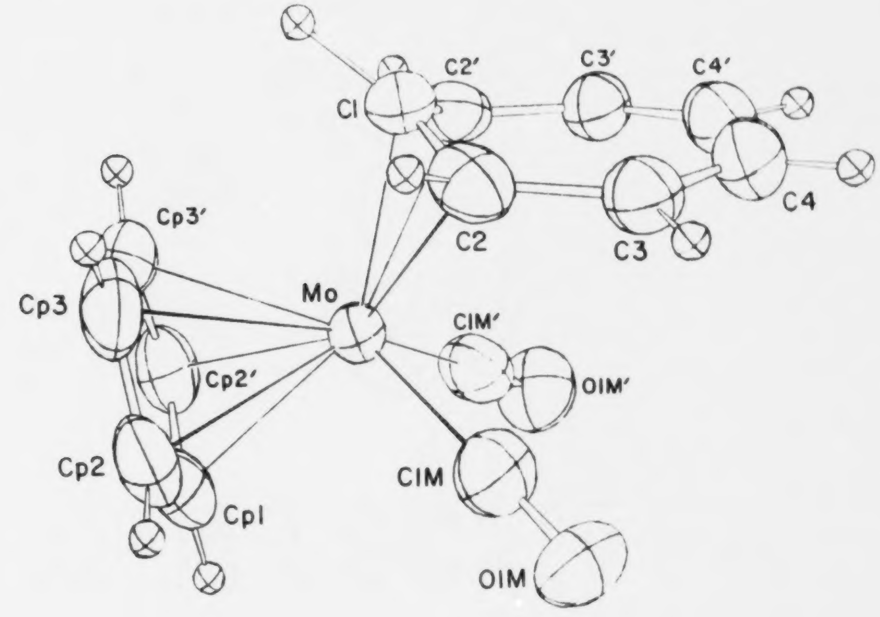

Figure 1.1 Molecular structure of $(\eta^3\text{-}C_7H_7)Mo(CO)_2(\eta^5\text{-}C_5H_5)$ (**19**).

It is noteworthy that a second dynamic process in this complex has also been identified by variable temperature IR spectroscopy. At room temperature there are four CO stretching bands due to the terminal CO ligands (1970, 1961, 1914, 1899 cm^{-1}). At -60°C two of the four bands disappear (1970 and 1914 cm^{-1}). The explanation of this observation is an equilibrium between two isomers (***exo*** -**A** and ***endo***-**B**), which is caused by the different orientations of the C_7H_7 ring with respect to the C_5H_5 ring (Scheme 1.7).[33a]

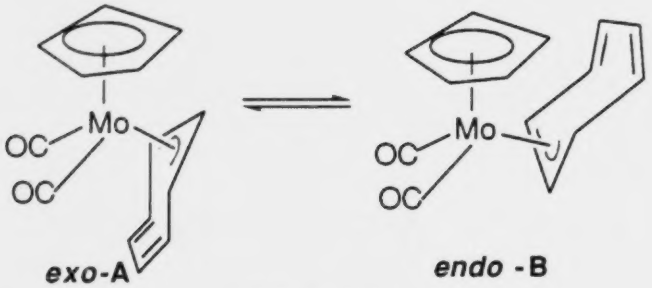

(Scheme 1.7)

Other interesting η^3-C_7H_7 complexes are $(\eta^3\text{-}C_7H_7)M(CO)_3^-$ (**20**) (M=Fe **a**, Ru **b**, Os **c**),[34,35] which are also the main subjects investigated in this thesis. Their formation is another excellent example of a very reactive organic ligand stabilized by a transition metal moiety. Due to its antiaromatic nature, the free anion $(C_7H_7)^-$ is rather unstable and consequently very difficult to prepare.[36] In contrast, the metal anions, $(\eta^3\text{-}C_7H_7)M(CO)_3^-$ (**20**) (M=Fe **a**, Ru **b**, Os **c**) can be easily prepared by deprotonation of $(\eta^4\text{-}C_7H_8)M(CO)_3$ (**21**) (M=Fe **a**, Ru **b**, Os **c**).

There are two bonding alternatives for the anions (Scheme 1.8) and both satisfy the 18-electron rule.[37] In structure **C** the $M(CO)_3$ moiety bonds to an η^4-diene unit with the negative charge formally localized on the allyl part of the C_7H_7 ring. Structure **D** corresponds to $(\eta^3\text{-allyl})M(CO)_3^-$ where the metal fragment formally carries the negative charge while the diene fragment remains uncoordinated.

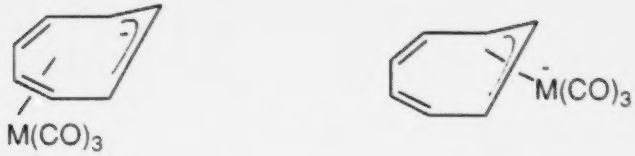

η^4-C **η^3-D**

M = Fe, Ru, Os

(Scheme 1.8)

X-ray crystallographic studies of all three metal anions have revealed that the η^3 form is the preferred bonding mode in the solid state (Figure 1.2).[34c,35]

The C_7H_7 ring of the anion **20** is fluxional as well. The low temperature limiting ^1H NMR spectrum of **20c** can be obtained at -110°C and consists of four peaks in the intensity ratio of 2:2:2:1. The chemical shifts of two peaks, which represent four protons, are in the free diene range. This indicates that in solution the η^3-**D** form is also the dominant structure.[35] These results are in accord with molecular orbital calculations which predicted the η^3-**D** form to be slightly more stable than η^4-**C** form. The energy difference between the two bonding modes is only ~14 kJ mol^{-1}.[37]

The anions, $(\eta^3\text{-}C_7H_7)M(CO)_3^-$ (**20**) (M=Fe **a**, Ru **b**, Os **c**) behave as mild nucleophiles with interesting ambident reactivity, and both ring and metal substituted products have been observed. These aspects will be fully discussed in the following chapters.

1.2.4. Complexes with an η^4-C_7H_8 Ligand.

Because the $M(CO)_3$ (M=Fe, Ru, Os) moieties have a strong tendency to coordinate to conjugated dienes,[38] it is not surprising that most η^4-cycloheptatriene complexes contain a group 8 metal.

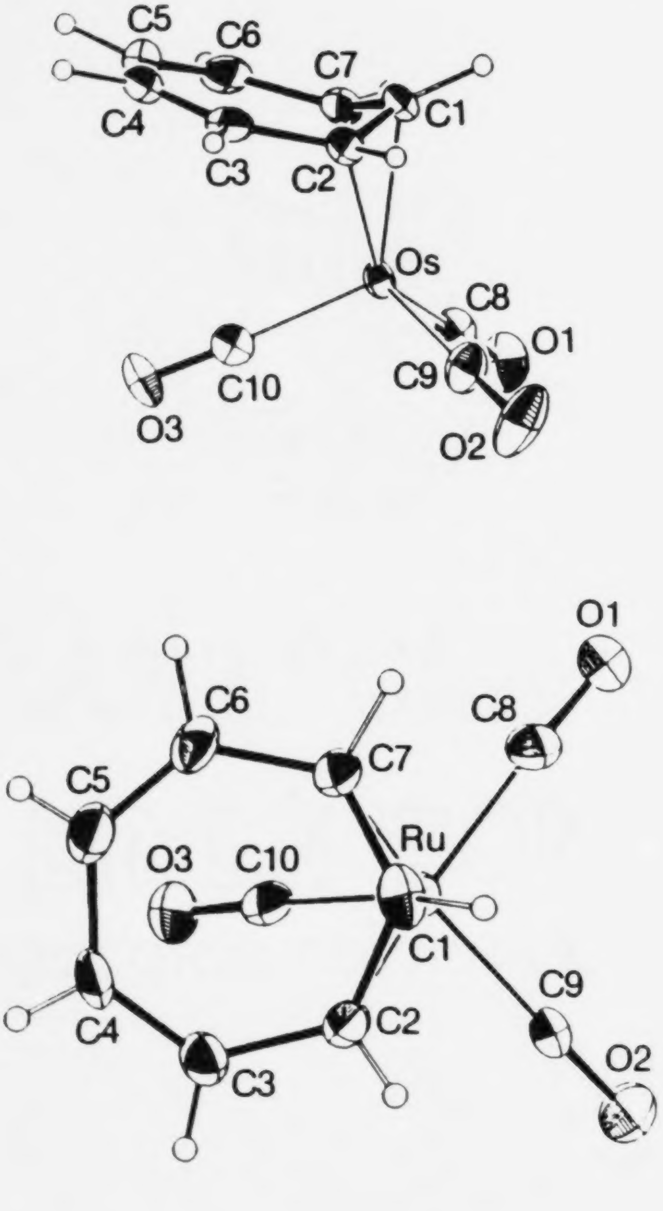
C5
C6
C7
C1
C4
C3
C2
Os
C8
O1
C10
C9
O3
O2
O1
C6
C8
C7
C5
Ru
O3
C10
C1
C9
C4
C2
O2
C3

Figure 1.2 Molecular structures of $(\eta^3\text{-}C_7H_7)M(CO)_3^-$ (**20**) (M=Ru **b**, Os **c**)

The complex, (η^4-C_7H_8)Fe(CO)$_3$ (**21a**) is a yellow liquid at room temperature. It is prepared by heating a toluene solution of cycloheptatriene and Fe(CO)$_5$ under reflux.[39] The analogous ruthenium complex, (η^4-C_7H_8)Ru(CO)$_3$ (**21b**) was first reported by Domingos et al.[40a] and Bau et al.,[40b,41] but the preparations were either inconvenient or gave **21b** in very low yields. A modified method, which involved photolysis of $Ru_3(CO)_{12}$ and excess of cycloheptatriene in benzene at 70°C, gave an 80-85% isolated yield of (η^4-C_7H_8)Ru(CO)$_3$ (**21b**).[42] The Os complex **21c** can be prepared in a similar fashion. However, due to the poor solubility of $Os_3(CO)_{12}$ in hydrocarbon solvents, the preparation scale is limited to only 300 mg at a time.[43]

The structural features of all three complexes are very similar. Their IR spectra show the characteristic stretching pattern of an M(CO)$_3$ group coordinated to an η^4-diene moiety, three strong bands, two of which are closely spaced (2050, 1989, 1975 cm^{-1} for Fe(CO)$_3$). The uncoordinated C=C double bond stretch occurs around 1660 cm^{-1}.[39]

The ^{1}H and ^{13}C NMR spectra show seven distinct resonances for the C_7H_8 ring which clearly establish that the molecules are static on the NMR time scale.[39,40b] The chemical shifts of bonded diene fragment experiences significant upfield shifts from that of the free ligand and the chemical shifts also roughly increase in the order of Fe<Ru<Os (Table 1.1). The latter most probably reflects the strength of the interaction between the M(CO)$_3$ moiety and C_7H_8 ring, which is expected to increase in the same order.

The derivative chemistry of (η^4-C_7H_8)M(CO)$_3$ (**21**) (M=Fe **a**, Ru **b**, Os **c**) is rich. Reactions can occur either at the C_7H_8 ring or at the metal center. This thesis focuses on the deprotonation of compound **21** and the reactions of formed anions with different electrophiles.

Table 1.1 ^{1}H NMR data of free C_7H_8 and (η^4-C_7H_8)M(CO)$_3$ (**21**) (M=Fe **a**, Ru **b**, Os **c**).[a,b]

	Free C_7H_8	Fe	Ru	Os
H1	5.28	3.3	3.25	2.75
H2	6.12	5.4	5.4	4.6
H3	6.55	5.4	5.45	4.7
H4	6.55	2.9	3.15	2.75
H5	6.12	5.7	5.8	5.7
H6	5.28	5.2	5.0	4.9
H7/H7'	2.20	2.3-2.5	2.0-2.2	1.6/0.9

[a]chemical shifts in ppm from TMS. [b]All signals are multiplets.

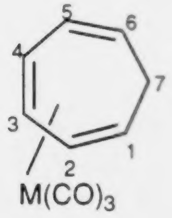

M = Fe, Ru, Os

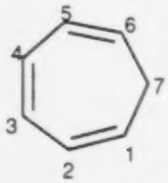

Cycloheptatriene is a very weak acid with an estimated pKa of 36[36] and its deprotonation is very difficult. On the other hand, attachment of an M(CO)$_3$ moiety leads to enhanced acidity of a C_7H_8 ring. Also, the resulting $C_7H_7^-$ anion is stabilized by the M(CO)$_3$ moiety. Therefore (η^3-C_7H_7)Fe(CO)$_3^-$ (**20a**) can be easily prepared by the deprotonation of (η^4-C_7H_8)Fe(CO)$_3$ (**21a**) with a variety of strong bases (Equation 1.7).[34]

In contrast to (η^3-C_7H_7)Fe(CO)$_3^-$ (**20a**), the preparation of the analogous Ru anion requires considerably more care. Although the deprotonation of (η^4-C_7H_8)Ru(CO)$_3$ (**21b**) with KO^{t}Bu proceeds rapidly and gives exclusively the desired anion, the reactions with KH or NaN(SiMe$_3$)$_2$ result in a mixture of mono- and dinuclear anionic species, [(C_7H_7)Ru$_2$(CO)$_5$]$^-$.[42]

$$\underset{\substack{\text{yellow}\\ \mathbf{21}}}{\eta^4\text{-}C_7H_8M(CO)_3} \xrightarrow[-H^+]{\text{Base}} \underset{\substack{\text{red}\\ \mathbf{20}}}{\eta^3\text{-}C_7H_7M(CO)_3^-} \qquad (1.7)$$

M = Fe Base = KH, NaN(SiMe$_3$)$_2$, BuLi, KO^{t}Bu
Ru KO^{t}Bu
Os KO^{t}Bu

It appears that KO^{t}Bu is also the only reagent for cleanly deprotonating (η^4-C_7H_8)Os(CO)$_3$ (**21c**). The resulting anion, (η^3-C_7H_7)Os(CO)$_3^-$ (**20c**) is the strongest base in the series.[43] This is reflected by the high sensitivity of **20c** toward protic solvents and the deprotonation equilibrium is temperature dependent. Low temperature favors the neutral, protonated form **21c**. Attempted deprotonation of (η^4-C_7H_8)Os(CO)$_3$ (**21c**) by other strong bases was not successful. Treatment of **21c** with BuLi gave a carbonyl attacked product, Li[(η^4-C_7H_8)Os(CO)$_2$(COBu)] (**22**) (Scheme 1.9).[43] It appears that the decreased acidity of (η^4-C_7H_8)Os(CO)$_3$ (**21c**) renders the carbonyl ligands the preferred site for a nucleophilic attack. Actually, nucleophilic attack of BuLi at carbonyl groups of Os and Ru clusters leading to stable acyl anions has been reported already.[44]

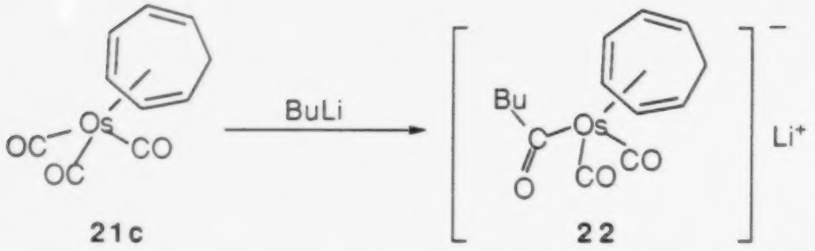

(Scheme 1.9)

1.2.5. Complexes with an η^5-C_7H_7 Ligand.

A typical neutral complex with an η^5-C_7H_7 moiety is the complex, (η^5-C_7H_7)Mn(CO)$_3$ (**23**). The compound was prepared by low temperature decarbonylation of (C_7H_7CO)Mn(CO)$_5$ (**24**) (Scheme 1.10).[45]

Complex **23** is fluxional. At 88°C the ^{1}H NMR spectrum displays only a time-averaged singlet for the C_7H_7 ring protons. On lowering the temperature the sharp signal broadens. The low temperature limiting spectrum is obtained at -48°C and shows four peaks in a ratio of 1:2:2:2 (3.53, 4.70, 5.42, 7.10 ppm). This is consistent with C_s molecular symmetry. Comparison of experimental and simulated spectra established that the rearrangement occurs through 1,2 metal shifts.[45b]

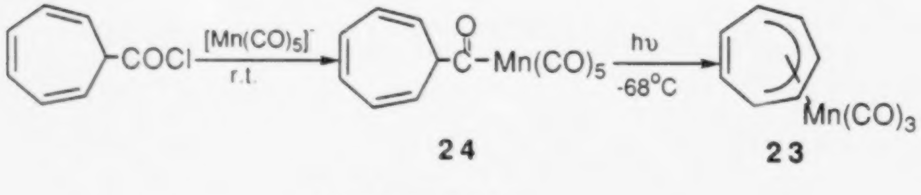

(Scheme 1.10)

Another interesting η^5-C_7H_7 complex is the cationic $[(\eta^5\text{-}C_7H_7)Fe(CO)_3]^+$ (**25**), which is isoelectronic with $(\eta^5\text{-}C_7H_7)Mn(CO)_3$ (**23**). The cation was prepared by protonation of $(\eta^4\text{-}C_7H_7OCH_3)Fe(CO)_3$ (**26**) with HBF_4 (Scheme 1.11).[47] Hydride abstraction from $(\eta^4\text{-}C_7H_8)Fe(CO)_3$ (**21a**) with $[Ph_3C][BF_4]$ is not a viable synthetic route since only electrophilic addition of $[Ph_3C]^+$ to the C_7H_8 ring is observed.

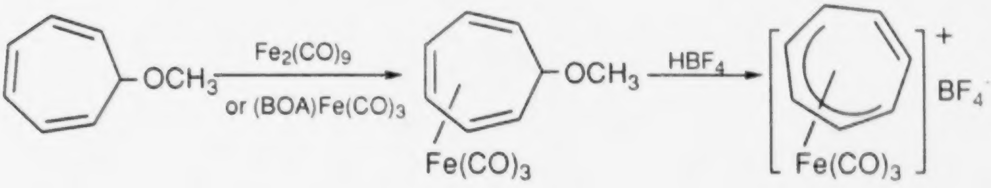

26 **25**

(Scheme 1.11)

The fluxional behavior of cation **25** is similar to that of the neutral Mn complex **23** except that the metal migration is more facile (T_c=-50°C, E_a=46 kJ mol^{-1} vs T_c=+20°C, E_a=63 kJ mol^{-1} in **23**). Based on detailed photoelectron spectroscopic studies and molecular orbital calculations, Whitesides et al. concluded that the differences are related to the extent of back-bonding from metal to the ring. An increase in back-bonding to the C_7H_7 ring results in an increase in the energy barrier to metal migration, and hence the cationic iron complex **25** with less back-bonding leads to a faster rate of rearrangement.[45b]

1.2.6. Complexes with an η^6-C_7H_8 Ligand.

The classical η^6-C_7H_8 complexes are those containing group 6 transition metals, $(\eta^6\text{-}C_7H_8)M(CO)_3$ (**27**) (M=Cr **a**, Mo **b**, W **c**). Indeed,

(η^6-C_7H_8)Mo(CO)$_3$ (**27b**) was the first metal complex containing a cycloheptatriene ligand.[46] The complexes, (η^6-C_7H_8)M(CO)$_3$ (**27**) (M=Cr **a**, Mo **b**, W **c**) can be prepared by heating M(CO)$_6$ in pure cycloheptatriene or in high boiling solvents under reflux (Scheme 1.12).[48]

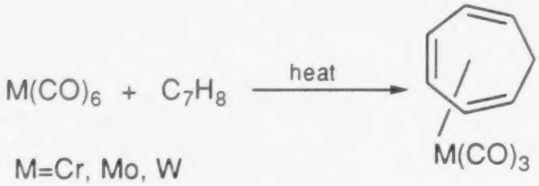

(Scheme 1. 12)

The molecular structure of the molybdenum complex **27b** is shown in Figure 1.3. The complex has approximate C_s symmetry and the mirror plane passes through the molybdenum atom, one carbonyl and the methylene group of the C_7H_8 ring. The cycloheptatriene ring is not planar, as the CH_2 group deviates from the plane of the remaining six carbon atoms by about 0.67 Å .[49]

The properties of (η^6-C_7H_8)M(CO)$_3$ (**27**) (M=Cr **a**, Mo **b**, W **c**) have been investigated in great detail. It was found that the Cr and Mo complexes readily undergo thermal 1,5 hydrogen shifts. The rearrangement of 7-substituted (η^6-C_7H_7R)Cr(CO)$_3$, which resulted only in an *exo*-R but not an *endo*-R isomer, demonstrates that only *endo*-hydrogen participates in the rearrangement (Scheme 1.13). Although a transition state involving the hydride intermediate **E** was originally suggested, the stepwise formation of substituted compounds and the stereospecifity of the shifts favour intermediate **F**.[50]

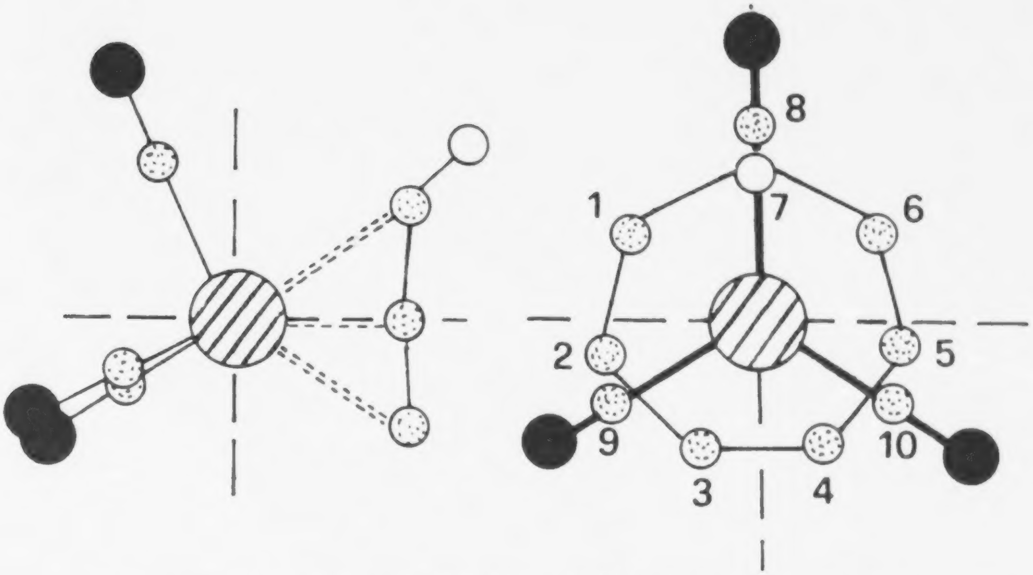
8
1
7
6
2
5
9
10
3
4

Figure 1.3 Molecular structure of (η^6-C_7H_8)Mo(CO)$_3$ (**27b**).

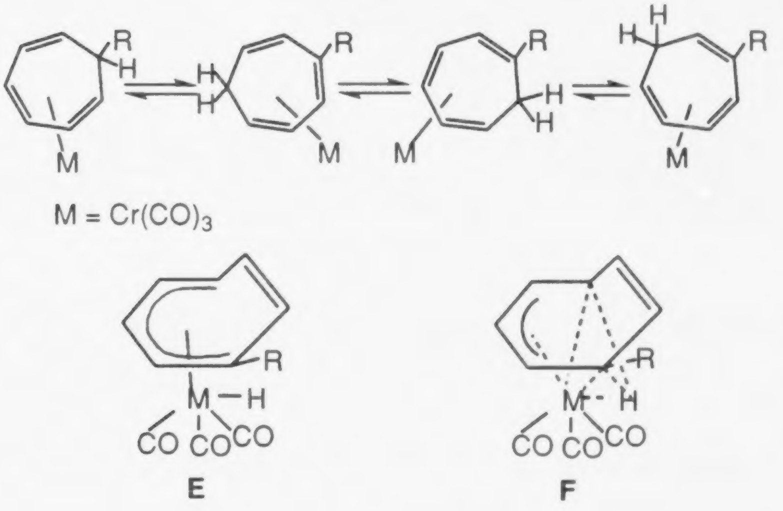
R
H
H
H
M
R
M
R
H
H
M
H
H
R
M
M = Cr(CO)3
R
M
H
CO
CO
CO
E
R
M
H
CO
CO
CO
F

(Scheme 1.13)

One of the important applications of (η^6-C_7H_8)Mo(CO)$_3$ (**27b**) is its usage as a source of Mo(CO)$_3$ group. The ready substitution of the C_7H_8 ligand by other neutral ligands and the almost exclusive formation of a *fac*-

isomer make using **27b** in many cases the best preparative method for *fac*-[Mo(CO)$_3$L$_3$] (**28**) (L = amines, phosphines, arsines, stibines, thioethers, etc.).[51]

Another important reaction of (η^6-C$_7$H$_8$)Mo(CO)$_3$ (**27b**) involves the facile hydride abstraction from the C$_7$H$_8$ ring. The obvious driving force for this reaction is the formation of the stable aromatic η^7-tropylium cation.[32] The properties and reactions of the cationic η^7-tropylium complexes will be discussed in the following section.

Beside η^6-C$_7$H$_8$ group 6 metal complexes, other metals can also bond to cycloheptatriene in an η^6-fashion. The displacement of all three carbonyl groups in (η^5-C$_5$H$_5$)Mn(CO)$_3$ by a C$_7$H$_8$ ligand gave (η^6-C$_7$H$_8$)Mn(η^5-C$_5$H$_5$) (**11**).[24] The crystal structure of the (η^5-CH$_3$C$_5$H$_4$)Mn(η^6-*exo*-7-PhC$_7$H$_7$) (**29**) has also been described.[52] The late transition metal complex (η^6-C$_7$H$_8$)Ru(η^4-C$_8$H$_{12}$) (**30**) has been prepared from the reaction of Ru(COD)(COT) (**31**) with CHT under a hydrogen atmosphere.[53]

1.2.7. Complexes with an η^7-C$_7$H$_7$ Ligand.

As mentioned before, hydride abstraction from (η^6-C$_7$H$_8$)M(CO)$_3$ (**27**) (M=Cr **a**, Mo **b**, W **c**) affords the cationic complexes (η^7-C$_7$H$_7$)M(CO)$_3^+$ (**32**).[32] The ^{1}H NMR spectrum of [(η^7-C$_7$H$_7$)Mo(CO)$_3$][BF$_4$] (**33b**) shows only one sharp singlet for the C$_7$H$_7$ ring which indicates fast rotation of the C$_7$H$_7$ ring in this molecule.

The planarity of the C$_7$H$_7$ ring has been confirmed by an X-ray structural investigation (Figure 1.4).[54] The Mo-CO distance (2.032 Å) is the longest found for Mo(CO)$_3$ complexes. On the other hand, the Mo-C$_{\text{ring}}$

distance (2.314 Å) is correspondingly one of the shortest so far found in molybdenum-aromatic ring compounds. Therefore the interaction between the metal and the C_7H_7 ring must be strong and the Mo-CO bond is relatively weak. These structural properties lead to characteristic reactivities of these cationic compounds.

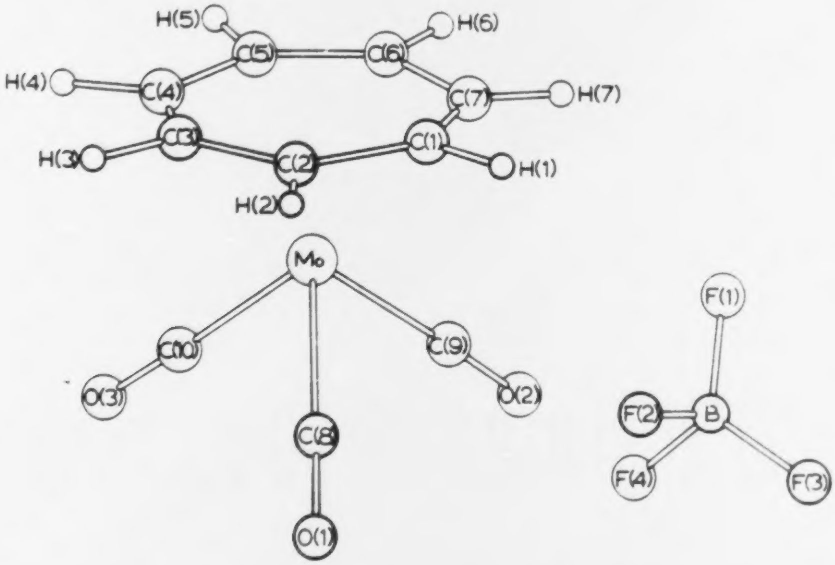

Figure 1.4 Molecular structure of $[(\eta^7\text{-}C_7H_7)Mo(CO)_3][BF_4]$ (**33b**).

The chemistry of the complex $(\eta^7\text{-}C_7H_7)Mo(CO)_3^+$ (**32b**) has been studied extensively. Both ring and metal moieties are reactive.[15] The weak metal-carbonyl bond leads to ready substitution of one carbonyl group by another neutral ligand (Scheme 1.14).[55] This reaction opens a synthetic route to otherwise inaccessible L-substituted complexes

$(\eta^6\text{-}C_7H_8)Mo(L)(CO)_2$ (**35**) by borohydride reduction of the resulting cation, $[(\eta^7\text{-}C_7H_7)Mo(L)(CO)_2]^+$ (**34**).[56]

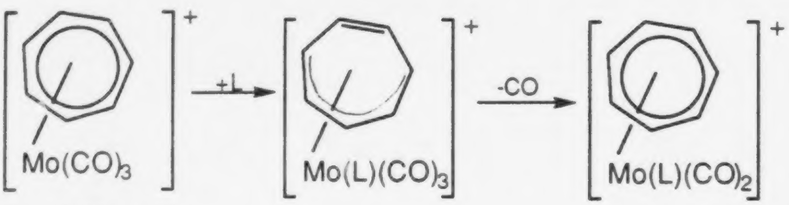

32b **33** **34**

(Scheme 1.14)

The typical ring reaction is nucleophilic attack on the C_7H_7 ring. Both neutral and anionic nucleophiles can react with $(\eta^7\text{-}C_7H_7)M(CO)_3^+$ (**32**) (M=Cr, Mo, W) to give substituted η^6-cycloheptatriene derivatives. Treatment of $(\eta^7\text{-}C_7H_7)Mo(CO)_3^+$ (**32b**) with phosphines affords the ring substituted phosphonium salts $[(\eta^6\text{-}C_7H_7PR_3)Mo(CO)_3][BF_4]$ (**36**).[57] But excess of phosphines leads to *fac*-$[M(CO)_3(PR_3)_3]$ (**37**) (M=Mo, W) (Scheme 1.15).[58]

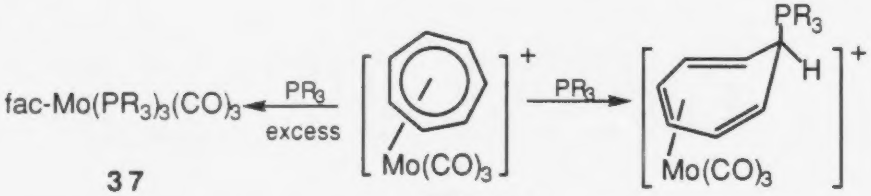

37 **32b** **36**

(Scheme 1.15)

Ambident reactivity has been observed in the reactions of $(\eta^7\text{-}C_7H_7)M(CO)_3^+$ (**32**) (M=Cr, Mo, W) with anionic nucleophiles (Scheme 1.16). For example, the reaction of $[(\eta^7\text{-}C_7H_7)Mo(CO)_3^+]$ with $(CH_3)_3CMgBr$

gave the corresponding ring substituted exo-^{t}Bu complex.[59] A kinetic investigation, using methoxide or acetylacetone as nucleophiles, suggested that the reaction occurs via direct addition to the tropylium ring. On the other hand, metal attacked products, $(\eta^7\text{-}C_7H_7)MX(CO)_2$ (**39**) were obtained from the reactions of $(\eta^7\text{-}C_7H_7)M(CO)_3^+$ (**32**) (M=Cr **a**, Mo **b**, W **c**) with NaX.[60] The formed dicarbonyl compounds are useful starting materials for the synthesis of η^7-cycloheptatrienyl dicarbonyl derivatives. Interestingly, it seems that such ambident reactivity is a characteristic property of C_7H_7 complexes because in following chapters such behavior will also be observed with the anions, $(\eta^3\text{-}C_7H_7)M(CO)_3^-$ (**20**) (M=Fe **a**, Ru **b**, Os **c**).

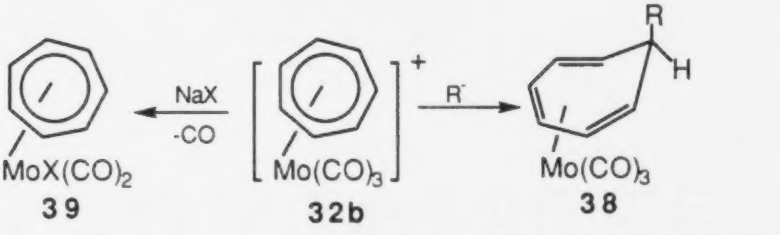

X=Cl, Br, I (Scheme 1.16) R=H, OCH_3, SH, t-Bu

1.3 Cycloheptatrienyl Bridged Heterobimetallic Complexes.

In the preceding pages the variable bonding capability of the cycloheptatriene (C_7H_8) and cycloheptatrienyl (C_7H_7) ligands to mononuclear metal fragments, ML_n, has been clearly demonstrated. The ligands also have the ability of bridging two metals together to give a variety of bimetallic complexes. A potential advantage of using these ligands as bridging groups is the possibility of producing unsaturated metal sites via ring slippage in these bimetallic complexes, that is via changes of the bonding mode of the μ-C_7H_8 or μ-C_7H_7 moieties. Since coordinatively unsaturated species are highly reactive, the variable bonding capability of these ligands promises rich derivative chemistry.

The first cycloheptatriene bridged binuclear complexes were homobimetallic complexes which were obtained from the reactions of cycloheptatriene with the respective di- or polymetallic carbonyl compounds (Scheme 1.17).[61]

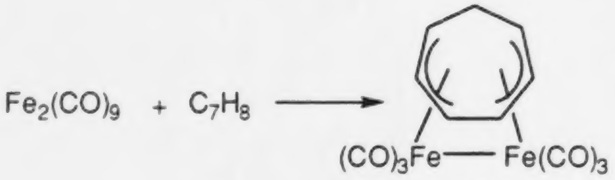

40

(Scheme 1.17)

Later, the cycloheptatrienyl bridged dirhodium complex was prepared by abstraction of a hydride from a coordinated cycloheptatriene ligand in CH_2Cl_2, as illustrated in scheme 1.18.[62]

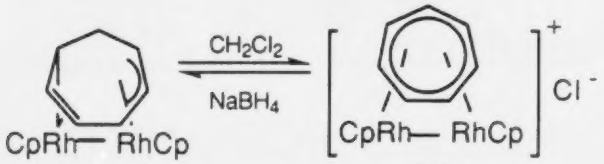

41 **42**

(Scheme 1.18)

The first cycloheptatrienyl bridged heterodinuclear complex was reported by Cotton et al. in 1969. The Fe-Mo complex was prepared by photochemical reaction of $(\eta^3\text{-}C_7H_7)Mo(CO)_2(\eta^5\text{-}C_5H_5)$ with $Fe(CO)_5$ or $Fe_2(CO)_9$. Spectral data and X-ray crystallography confirmed the trans-(μ-η^3,η^4-C_7H_7) structure for this compound, in which (η^5-C_5H_5)Mo(CO)$_2$ and Fe(CO)$_3$ fragments are bonded to opposite faces of the C_7H_7 ring with η^3- and η^4- bonding modes, respectively (Scheme 1.19).[30]

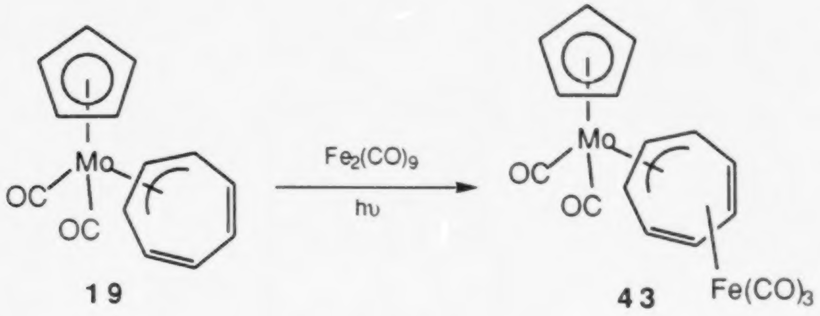

(Scheme 1.19)

It was also found that the complex is fluxional. At room temperature the ^1H NMR spectrum showed only one broad signal for the C_7H_7 ring. Upon lowering the temperature the peak broadened. The low temperature limiting spectrum was reached at -50°C and gave four peaks in a ratio of 2:2:2:1, consistent with C_s molecular symmetry. Line shape analysis suggested that the rearrangement proceeds by a 1,2 or a mixture of 1,2 and 1,3 metal shifts.[30]

In 1976 Bennett et al. reported, for the first time, a different strategy to synthesize cycloheptatrienyl bridged heterobimetallic complexes.[63] In this route a metal anion, (η^3-C_7H_7)Fe(CO)$_3^-$ (**20a**) was reacted with transition metal carbonyl halides to give C_7H_7 bridged heterobimetallic complexes. Interestingly, the products of these reactions exhibited a cis arrangement of two metal moieties with a metal-metal bond (Scheme 1.20), different from above trans FeMo complex **43**.

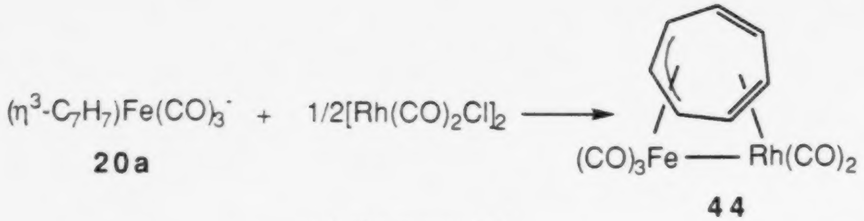

20a

44

(Scheme 1.20)

The method has proved versatile and provided a series of cycloheptatrienyl bridged heterobimetallic complexes, cis-(μ-C_7H_7)Fe$(CO)_3$M'L_n (M'= Rh, Ir, Mn, Re, Pd; L= CO, olefin).[62-64] Recently, by using the analogous Ru and Os anions, (η^3-C_7H_7)M$(CO)_3^-$ (**20**) (M=Ru **b**, Os **c**), the corresponding Ru/Os-Rh/Ir complexes have also been synthesized.[42,43,65]

A noteworthy feature of this method is the metal-dependent reactivity of the anions. Thus, the reactions of Fe and Ru anions with transition metal halides always yielded cis type products, but the Os anion gave both cis and trans compounds (Scheme 1.21).[66]

A most distinct characteristic of these cycloheptatrienyl bridged heterobimetallic complexes is the whizzing of the C_7H_7 ring, but, the speed of rotation is very different between cis and trans type compounds. For instance in cis-(μ-C_7H_7)Fe$(CO)_3$Rh$(CO)_2$ (**44**) the rotation of the C_7H_7 ring could not be frozen out even at -164°C.[63] However, the related trans-(μ-C_7H_7)Os$(CO)_3$Rh(COD) (**45**) has a coalescence temperature of -50°C.[66]

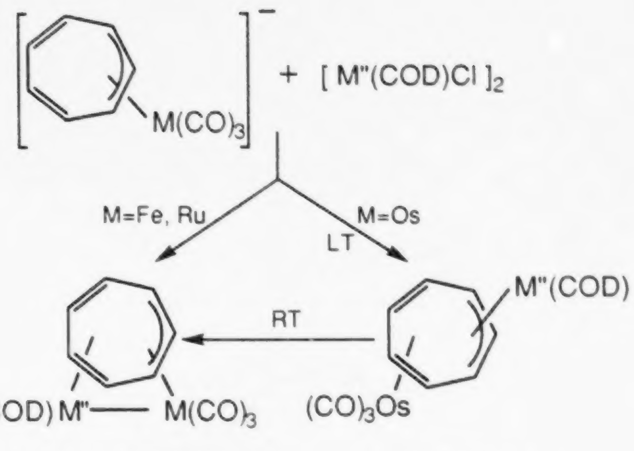
M(CO)3
+ [M"(COD)Cl]2
M=Fe, Ru
M=Os
LT
RT
M"(COD)
(COD) M"
M(CO)3
(CO)3Os

(M=Fe, Ru, Os; M"=Rh, Ir) (M"=Rh, Ir)

(Scheme 1.21)

Although most cycloheptatrienyl bridged heterobimetallic complexes have a coordinatively saturated C_7H_7 ring, very recently Airoldi et al. prepared cis-(μ-η^3,η^2-C_7H_7)Fe(CO)$_3$Pd(η^5-C_5H_5) (**46**) which has a free double bond in the C_7H_7 ring. The (μ-η^2,η^3-C_7H_7) structure has been confirmed by X-ray crystallography (Figure 1.5).[67]

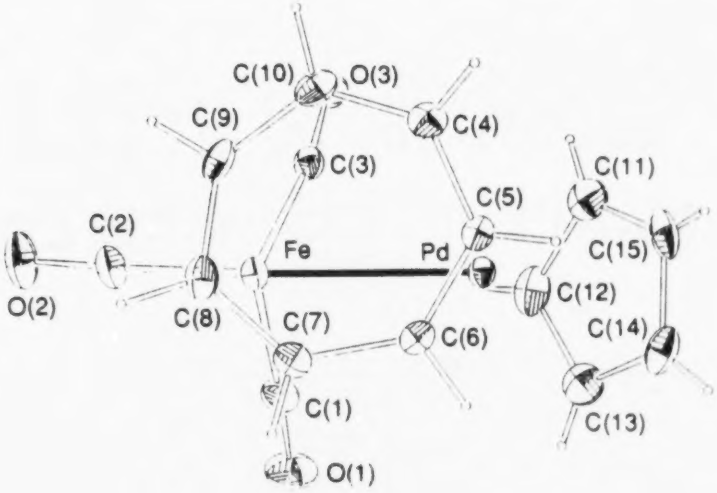
C(10)
O(3)
C(9)
C(4)
C(3)
C(11)
C(5)
C(2)
Fe
Pd
C(15)
O(2)
C(12)
C(8)
C(7)
C(6)
C(14)
C(1)
C(13)
O(1)

Figure 1.5 ORTEP drawing of (μ-η^3,η^2-C_7H_7)Fe(CO)$_3$Pd(η^5-C_5H_5) (**46**).

Complementing the above synthetic routes, nucleophilic attack on an electrophilic tropylium complex can also afford μ-C_7H_7 bridged heterobimetallic compounds. Muller et al.[68] and Beddoes et al.[69] treated the cationic tropylium complex, $(\eta^7\text{-}C_7H_7)Mo(CO)_3^+$ (**32b**) with $Na[Re(CO)_5]$ (**10**) or $K[Ru(CO)_2(\eta^5\text{-}C_5Me_5)]$ (**47**) and obtained $(\mu\text{-}\eta^6,\eta^1\text{-}C_7H_7)Mo(CO)_3Re(CO)_5$ (**48**) and $(\mu\text{-}\eta^6,\eta^1\text{-}C_7H_7)Mo(CO)_3Ru(CO)_2(\eta^5\text{-}C_5Me_5)$ (**49**) (Scheme 1.22). Both compounds are fluxional as well.

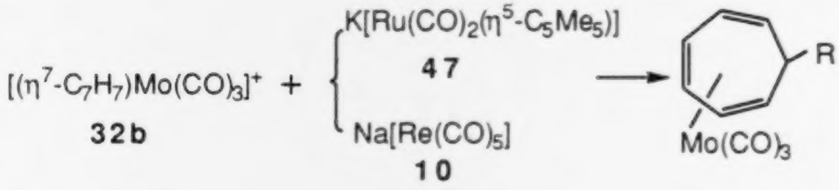

(R=$Re(CO)_5$ **48**, $Ru(CO)_2(\eta^5\text{-}C_5Me_5)$ **49**)

(Scheme 1.22)

1.4. Further Reactions of the Anionic Complexes, $(\eta^3\text{-}C_7H_7)M(CO)_3^-$ (M=Fe, Ru, Os), with Electrophiles: Scope of the Thesis

It has been demonstrated that the anionic complexes $(\eta^3\text{-}C_7H_7)M(CO)_3^-$ (M=Fe, Ru, Os) are effective starting materials for the formation of C_7H_7 bridged heterobimetallic complexes. However, the metal-dependent reactivity and electrophilic discrimination of these anions are far from being understood. Clearly, in order to rationalize the variable reactivities, more information about the reactions of the anions is desirable.

In this thesis the reactions of $(\eta^3\text{-}C_7H_7)M(CO)_3^-$ (**20**) (M=Fe **a**, Ru **b**, Os **c**) with a range of metal electrophiles have been carried out. It was found that reactions of **20b** and **20c** with group 7 halides gave only cis-C_7H_7 ring bridged Ru/Os-Mn/Re complexes. The complex, cis-$(\mu\text{-}\eta^3,\eta^2\text{-}C_7H_7)Os(CO)_3Re(CO)_4$ (**50**) was detected in the reaction of $(\eta^3\text{-}C_7H_7)Os(CO)_3^-$ (**20c**) with $[Re(CO)_4Br]_2$. The detection of this complex is helpful to understand the formation of cis-C_7H_7 ring bridged Ru/Os-Mn/Re complexes.

The reactions of **20** with $(\eta^5\text{-}C_9H_7)/(\eta^5\text{-}C_5H_5)Mo(CO)_2^+$ (C_9H_7=indenyl, C_5H_5=cyclopetadienyl) have been carried out. Surprisingly, in all three cases trans type products have been produced. The osmium anion again proved to be the exception and gave two products, the trans compound and a cis compound without a metal-metal bond. The reactions again demonstrate that the nature of the electrophiles is very important for the outcome of the reactions.

The reaction of Fe anion **20a** with $[Pd(\eta^3\text{-}C_3H_5)Cl]_2$ gave a normal cis-FePd compound. But the reaction of the Ru anion resulted in allyl transfer and gave $(\eta^3\text{-}C_7H_7)Ru(CO)_2(\eta^3\text{-}C_3H_5)$ and $(\mu\text{-}C_7H_7)Ru(CO)_3Ru(CO)(\eta^3\text{-}C_3H_5)$, another example of the nucleophilic metal-dependence.

Finally, with a view to utilizing the anionic complexes in organic synthesis, the deprotonation of the functionalized derivative, $(\eta^4\text{-}C_7H_7CHO)Fe(CO)_3$ was carried out, and the reactions of the anion, $[(\eta^3\text{-}C_7H_6CHO)Fe(CO)_3]^-$ with CH_3I and Me_3SiCl were investigated.

1.5. References.

1. Sinfelt, J. H., *"Bimetallic Catalysts: Discoveries, Concepts and Applications"*, Wiley, New York, **1983**

2. Sachtler, W. M. H., *J. Mol. Catal.*, **1984**, *25*, 1

3. Ponec, V., *Adv. Catal.*, **1983**, *32*, 149

4. Sinfelt. J. H., *Accts. Chem. Res.*, **1977**, *10*, 15

5. Sinfelt, J. H., *Catal. Rev.-Sci. Engng*, **1974**, *9*, 147.

6. Guczi, L., *J. Mol. Catal.*, **1984**, *25*, 13

7. Rodriguez, J. A.; Goodman, D.W., *Science*, **1992**, *257*, 897

8. Sinfelt, J. H., *Sci. Am.*, **1985**, *253*, 90

9. (a). Bond, G. C., *"Heterogenous Catalysis: Principles and Applications"* Oxford University Press, Oxford, **1987**.

   (b). Leach, B. E. (Ed.), *"Applied Industrial Catalysis"*, Academic Press, New York, **1983**, Vol. *1-3*

10.(a). Johnson, B. F. G. (Ed.), *"Transition Metal Clusters"*, Wiley, Chichester, **1980**

   (b). Adams, R. O.; Horvath, I. T., *Prog. Inorg. Chem.*,**1985**, *33*,127

   (c). Kaesz, H. D., *"Metal Clusters in Catalysis"*, Elsevier, Amsterdam, **1986**

   (d). Roberts, D. A.; Geoffroy, G. L., *"Comprehensive Organonetallic Chemisty"*, (Edited by Wilkinson, G.; Stone, F. G. A.; Abel, E. W.), Pergamon Press, Oxford, **1982**, Chapter. *40*

   (c). Farrugia, L. J., *Adv. Organomet. Chem.*, **1990**, *31*, 301

11. Adams, R. D.; Li, Z.; Swepston, P.; Wu, W.; Yamamoto, J., *J. Am. Chem. Soc.*, **1992**, *114*, 10657.

12. Parshall, G. W., *"Homogeneous Catalysis"*, Wiley, New York, **1980**

13.(a). Holton, J.; Lappert, M. F.; Pearce, R.; Yarrow, P. I. W., *Chem. Rev.*, **1983**, *83*, 135.

(b). Casey, C. P; Audett, J. D., *Chem. Rev.*,**1986**, *86*,339

(c). Bullock, R. M.; Casey, C. P., *Acc. Chem. Res.*, **1987**, *20*, 167

(d). White, G. S.; Stephan, D. W., *Organometallics*, **1988**, *7*, 903

(e). Breimair, J.; Niemer, B.; Raab, K.; Beck, W., *Chem. Ber.*, **1991**,*124*,1059

(f). Puddephatt, R. J., *Chem. Soc. Rev.*, **1983**,*12*, 99

(g). Hostetler, M. J.; Butts, M. D.; Bergman, R. G., *Inorg. Chim. Acta*, **1992**, *198*, 377.

14.(a). Collman, J. P.; Hegedus, L. S.; Norton, J. R.; Finke, R. G., *"Principles and Appilcations of Organotransition Metal Chemistry"*, University Science Books, Mill Valley, **1987**, chapter *12*, p. 653

(b). Brady III, R. C.; Pettit, R., *J. Am. Chem. Soc.*, **1980**, *102*, 6181

(c). Brady III, R. C.; Pettit, R., *J. Am. Chem. Soc.*, **1981**, *103*, 1287

15. Deganello, G., *"Transition Metal Complexes of Cyclic Polyolefins,"* Academic Press, London, **1979**, Chapter *1*

16. Cotton, F. A.; *J. Am. Chem. Soc.*, **1968**, *90*, 6230

17. Fischer, E. O.; Fritz, H. P., *Adv. Inorg. Chem. Radiochem.*, **1959,** *1*, 55.

18. Abel, E. W.; Bennett, M. A.; Burton, R.; Wilkinson, G., *J. Chem. Soc.*, **1958**, 4559

19. Werner, R. P. M.; Manastyrskyj, S. A., *J. Am. Chem. Soc.*, **1961**, *83*, 2023

20. Ciappenelli, D.; Rosenblum, M., *J. Am. Chem. Soc.*, **1969**, *91*, 3673; 6876

21. Heinekey, D. M.; Graham, W. A. G., *J. Am. Chem. Soc.*, **1979**, *101*, 6115

22. Heinekey, D. M.; Graham, W. A. G., *J. Organomet. Chem.*, **1982**, *232*, 335

23. Heinekey, D. M.; Graham, W. A. G., *J. Am. Chem. Soc.*, **1982**, *104*, 915

24. Pauson, P. L.; Seagal, J. A., *J. Chem. Soc. Dalton Trans,* **1975**, 2387

25. Benson, I. B.; Knox, S. A. R.; Starisfield, R. F. O.; Woodward, P., *J. Chem. Soc. Chem. Commun.*, **1977**, 404.

26. Reger, D. L.; Colleman, C. J.; McElligott, P. J., *J. Organomet. Chem.*, **1979**, *171*, 73

27. Sweet, J. R.; Graham, W. A. G., *J. Organomet. Chem.*, **1981**, *217*, C37

28. Lu, Z.; Abboud, K. A.; Jones,W. M., *J. Am. Chem. Soc.*, **1992**, *114*, 10991

29. King, R. B.; Bisnette, M. B., *Inorg, Chem.*, **1964**, *3*, 785

30. Cotton, F. A.; Reich, C.R., *J. Am. Chem. Soc.*, **1969**, *91*, 847

31. Cotton, F. A.; DeBoer, B. G.; LaPrade, M.D., *Abstract of the XXIIIrd IUPAC Conference,* Boston, **1971**, Vol. *3*, p. 1

32.(a). King, R.B.; Fronzaglia, A., *Inorg. Chem.*, **1966**, *5*, 1837

(b). Munro, J. D.; Pauson, P. L., *J. Chem. Soc.,* **1961**, 3475

33.(a). Bennett, M. A.; Bramley, R.; Watt, R., *J. Am. Chem. Soc.*, **1969,** *91*, 3089

(b). Faller, J.W., *Inorg. Chem.*, **1969**, *8*, 767

34.(a). Maltz, H., Kelly, B. A.; *J. Chem. Soc. Chem. Commun.,* **1971**, 1390 (b). Deganello, G., Boschi, T., Toniolo, L.; *J. Organomet. Chem.*, **1975**, *97*, C46

(c). Sepp, E.; Purzer, A.; Thiele, G.; Bebrens, H., *Z. Naturforsch.*, **1978**, *33b*, 261

35. Astley, S. T.; Takats, J., *Organometallics*, **1990**, *9*, 184

36.(a). Dauben Jr., H. J.; Rifi, M. R., *J. Am. Chem. Soc.*,**1963**, *85*, 3041

(b). Doering, W. von E.; Gaspar, P.P., *J. Am. Chem. Soc.*, **1963**, *85*, 3043

37. Hofmann, P., *Z. Naturforsch.*, **1978**, *33b*, 251

38. Pearson, A. J., *"Metallo-organic Chemistry"* Wiley, Chichester, **1985**.

39. Burton, R.; Pratt, L.; Wilkinson, G., *J. Chem. Soc.*, **1961**, 594

40.(a). Domingos, A. J. P.; Johnson, B. F. G.; Lewis, J., *J. Organomet. Chem.*, **1973**, *49*, C33

(b). Bau, R.; Burt, J. C.; Knox, S. A. R.; Laine, R. M.; Phillips, R. P.; Stone, F. G. A., *J. Chem. Soc. Chem. Commun.*, **1973**, 726

41. Burt, J. C.; Knox, S. A. R.; Stone, F. G. A., *J. Chem. Soc. Dalton*, **1975,** 731

42. Edelmann, F.; Kiel, G. Y.; Takats, J.; Vasudevamurthy, A.; Yeung, M. Y., *J. Chem. Soc., Chem. Commun.*, **1988**, 296

43. Astley, S. T., *Ph. D. Thesis*, University of Alberta, **1989**, Chapter *3*

44. Kaesz, H. D.; Jensen, C. M., *Polyhedron*, **1988**, *7*, 1035

45.(a). Whitesides, T. H.; Budnik, R. A., *J. Chem. Soc. Chem. Commun.*, **1971**, 1514

(b). Whitesides, T. H.; Budnik, R. A., *Inorg. Chem.*, **1976**, *14*, 68

46. Abel, E. W.; Bennett, M. A.; Wilkinson, G., *Proc. Chem. Soc.*, **1958**, 152

47. Mahler, J. E.; Jones, D. A. K.; Pettit, R., *J. Am. Chem. Soc.*, **1964**, *86*, 3589

48.(a). Abel, E. W.; Bennett, M. A.; Burton, R.; Wilkinson, G., *J. Chem. Soc.*, **1958**, 4559

(b). Strohmeier, W., *Chem. Ber.*, **1961**, *94*, 2490

(c). Bennett, M. A.; Pratt, L.; Wilkinson, G., *J. Chem. Soc.*, **1961**, 2037

49. Dunitz, J. D.; Pauling, P., *Helv. Chim. Acta*, **1960**, *43*, 2188

50.(a). Foreman, M. I.; Knox, G. R.; Pauson, P. L.; Todd, K. H.; Watts, W. E., *J. Chem. Soc. Chem. Commun.*, **1970**, 843; *Perkin II*, **1972**, 1141

(b). Roth, W. R.; Grimme, W., *Tetrahedron Lett.*, **1966**, 2347

51.(a). Abel, E. W.; Bennett, M. A.; Wilkinson, G., *J. Chem. Soc.*, **1959**, 2323

(b). Cotton, F. A.; Zingales, F., *Chem. Ind. (London)*, **1960**, 1219

(c). King, R. B., *Inorg. Chem.*, **1963**, *2*, 936

(d). Chandrasegaran, L.; Rodley, G. A., *Inorg. Chem.*, **1965**, *4*, 1360

52. Jeffreys, J. A. D.; MacFie, J., *J. Chem. Soc. Dalton Trans.*, **1978**, 144

53. Deganello, G., Mantovani, A., Sandrini, P. L., Pertici, P., Vitulli, G.; *J. Organomet. Chem.*, **1977**, *135*, 215

54. Clark, G. R., Palenik, G. J.; *J. Organomet. Chem.*, **1973**, *50*, 185

55. Deganello, G.; Boschi, T.; Toniolo, L.; Albertin, G., *Inorg. Chim. Acta*, **1974**, *10*, L3

56. Isaacs, E. E.; Graham, W. A. G., *J. Organomet. Chem.*, **1975**, *90*, 319

57. Salzer, A., *Inorg. Chim. Acta*, **1976**, *17*, 221

58. Sweigart, D. A.; Gower, M.; Kane-Maguire, L. A. P., *J. Organomet. Chem.*, **1976**, *108*, C15

59.(a). Munro, J. D.; Pauson, P. L., *Proc. Chem. Soc.*, **1959**, 267.

(b). Al-Kathumi, K. M.; Kane-Maguire, L. A. P., *J. Organomet. Chem.*, **1975**, *102*, C4

60. Isaacs, E. E.; Graham, W. A. G., *Can. J. Chem.*, **1975**, *53*, 975

61.(a). Emerson, G. F.; Mahler, J. E.; Pettit, R.; Collins, R., *J. Am. Chem. Soc.*, **1964**, *86*, 3590

(b). Cotton, F. A., DeBoer, B. G., Marks, T. J.; *J. Am. Chem. Soc.*, **1971**, *93*, 5069

(c). Deganello, G.; *J. Organomet. Chem.*, **1973**, *59*, 329

62. Salzer, A.; Egolf, T.; Philipsborn, W. von, *Helv. Chim. Acta*, **1982**, *65*,1145

63. Bennett, M. J.; Pratt, J. L.; Simpson, K. A.; LiShingMan, L. K. K.; Takats, J., *J. Am. Chem. Soc.*, **1976**, *98*, 4810

64.(a). Edelmann, F.; Takats, J., *J. Organomet. Chem.*, **1988**, *344*, 351

(b). Ball, R. G.; Edelmann, F.; Kiel, G.-Y.; Takats, J.; Drews, R., *Organometallics*, **1986**, *5*, 829

(c). Lin, G. Y.; Takats, J., *J. Organomet. Chem.*, **1984**, *269*, C4

65.(a). Vasudevamurthy, A.; Takats, J., *Organometallics*, **1987**, *6*, 2005

(b). Astley, S. T.; Takats, J., *J. Organomet. Chem.*, **1989**, *363*, 167

66. Astley, S. T., *Ph. D. Thesis*, University of Alberta, **1989**, Chapter *4*

67. Airoldi, M.; Deganello, G.; Gennaro, G.; Moret, M.; Sironi, A., *J. Chem. Soc. Chem. Commun.*, **1992**, 850

68. Müller, H. J.; Nagel, U.; Steinmann, M.; Polborn, K.; Beck, W., *Chem. Ber.*, **1989**, *122*, 1387

69. Beddoes, R. L.; Davies, E. S.; Hellinwell, M.; Whiteley, M. W., *J. Organomet. Chem.*, **1991**, *421*, 285

Chapter 2.

Synthesis and Spectroscopic Characterization of cis-(μ-C_7H_7)M(CO)$_3$M'(CO)$_3$ (M=Ru, Os; M'=Mn, Re)

2.1. Introduction.

As mentioned in chapter one, the reactions of the ambident organometallic anions, (η^3-C_7H_7)M(CO)$_3^-$ (M=Fe **1a**, Ru **1b**, Os **1c**) with transition metal electrophiles have exhibited interesting metal-dependence. The reactions of **1a** and **1b** with [M"(COD)Cl]$_2$ (M"=Rh, Ir; COD=1,5-cyclooctadiene) lead to the formation of cis type products, cis-(μ-C_7H_7)M/M" (M"=Rh, Ir), which have the two metal moieties occupying the same face of the C_7H_7 ring. In these compounds the two metal units are joined by a metal-metal bond (Scheme 2.1).[1-3] However, the reactions of **1c** with [M"(COD)Cl]$_2$ (M"=Rh, Ir) unexpectedly gave trans-(μ-C_7H_7)Os(CO)$_3$M"(COD) (M"=Rh, Ir), where two metal fragments occupy opposite sides of the bridging C_7H_7 ring (Scheme 2.1).[4] The trans compounds appear as the kinetic products and easily convert to thermodynamically more stable cis compounds. The driving force for this isomerization is presumably the saturated 18 electron configuration of the Rh/Ir centers in the cis compounds, compared to the 16 electron Rh/Ir centers in the trans arrangement.

The rationale for such variable reactivity of anions **1** has, for a long time, been attributed to the possible existence of two alternative structures (η^3-**A** and η^4-**B**) (Scheme 2.2).[5] Formally, the location of the negative charge is very different in these two structures, at the metal atom in η^3-**A** and on the C_7H_7 ring in η^4-**B**. Hence electrophilic attack is expected to occur at the metal center in η^3-**A** to give metal-metal bonded bimetallic compounds, or at the ring carbon in η^4-**B** to afford ring substituted products.

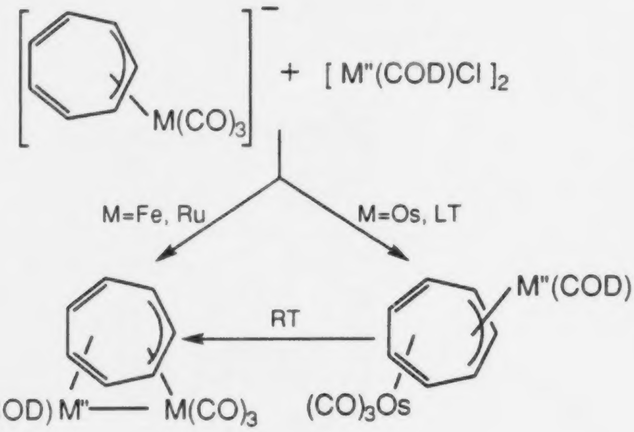

(M=Fe, Ru, Os; M"=Rh, Ir)   (M"=Rh, Ir)

(Scheme 2.1)

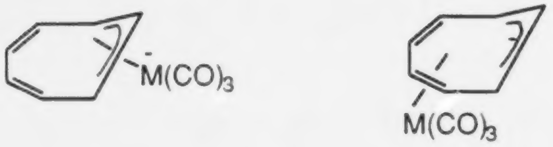

η^3-**A**

(M=Fe, Ru, Os)

η^4-**B**

(Scheme 2.2)

However X-ray crystallography has revealed that the solid structures of all three anions **1a-1c**, irrespective of the metal, conform to the η^3-**A** bonding mode.[6] Also, variable temperature ^1H NMR studies of the Os anion indicated that even in solution anion **1c** takes an η^3-**A** bonding form as its ground state structure.[6] These experimental observations are also consistent with the results of extended Hückel MO calculations which indicates that the η^3-**A** form is slightly more stable than the η^4-**B** form.[7] Thus the variable reactivity of the anions may just reflect the relative amount of the negative charge distributed between the metal center and the η^3-C_7H_7 ring as the metal center is changed. This is supported by the ^{13}C chemical shift trend of the C_7H_7 ring ($\delta_{C_7H_7}$ **1a**, 95.2; **1b**, 92.8; **1c**, 89.0 ppm, all in THF-d_8)[6]. The upfield shifts of the C_7H_7 ring signal of **1c** implies that electron density on the C_7H_7 ring in **1c** is higher than in the other anions. Hence reactions of **1c** may favor ring attacked, trans type products.

In order to further probe this metal-dependent reactivity, and with the hope of producing more trans type products to give further support to the above nucleophilic trend, it was decided to react the anions, $(\eta^3\text{-}C_7H_7)M(CO)_3^-$ (M=Ru **1b**, Os **1c**) with $[M'(CO)_4X]_2$ (M'=Mn, Re). We reasoned that if trans-$(\mu\text{-}C_7H_7)M(CO)_3M'(CO)_4$ (M=Ru, Os; M'=Mn, Re) were formed, they, as opposed to trans-$(\mu\text{-}C_7H_7)Os(CO)_3M''(COD)$ (M"=Rh, Ir), should be more stable because of the 18 electron, closed-shell configuration of both Ru/Os and Mn/Re centers. However, as will be seen, only cis type compounds were obtained from these reactions.

This chapter describes the preparation and spectroscopic characterization of cis-$(\mu\text{-}C_7H_7)M(CO)_3M'(CO)_3$ (M=Ru, Os; M'=Mn, Re) (**2-5**). Comparison with the analogous compounds, cis-$(\mu\text{-}C_7H_7)Fe(CO)_3M'(CO)_3$ (M'=Mn **6**, Re **7**) will be made as well. In addition, in the reaction of $[Ph_4As][(\eta^3\text{-}C_7H_7)Os(CO)_3]$ with $[Re(CO)_4Br]_2$ another minor product, cis-$(\mu\text{-}C_7H_7)Os(CO)_3Re(CO)_4$ (**8**) was detected. The structure of **8** was probed by variable temperature ^1H NMR spectroscopy.

2.2. Results and Discussion.

2.2.1. Reactions of $(\eta^3\text{-}C_7H_7)M(CO)_3^-$ (M=Ru, Os) with $[M'(CO)_4X]_2$ (M'=Mn, Re; X=Cl, Br).

Addition of $K[(\eta^3\text{-}C_7H_7)M(CO)_3]$ (M=Ru **1b**, Os **1c**) to $[Mn(CO)_4Cl]_2$ or $[Re(CO)_4Br]_2$ in THF at low temperature caused immediate disappearance of the dark red color of the anions. Work-up, followed by column chromatography afforded very poor yields (~2%) of the bimetallic compounds **2-5** and a large amount of $(\eta^4\text{-}C_7H_8)M(CO)_3$ (M=Ru, Os) (~70%). Crystallization from hexane solution gave yellow or light yellow crystals **2-5** which are air stable and moderately soluble in common organic solvents. (Equation 2.1)

$$K[(\eta^3\text{-}C_7H_7)M(CO)_3] + 1/2[M'(CO)_4X]_2 \xrightarrow[\text{LT-RT}]{\text{THF}} \underset{\textbf{2-5}}{(\mu\text{-}C_7H_7)MM'(CO)_6} + (\eta^4\text{-}C_7H_8)M(CO)_3 + CO \qquad (2.1)$$

(M=Ru, Os; M'=Mn, Re)

The poor yields of the bimetallic products are similar to that of the previous FeMn/Re reactions (~2%) which were carried out under similar conditions.[1] Interestingly, in the present reactions no by-products of $[(C_7H_7)M(CO)_3]_2$ (M=Ru, Os) were observed, whereas in the FeMn/Re reactions varying amounts of $[(C_7H_7)Fe(CO)_3]_2$ were also obtained.[1] It appears that in the present cases the major competition reaction is protonation of the anions to form $(\eta^4\text{-}C_7H_8)M(CO)_3$, as opposed to redox coupling with formation of $[(C_7H_7)M(CO)_3]_2$ (M=Ru, Os).

As discussed before, due to the ambident nature of anions **1** two possible products could result from reaction 2.1, a trans compound with a $Mn/Re(CO)_4$ moiety or a cis compound with a $Mn/Re(CO)_3$ fragment (Scheme 2.3).

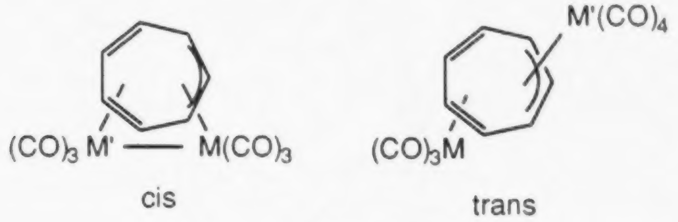

(M=Ru, Os; M'=Mn, Re)

(Scheme 2.3)

Elemental analysis and the mass spectra of compounds **2-5** led to their formulation as $(C_7H_7)MM'(CO)_6$ (M=Ru, Os; M'=Mn, Re). In particular, the mass spectra of **2-5** exhibited parent ions followed by successive loss of six carbonyl ligands. These results suggest the formation of cis compounds.

Further corroboration of cis type products came from the IR spectra of **2-5**. Previous work has shown that for a trans compound, with little interaction between the two metal centers, one would expect the spectrum to be a simple composite of the two individual metal carbonyl groups. For example, the IR spectrum[8] of trans-$(\mu\text{-}\eta^4,\eta^3\text{-}C_7H_7)Fe(CO)_3Mo(CO)_2(\eta^5\text{-}C_5H_5)$ shows five bands at 2040, 1980, 1975, 1950, 1880 cm^{-1}, corresponding to $(\eta^4\text{-}C_7H_8)Fe(CO)_3$ (2050s, 1989s, 1975s cm^{-1})[9] and $(\eta^3\text{-}C_7H_7)Mo(CO)_2(\eta^5\text{-}C_5H_5)$ (1966/1960 and

1911/1896 cm^{-1})[10]. On the other hand, a cis compound, such as cis-(μ-C_7H_7)Fe(CO)$_3$Mn(CO)$_3$ (**6**), gives a multiple band pattern (2052s, 1997s, 1995sh, 1992sh, 1944w and 1939m cm^{-1}) with little resemblance to the original mononuclear compounds.[1] In fact, it is the latter situation that is observed for compounds **2-5**. For instance, the IR spectrum of the RuMn compound **2** displays five bands at 2070s, 2014s, 2001vs, 1988w, 1934s cm^{-1}. The hypsochromic shifts of the first three bands, compared to the FeMn compound, can be considered as the result of replacing the Fe atom by the Ru atom. The positions of the bands are far different from the simple combination of (η^4-C_7H_8)Ru(CO)$_3$ (2066, 2002, 1991 cm^{-1})[11] and (η^3-C_7H_7)Mn(CO)$_4$ (2063, 2001, 1970, 1960 cm^{-1}).[12]

More evidence for the cis type structure was obtained from the ^{1}H and ^{13}C NMR spectra of the products. It is well known[1-3] that the most distinguishing characteristic of a cycloheptatrienyl bridged cis-bimetallic compound is the rapidly whizzing C_7H_7 ring, even at low temperature. Indeed, attempts to obtain the slow-exchange limiting ^{1}H NMR spectrum for cis-(μ-C_7H_7)Fe(CO)$_3$Mn(CO)$_3$ (**6**) failed even at -140°C.[1]

At room temperature both ^{1}H and ^{13}C NMR spectra of **2-5** show a single, time-averaged signal for the C_7H_7 ring (at 3.92 and 64.68 ppm for **2** respectively). These single peaks remain sharp as the temperature is lowered to -70°C, and indicate that ring whizzing in these complexes is very fast. The behavior is similar to other cis-(μ-C_7H_7)MM' compounds.[1]

Another similarity between **2-5** and cis FeMn/Re complexes is the behavior of the CO ligands. At room temperature the ^{13}C NMR spectra displayed two singlets for M(CO)$_3$ (M=Ru, Os) and Re(CO)$_3$ moieties, indicating rapid CO scrambling at the respective metal centers. The tentative assignment of these CO signals are based on the comparison with other similar compounds. The signal for $Mn(CO)_3$ was not observed due to the quadrupolar property of the Mn nucleus.[1] Raising the temperature to 70°C caused no line broadening of the CO signals in the OsRe compound **5**. Thus, no intermetallic CO exchange occurs and the process must be a high energy process.

At this stage we can conclude that reactions 2.1 result only in the formation of cis type compounds. In order to improve the yield, reactions of **1b** and **1c** with $[Mn(CO)_3(CH_3CN)_2Br]$ and $[Re(CO)_3(THF)_2Br]$ were carried out. These reagents should more easily give cis compounds **2-5** without the necessary CO loss from the Mn/Re moieties. This strategy has been used before in the Fe-Mn/Re reactions. Indeed, reactions 2.2 afforded the same cis-products, but in somewhat better yields (see experimental section).

$$K[(\eta^3\text{-}C_7H_7)M(CO)_3] + M'(CO)_3L_2X \xrightarrow[\text{LT-RT}]{\text{THF}} \underset{\textbf{2-5}}{(\mu\text{-}C_7H_7)MM'(CO)_6} + (\eta^4\text{-}C_7H_8)M(CO)_3 \qquad (2.2)$$

(M=Ru, Os; M'=Mn, Re)
(L=CH_3CN, THF)

2.2.2. Reaction of $[Ph_4As][(\eta^3\text{-}C_7H_7)Os(CO)_3]$ with $[Re(CO)_4Br]_2$.

The absence of trans compounds from reactions of the Os anion with Mn/Re electrophiles was not anticipated. Since the Os anion reacted with $[M''(COD)Cl]_2$ (M"=Rh, Ir) to give kinetic trans products, we were expecting similar reactions to occur with the manganese and rhenium electrophiles. Furthermore, the trans compounds containing the $Mn/Re(CO)_4$ moieties should be more stable than the 16 electron OsRh/Ir compounds because of the saturated 18 electron configuration at both Os and Mn/Re centers.

Another unexpected feature of reactions 2.1 was the formation of large amounts of $(\eta^4\text{-}C_7H_8)M(CO)_3$ (M=Ru, Os), which obviously arose from protonation of the anions. A potential proton source was traced to ^{t}BuOH which existed as a result of using KO^{t}Bu to deprotonate the neutral molecules, $(\eta^4\text{-}C_7H_8)M(CO)_3$. In addition to lowering the yield of the products, we were concerned that the presence of ^{t}BuOH might also influence the course of the electrophilic attack. In order to rule out this possibility, an experiment that eliminated any trace of ^{t}BuOH was carried out.

Instead of the potassium salt, a carefully prepared tetraphenylarsonium salt, $[Ph_4As][(\eta^3\text{-}C_7H_7)Os(CO)_3]$ was reacted with $[Re(CO)_4Br]_2$ at -78°C under a CO atmosphere in THF. ^{1}H NMR spectroscopy confirmed that the anion did not contain any residual ^{t}BuOH. The use of CO atmosphere was to prevent CO loss from the product and thereby allow isolation of the trans compound, if formed at all.

In order to avoid possible decomposition and conversion of the initially formed products, the solvent was removed at -70°C. ^{1}H NMR spectroscopy was used to probe the composition of the crude reaction mixture and showed the formation of two major products in a 1:1 ratio. It was also found that there was still a considerable amount of $(\eta^4\text{-}C_7H_8)Os(CO)_3$ formed in this reaction. It is not clear how this protonation occurs. Work-up and crystallization at -78°C from hexane solution failed to afford any solid product. Purification via column chromatography resulted only in separating the by-product, $(\eta^4\text{-}C_7H_8)Os(CO)_3$. Further attempts to separate the two products were not successful due to their very close Rf values although one or the other component could be obtained in very small amount by collecting partial eluates. The overall isolated yield of combined products was very low (<1%).

The IR spectrum of the slower moving component was the same as the previously obtained cis-(μ-C_7H_7)$Os(CO)_3Re(CO)_3$ (**5**). The other component **8** displayed a complex set of IR bands (2084m, 2037s, 2004vs, 1987s, 1970w, 1949s cm^{-1}) and offered no definite structural suggestion although the overall appearance of the band pattern was reminiscent of cis bimetallic compounds (Figure 2.1).

The room temperature ^1H NMR spectrum of the mixture displayed two single peaks, one sharp and one broad, in the C_7H_7 ring region (4.07 and 4.7 ppm) (Figure 2.2). The upfield signal, which only broadens a little even at -60°C, is at the same position as that of cis-(μ-C_7H_7)$Os(CO)_3Re(CO)_3$ (**5**) and further corroborates one of the components as the cis OsRe compound **5**. Interestingly, the downfield signal begins to broaden at 0°C and decoalesces at about -60°C (Figure 2.2). The low temperature (-110°C) spectrum shows seven distinct resonances with relative intensity of one for each peak which indicates asymmetric disposition of the C_7H_7 ring. It was also found that compound **8** is not stable and slowly converts to compound **5** at room temperature.

On the basis of the available IR and NMR data, the stable component in the mixture could be confidently assigned to cis-(μ-C_7H_7)$Os(CO)_3Re(CO)_3$ (**5**). The structure of the other component **8** is more difficult to deduce with certainty. But it is clear that a trans structure is not consistent with the spectroscopic data of **8**. In particular, the low temperature ^1H NMR spectrum shows seven signals for the C_7H_7 ligand whereas for the trans structure, with its C_s symmetry, four signals in the ratio of 2:2:2:1 would be expected.[4,8]

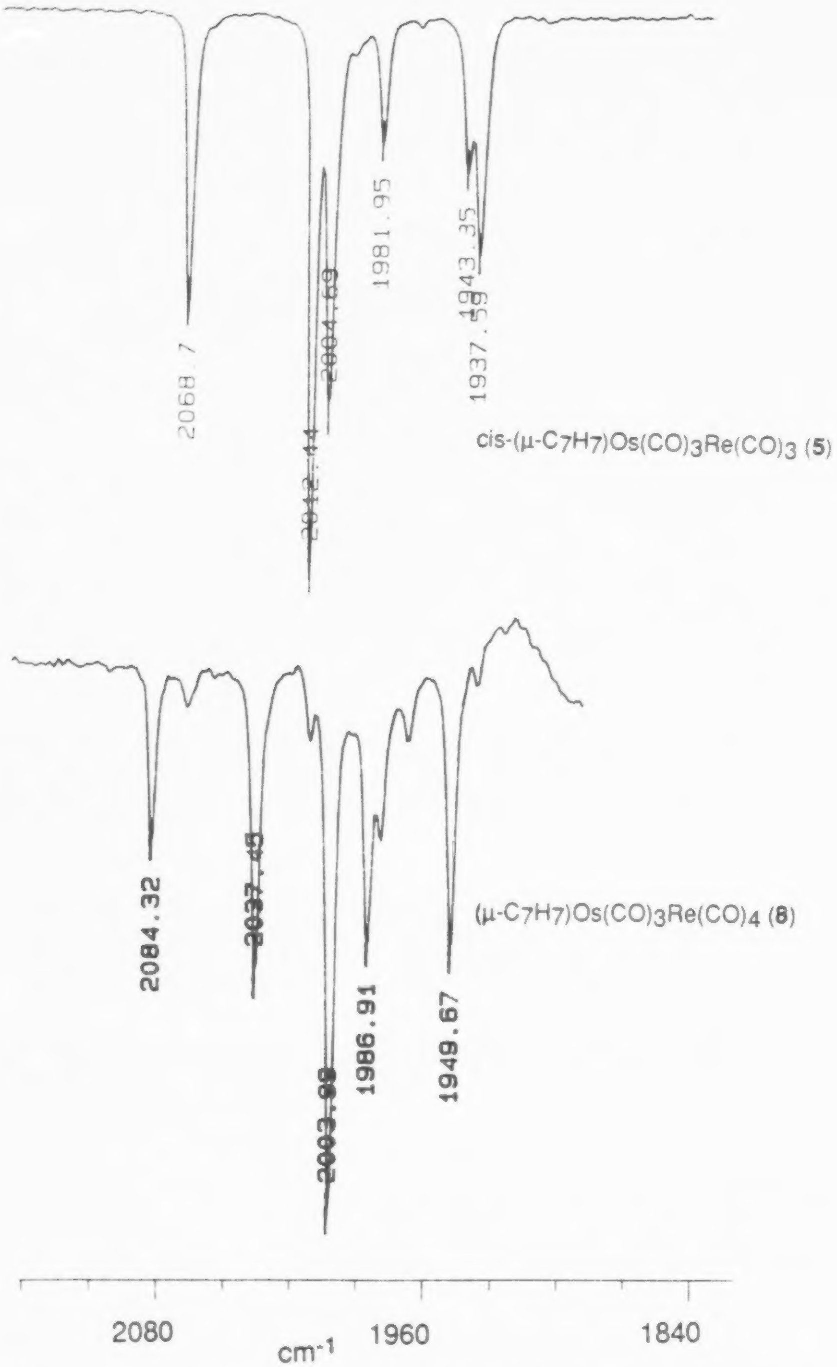

Figure 2.1 IR spectra of cis-(μ-C_7H_7)Os$(CO)_3$Re$(CO)_3$ (**5**) and cis-(μ-C_7H_7)Os$(CO)_3$Re$(CO)_4$ (**8**).

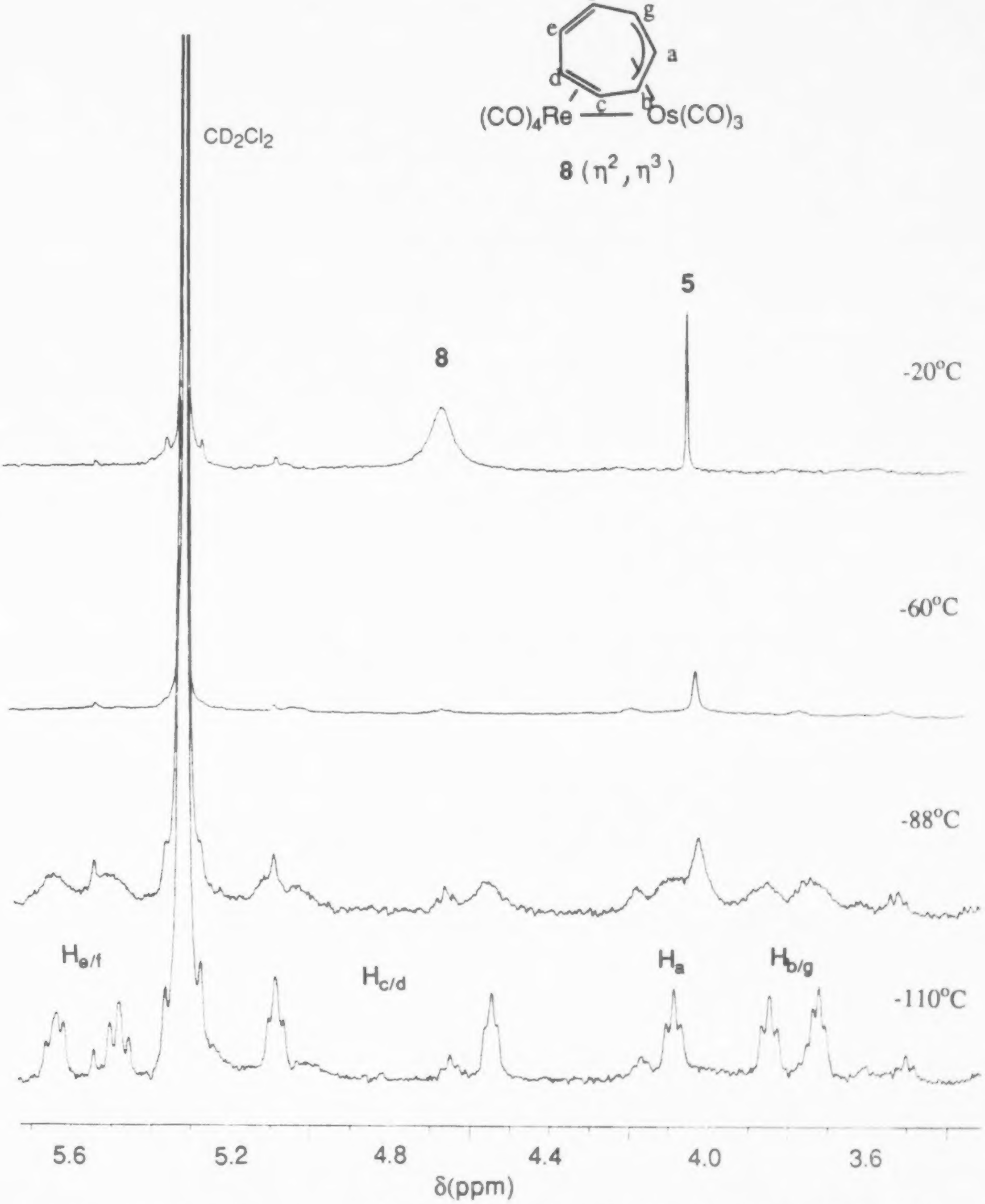

Figure 2.2 Variable temperature ^{1}H NMR spectra (400 MHz) of cis-(μ-C_7H_7)Os$(CO)_3$Re$(CO)_3$ (**5**) and cis-(μ-C_7H_7)Os$(CO)_3$Re$(CO)_4$ (**8**).

On the other hand, the fact that compound **8** slowly converts to **5** implies that the two components **5** and **8** are closely related. On this basis, and to account for the fluxionality and the asymmetric nature of the C_7H_7 ring, the structure of **8** is postulated as cis-(μ–η^3,η^2-C_7H_7)$Os(CO)_3Re(CO)_4$ (Scheme 2.4).

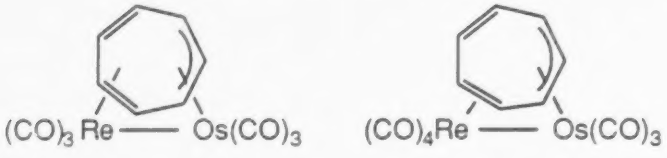

5 (η^4 , η^3)

8 (η^2 , η^3)

(Scheme 2.4)

In this structure, both metal centers are still located on the same face of the bridging C_7H_7 ring and achieve the 18 electron configuration by formation of an Os-Re bond. Because the $Re(CO)_4$ center retains its four CO ligands, the C_7H_7 ring will leave one double bond uncoordinated. Since the compound has a cis configuration it is not surprising that the C_7H_7 ring still rotates very fast. However, the uncoordinated double bond certainly disrupts the π-conjugation in the C_7H_7 ring and renders metal migration a higher energy process. Indeed, as figure 2.2 shows, the decoalescence temperature of **8** (-60°C) is some 50°C higher than that of **5** (ca. -110°C).

It is noteworthy that recently Airoldi et al.[13] reported a compound that contains a μ-C_7H_7 moiety with an identical bonding mode as postulated for **8**. The structure of cis-(μ-η^3,η^2-C_7H_7)$Fe(CO)_3Pd$(η^5-C_5H_5) and the (μ-η^2,η^3) bonding mode of the μ-C_7H_7 ring were confirmed by X-ray crystallography. The ^1H NMR spectrum of the FePd complex and its temperature dependent behavior also resemble that of the complex **8**. Thus at room temperature the

FePd compound shows a singlet for the C_7H_7 ring at 4.72 ppm. As the temperature is lowered the single, sharp signal broadens and reemerges as five signals at -110°C, in a ratio of 1:2:2:1:1.

Although separation of **5** and **8** could not be achieved and hence full characterization of **8** is not at hand, we are confident that the obtained spectroscopic data and the close relationship to the fully characterized complex, cis-(μ-η^3,η^2-C_7H_7)Fe$(CO)_3$Pd(η^5-C_5H_5) are sufficient to establish the structure of **8** as cis-(μ–η^3,η^2-C_7H_7)Os$(CO)_3$Re$(CO)_4$.

2.3. Conclusion.

The reactions of anions (η^3-C_7H_7)M$(CO)_3^-$ (M=Ru **1b**, Os **1c**) with $[M'(CO)_4X]_2$ and $[M'(CO)_3L_2X]$ (M'=Mn, Re) followed the same path as **1a** (M=Fe) and led to the formation of cis-(μ-C_7H_7)M$(CO)_3$M'$(CO)_3$ complexes, regardless of the metal centers. These results provide evidences that the reactivity of the anions (η^3-C_7H_7)M$(CO)_3^-$ (M=Fe **1a**, Ru **1b**, Os **1c**) is controlled by subtle factors and the nature of the electrophiles is also very important in guiding product formation. The observation of cis-(μ–η^3,η^2-C_7H_7)Os$(CO)_3$Re$(CO)_4$ (**8**) and its conversion to the cis-(μ–η^3,η^4-C_7H_7)Os$(CO)_3$Re$(CO)_3$ (**5**) is interesting and allows us to postulate how the initial step in these reactions occurs. The following scenario (Scheme 2.5) seems to be a possible reaction route for the formation of complexes **5** and **8**.

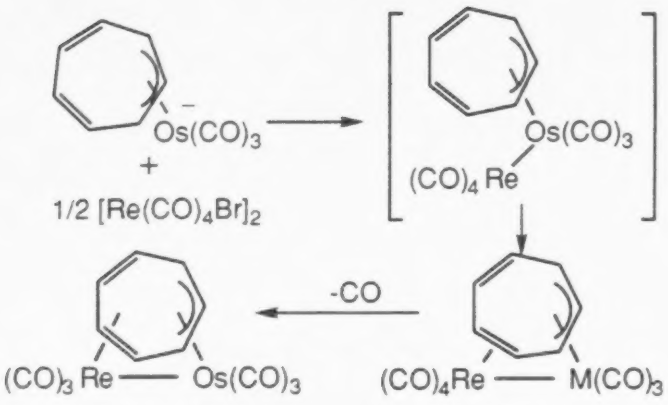

(η^4, η^3- **5**) (η^2, η^3- **8**)

(Scheme 2.5)

2.4. Experimental.

2.4.1. General Techniques and Reagents.

All experimental procedures were performed in standard Schlenk vessels under a static atmosphere of rigorously purified nitrogen or argon. Nitrogen and argon were purified by passage through a heated column (100°C), containing BASF (Cu-based) catalyst R3-11 to remove oxygen and a column of Mallinkrodt Aquasorb (P_2O_5 on an inert base) to remove water. Solvents were dried by refluxing under nitrogen with the appropriate drying agents (Table 2.1) and distilled just prior to use.

Pentane and hexane were preconditioned before refluxing and distillation by washing with H_2SO_4 and water and drying over Na_2SO_4 in order to remove alkenes. All deuterated solvents were dried over molecular sieves except THF-d_8 which was distilled from Na-benzophenone prior to use. Glassware was cleaned by treatment with KOH-ethanol solution and was oven-dried at 120°C.

Table 2.1. Drying agents used in the distillation of solvents

Solvent	Drying Agent
Pentane	CaH_2
Hexane	Potassium metal
Benzene	Potassium metal
Toluene	Sodium metal
THF	Potassium metal/benzophenone
CH_2Cl_2	P_2O_5.

Potassium tertiarybutoxide (KO^tBu) and tetraphenylarsonium chloride (Ph_4AsCl) were purchased from Aldrich. Potassium tertiarybutoxide (KO^tBu) was sublimed prior to use (150°C, 10^{-3} mmHg). Tetraphenylarsonium chloride (Ph_4AsCl) was dried at 180°C under vacuum (1 mmHg) overnight. $[Mn(CO)_3(CH_3CN)_2Br]$,[14] $[Re(CO)_3(THF)_2Br]$,[15] $[Mn(CO)_4Cl]_2$,[16] $[Re(CO)_4X]_2$ (X=Cl, Br),[17] $(\eta^4\text{-}C_7H_8)Ru(CO)_3$[18] and $(C_7H_8)Os(CO)_3$[4] were prepared according to literature methods. Silica gel 60 (230-400 mesh ASTM) was used as received from BDH Chemicals, except for drying by heating overnight at 200°C.

Infrared spectra were obtained with a Nicolet MX-1 or a Bomem MB-100 Fourier Transform interferometers. Mass spectra were taken with an A.E.I. MS-12 spectrometer operating at 16eV or 70eV. NMR spectra were recorded on Bruker WH 200, Bruker WH 360, Bruker AM 400 or Bruker AM 300 spectrometers. Elemental analyses were performed by the Microanalytical Laboratory of this department.

2.4.2. Preparation of cis-(μ-C_7H_7)Ru(CO)$_3$Mn(CO)$_3$ (2).

Method A: K(η^3-C_7H_7)Ru(CO)$_3$ (1.08 mmol) was prepared by the addition of an equimolar quantity of KO^{t}Bu to (η^4-C_7H_8)Ru(CO)$_3$ (300 mg, 1.08 mmol) in THF (20 ml) at -78°C. The cold anion solution was added dropwise via a canula to a slurry of [Mn(CO)$_4$Cl]$_2$ (220 mg, 0.51 mmol) in THF (25 ml) at room temperature. Initially, the dark red color of the anion quickly disappeared. The addition continued for 1.5 hr and resulted in a reddish mixture. The mixture was stirred for 2 hr at room temperature, filtered and the solvent evaporated under vacuum to give a dark reddish oil. The residue was extracted with pentane (2 x 20 ml), concentrated to 2ml and chromatographed on a silica gel column (1 X 10 cm). Elution with pentane produced a large orange band which proved to be (η^4-C_7H_8)Ru(CO)$_3$ (145 mg, 70%). Further elution with pentane-toluene (1:1) gave, after solvent removal, a reddish solid. Washing the residue with pentane (2 ml) gave compound **2** as a yellow-orange solid (10 mg, 2%).

Anal. Calcd. for $C_{13}H_7O_6MnRu$: C, 37.61, H, 1.70. Found: C, 37.39, H, 1.74.

Mass spectrum (16eV, 120°C); M^+ (416), M^+-nCO (n=1-6)

IR (hexane) : υ_{CO} 2070(s), 2014(s), 2001(vs), 1988(w), 1934(s) cm^{-1}.

^{1}H NMR (360 MHz, 22°C, CD_2Cl_2): δ 3.92 (s, 7 H, C_7H_7).

^{13}C {^{1}H} NMR (90 MHz, 24°C, $CDCl_3$): δ 64.68 (s, C_7H_7), 196.27 (s, CO_{Ru}); (-67°C,CD_2Cl_2): δ 64.51 (s, C_7H_7), 196.53 (s, CO_{Ru}), 225.25 (s,CO_{Mn}).

Method B: A cold THF solution of K(η^3-C_7H_7)Ru(CO)$_3$ (2.7 mmol), prepared as above, was added over a period of 3 hr to [Mn(CO)$_3$(CH$_3$CN)$_2$Br] (0.81 g, 2.7 mmol) in THF (60 ml) at room temperature. The solution was stirred for another hour at room temperature. Work-up and chromatographic separation were carried out as above. Crystallization from hexane gave orange crystals of **2** (107mg, 10%).

2.4.3. Preparation of cis-(μ-C_7H_7)Ru(CO)$_3$Re(CO)$_3$ (3).

Method A: K(η^3-C_7H_7)Ru(CO)$_3$ (0.94 mmol) in THF (20 ml) was added dropwise to a slurry of [Re(CO)$_4$Cl]$_2$ (320 mg, 0.48 mmol) in THF (40 ml) and was stirred at room temperature for 2 hr. The resulting orange mixture was filtered to remove a white precipitate (KCl) and the solvent was removed under vacuum. The residue was extracted with hexane (2 x 25 ml). The combined extracts were concentrated to 1 ml and chromatographed on a silica gel column (1x10 cm). Elution with hexane gave (η^4-C_7H_8)Ru(CO)$_3$ (145 mg, 67%). Changing the solvent to benzene eluted a yellow band. Removal of the solvent gave **3** as an orange-red solid (50 mg, 10%).

Anal. Calcd. for $C_{13}H_7O_6ReRu$: C, 28.57, H, 1.29. Found: C, 28.87, H, 1.30

Mass spectrum (16eV, 100°C); M^+ (546), M^+-nCO (n=1-6)

IR (hexane) : υ_{CO} 2069(s), 2012(vs), 1991(w), 1941(s), 1936(s) cm^{-1}.

^1H NMR (360 MHz, 22°C, CD_2Cl_2): δ 4.15 (s,7 H, C_7H_7).

^{13}C {^1H} NMR (90 MHz, 24°C, $CDCl_3$): δ 62.01 (s, C_7H_7), 194.59 (s, CO_{Ru}) 192.70 (s, CO_{Re}) (the tentative assignment of CO ligands is based on the comparison with other Ru or Re compounds); (-70°C,CD_2Cl_2): δ 62.40 (s, C_7H_7), 196.03 (s, CO_{Ru}), 193.38 (s,CO_{Re}).

Method B: A cold THF (20 ml) solution of K(η^3-C_7H_7)Ru(CO)$_3$ (0.97 mmol) was added dropwise to [Re(CO)$_3$(THF)$_2$Br] (405 mg, 0.97 mmol) in THF (20 ml) at room temperature. After addition was complete the white precipitate (KBr) was filtered out and the solvent was removed under vacuum to give a reddish oil. The residue was extracted with benzene (2 x 20 ml) and the combined extracts were concentrated to 1 ml and separated on the silica gel column chromatography (1 x 10 cm). Elution with hexane gave $(\eta^4\text{-}C_7H_8)Ru(CO)_3$ (134 mg, 50%). Changing the solvent to hexane-benzene (1:1) gave an orange-red band. Removal of the solvent gave **3** as an orange-red solid (180 mg, 35%).

2.4.4. Preparation of cis-$(\mu\text{-}C_7H_7)Os(CO)_3Mn(CO)_3$ (4).

Method A: A THF solution of $K(\eta^3\text{-}C_7H_7)Os(CO)_3$ (0.65 mmol) was added dropwise to a cold (-78°C) slurry of $[Mn(CO)_4Cl]_2$ (135 mg, 0.33 mmol) in THF (15 ml). After the addition was completed the solution was allowed to slowly warm up to room temperature. An orange solution with some white precipitate (KCl) was formed. The precipitate was filtered out and the solvent was removed under vacuum to give a reddish oil. The residue was extracted with hexane (2 x 20 ml). The combined extracts were concentrated to 1ml and chromatographed on a silica gel column (1 x 10 cm). Elution with hexane gave $(\eta^4\text{-}C_7H_8)Os(CO)_3$ (190 mg, ~80%). Changing the solvent to hexane-CH_2Cl_2 (3:1) eluted a yellow band. Removal of the solvent and crystallization from hexane afforded yellow crystals of **4** (9 mg,<1%).
Anal. Calcd. for $C_{13}H_7O_6MnOs$: C, 30.96, H, 1.40. Found: C, 33.74, H, 2.41
Mass spectrum (70 eV, 100°C); M^+ (504), M^+-nCO (n=1-6)
IR (hexane) : υ_{CO} 2071(s), 2007(s), 1999(vs), 1983(vw), 1935(s) cm^{-1}.
^1H NMR (360 MHz, 22°C, CD_2Cl_2): δ 3.87 (s,7 H, C_7H_7).
^{13}C $\{^1H\}$ NMR (90 MHz, 22°C,CD_2Cl_2): δ 61.28 (s, C_7H_7), 173.49 (s, CO_{Os})

Method B: $[Ph_4As][(\eta^3\text{-}C_7H_7)Os(CO)_3]$ was prepared as follows. A THF solution of $K(\eta^3\text{-}C_7H_7)Os(CO)_3$ (0.19 mmol) was added dropwise to Ph_4AsCl (92 mg, 0.21 mmol) at room temperature and the slurry was stirred for 15 min. IR spectrum of the solution indicated that the exchange of the cations was complete (the bands of the potassium salt: 1960s, 1884s 1863sh, br cm^{-1} were replaced by those of the tetraphenylarsonium salt: 1961s, 1882s 1863s cm^{-1}, Figure 2.3). The slurry was filtered to give clear red-orange solution. Addition of heptane (15 ml) to the anion solution resulted in the formation of some reddish precipitate. Removal of THF under vacuum gave more precipitate. The solids were filtered, washed with pentane (10 ml) and dried to give a yellow solid of $[Ph_4As][(\eta^3\text{-}C_7H_7)Os(CO)_3]$ (120 mg, 98%).

The solid was redissolved in THF (10 ml) and added to $[Mn(CO)_3(CH_3CN)_2Br]$ (100 mg, 0.19 mmol) in THF (5 ml) at -78°C. After the addition was complete the mixture was kept at -78°C overnight. Then 20 ml of heptane were added to the solution and the THF was removed under vacuum to give a yellow solution and some precipitate. The mixture was filtered and residue was washed with heptane (10 ml). The combined filtrates were concentrated to 5 ml and kept at -78°C to give **4** as a yellow solid (20 mg, 21%). The mother liquor was concentrated to 1 ml and chromatographed on a silica gel column (1 x 10 cm) to afford more solid **4** (10 mg) (over all yield, 31%)

2.4.5. Preparation of cis-(μ-C_7H_7)$Os(CO)_3Re(CO)_3$ (5).

Method A: A cold THF (20 ml) solution of $K[(\eta^3\text{-}C_7H_7)Os(CO)_3]$ (398 mg, 0.58 mmol) was added dropwise to a cold (-78°C) slurry of $[Re(CO)_4Cl]_2$

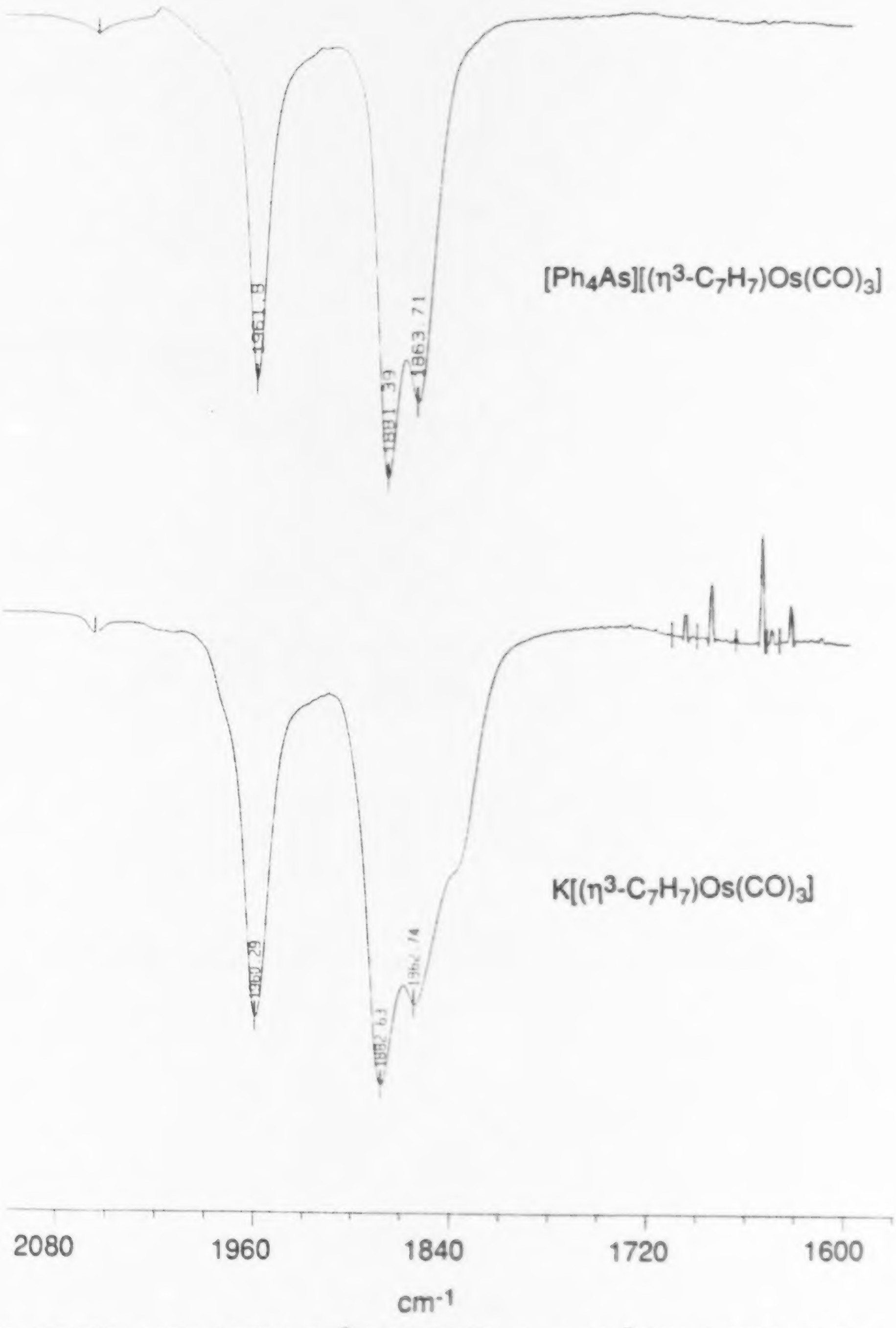

Figure 2.3 IR spectra of $[Ph_4As][(\eta^3\text{-}C_7H_7)Os(CO)_3]$ and $K[(\eta^3\text{-}C_7H_7)Os(CO)_3]$ in THF.

(166 mg, 0.25 mmol) in THF (5 ml). After the addition was completed the solution was allowed to slowly warm up to room temperature. The precipitate (KCl) was filtered out and the solvent was removed under vacuum. The residue was extracted with hexane (2 x 20 ml). The combined extracts were concentrated to 1ml and chromatographed on a silica gel column (1 x 10 cm). Elution with hexane gave $(\eta^4\text{-}C_7H_8)Os(CO)_3$ (167 mg, ~80%). Changing solvent to hexane-CH_2Cl_2 (2:1) eluted a yellow band. Removal of the solvent and crystallization from hexane afforded **5** as a yellow solid (20 mg, 6%).

Anal. Calcd. for $C_{13}H_7O_6ReOs$: C, 24.57, H, 1.11. Found: C, 25.18, H, 1.19

Mass spectrum (16 eV, 190°C); M^+ (636), M^+-nCO (n=1-6)

IR (hexane) : υ_{CO} 2069(s), 2012(vs), 2005(s), 1982(m), 1943(m), 1938(s) cm^{-1}

^1H NMR (360 MHz, 22°C, CD_2Cl_2): δ 4.07 (s,7 H, C_7H_7).

^{13}C $\{^1H\}$ NMR (90 MHz, 20°C,$CDCl_3$): δ 57.69 (s, C_7H_7), 171.57 (s, CO_{Os}), 191.33 (s,CO_{Re}).

Method B: $[Ph_4As][(\eta^3\text{-}C_7H_7)Os(CO)_3]$ (392 mg, 0.52 mmol) in THF (20 ml) and $[Re(CO)_3(THF)_2Br]$ (263 mg, 0.59 mmol) in THF (5 ml) at -78°C afforded **5** after the usual work-up (180mg, 48%)

2.4.6. Reaction of $[Ph_4As][(\eta^3\text{-}C_7H_7)Os(CO)_3]$ with $[Re(CO)_4Br]_2$.

$[Ph_4As][(\eta^3\text{-}C_7H_7)Os(CO)_3]$ (202 mg, 0.28 mmol) in THF (10 ml) was added dropwise to $[Re(CO)_4Br]_2$ (132 mg, 0.175 mmol) in THF (5 ml) at -78°C under a CO atmosphere (1.5 atm). After the addition was complete the original slurry changed to a clear yellow solution. The solution was stirred at -78°C for 1 hour. Then heptane (20 ml) was added. Removal of THF under vacuum at -60°C produced some yellow precipitate. The mixture was filtered and the filtrate was concentrated to 10 ml. The solution was kept at -70°C to effect crystallization. Three days later no solid was formed. At this point flash column chromatography (silica gel, 1 x 10 cm) was carried out. Elution with hexane gave a light yellow band which was confirmed to be $(\eta^3\text{-}C_7H_8)Os(CO)_3$. The solvent was changed from hexane to hexane-CH_2Cl_2 (2:1) and resulted in the development of a yellow band. The IR spectrum and a TLC test of the second band indicated that it contained a mixture of two compounds. Further efforts to separate the mixture failed due to the close Rf values of the two components. After separation was completed the ratio of the components in mixture was 3:1 (**5:8**) based on the ^1H NMR spectrum. No ^{13}C NMR spectral data of **8** is reported due to insufficient sample.

For **8**: IR (hexane) : υ_{CO} 2085(m), 2037(s), 2003(vs), 1987(s), 1970(w), 1949(s) cm^{-1}.

^1H NMR (400 MHz, 20°C, CD_2Cl_2): δ 4.70 (s,7 H, C_7H_7); (-110°C,CD_2Cl_2): δ 5.64 (m, 1H, C_7H_7), 5.48 (m, 1H, C_7H_7), 5.09 (m, 1H, C_7H_7), 4.53 (m, 1H, C_7H_7), 4.09 (m, 1H, C_7H_7), 3.85 (m, 1H, C_7H_7), 3.71 (m, 1H, C_7H_7).

2.5. References.

1. Bennett, M. J.; Pratt, J. L.; Simpson, K. A.; LiShingMan, L. K. K.; Takats, J., *J. Am. Chem. Soc.*, **1976**, *98*, 4810
2. Edelmann, F.; Takats, J., *J. Organomet. Chem.*, **1988**, *344*, 351
3. Astley, S. T.; Takats, J., *J. Organomet. Chem.*, **1989**, *363*, 167
4. Astley, S. T., *Ph. D. Thesis*, University of Alberta, **1990**, Chapter *4*, p. 68
5. Deganello, G., *"Transition Metal Complexes of Cyclic Polyolefins"*, Academic Press, London, **1979**, Chapter *1*, p. 67
6. Astley, S.T.; Takats, J.; Huffman, J. C.; Streib, W. E., *Organometallics*, **1990**, *9*, 184
7. Hofmann, P., *Z. Naturforsch.*, **1978**, *336*, 251
8. Cotton, F. A.; Reich, C. R., *J. Am. Chem. Soc.*, **1969**, *91*, 847
9. Burton, R.; Pratt, L.; Wilkinson, G., *J. Chem. Soc.*, **1961**, 594
10. Faller, J. W., *Inorg. Chem.*, **1969**, *8*, 767
11. Bau, R.; Burt, J. C.; Knox, S. A. R.; Laine, R. M.; Phillips, R. P.; Stone, F. G. A., *J. Chem. Soc. Chem. Commun.*, **1973**, 726
12. Heinekey, D. M., *Ph. D. Thesis*, University of Alberta, **1981**, Chapter *2*, p. 15
13. Airoldi, M.; Deganello, G.; Gennaro, G.; Moret, M.; Sironi, A., *J. Chem. Soc. Chem. Commun.*, **1992**, 850
14. Farona, M. F.; Kraus, K. F., *Inorg. Chem.*, **1970**, *9*, 1700
15. Vitali, D.; Calderazzo, F., *Gazzetta Chimica Italiana*, **1972**, *102*, 587
16. Zingales, F.; Sartorelli, U., *Inorg. Chem.*, **1967**, *6*, 1243
17. Abel, E. W.; Hargreaves, G. B.; Wilkinson, G., *J. Chem. Soc.*, **1958**, 3149
18. Edelmann, F.; Kiel, G. Y.; Takats, J.; Vasudevamurthy, A.; Yeung, M. Y., *J. Chem. Soc. Chem. Commun.*, **1988**, 296

Chapter 3.

Reactions of $(\eta^3\text{-}C_7H_7)M(CO)_3^-$ (M=Fe, Ru) with $[(\eta^3\text{-}C_3H_5)PdCl]_2$: Unexpected Allyl Ligand Transfer between Ru and Pd Complexes.

3.1. Introduction.

One of the major events that stimulated the development of organopalladium chemistry was the discovery of the Wacker process in 1956 (Equation 3.1).[1] In this palladium catalyzed ethylene oxidation process it is believed that the key step involves nucleophilic attack by a hydroxide on an ethylene palladium intermediate.[2] Since then, the application of palladium complexes to mediate a variety of organic transformations has developed very rapidly, and palladium has become one of few transition metals that is effective in almost all the important organometallic reactions such as oxidative addition, reductive elimination, nucleophilic addition, insertion and β-elimination.[3]

$$CH_2{=}CH_2 + \ 1/2\ O_2 \xrightarrow[CuCl_2]{PdCl_2} CH_3CHO \qquad (3.1)$$

Since organopalladium compounds are so reactive, the introduction of a palladium metal into the versatile cycloheptatrienyl ring system should be interesting. It may lead to some unusual reactivities and perhaps even to unique catalytic chemistry. Also, the preparation of bimetallic compounds

(μ-C_7H_7)MPd (M=Fe, Ru, Os) would further extend our previous studies on the reactivity of the anions, (η^3-C_7H_7)M(CO)$_3^-$ (M=Fe **1a**, Ru **1b**, Os **1c**).[4-6]

Such considerations led us to investigate the reactions of (η^3-C_7H_7)M(CO)$_3^-$ (M=Fe **1a**, Ru **1b**, Os **1c**) with an allylpalladium chloride, [(η^3-C_3H_5)PdCl]$_2$. In fact, Salzer et al. has shown that the Fe-Pd complex, cis-(μ-C_7H_7)Fe(CO)$_3$Pd(η^3-C_3H_5) (**2**) can be obtained from this synthetic route.[7] Since the fluxional behavior of **2** was not yet studied it was decided to include complex **2** in our studies as well. The preparation of cis-(μ-C_7H_7)Fe(CO)$_3$Pd(η^3-C_3H_5) (**2**) was carried out as described by Salzer et al. Unexpectedly, the reaction of (η^3-C_7H_7)Ru(CO)$_3^-$ (**1b**) with [(η^3-C_3H_5)PdCl]$_2$ proceeded via an allyl transfer between the palladium and ruthenium complexes and yielded (η^3-C_7H_7)Ru(CO)$_2$(η^3-C_3H_5) (**3**) and (μ-C_7H_7)Ru(CO)$_3$Ru(CO)(η^3-C_3H_5) (**4**). No Ru-Pd product was obtained in this reaction. Compounds **2-4** were characterized by IR and NMR spectroscopies and the structure of **4** was further corroborated by the X-ray crystallographic study. The fluxional behavior of **3** and **4** was investigated by variable temperature ^{1}H NMR spectroscopy.

3.2. Results and Discussion.

3.2.1. Synthesis and Fluxionality of (μ-C_7H_7)Fe(CO)$_3$Pd(η^3-C_3H_5).

The reaction of Na [(η^3-C_7H_7)Fe(CO)$_3$] (**1a**) with [Pd(η^3-C_3H_5)Cl]$_2$ at -10°C gave, after work-up and chromatographic separation, **2** as dark red crystals in 35% isolated yield (Scheme 3.1). Compound **2** is moderately air stable and soluble in most organic solvents. However even under an inert atmosphere in solution, at room temperature, it decomposes to a black solid.

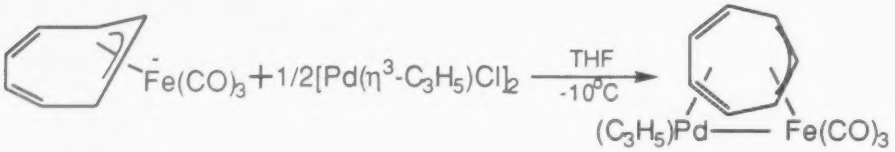

1a

2

(Scheme 3.1)

The spectroscopic data for **2** are in good agreement with the previous report.[7] The IR spectrum shows three terminal CO stretching bands at 2003vs, 1945s, 1934s cm^{-1}. At ambient temperature both ^{1}H and ^{13}C NMR spectra show a single, time-averaged signal for the C_7H_7 ring. The single C_7H_7 resonance remains sharp even at -80°C. It indicates rapid ring whizzing in this molecule. Such a highly fluxional C_7H_7 ring is consistent with the expected cis cycloheptatrienyl bridging structure, cis-(μ-C_7H_7)Fe(CO)$_3$Pd(η^3-C_3H_5) (**2**), because rapid ring whizzing is typical for cis cycloheptatrienyl bridged bimetallic complexes.[4]

At room temperature there are three sets of proton signals for the η^3-allyl group with a ratio of 2:2:1 (Figure 3.1). Based on signal intensity, the multiplet at 5.34 ppm (J=7 Hz, 13 Hz) is assigned to the central proton, H_3 which shows coupling to the other two types of protons. The remaining two doublets are assigned to syn protons, H_2/H_4 (4.67 ppm, J=7 Hz) and anti protons, H_1/H_5 (3.07 ppm, J=13 Hz) on the basis of coupling considerations (smaller coupling for the two syn protons and larger coupling for two anti protons) (Figure 3.1).

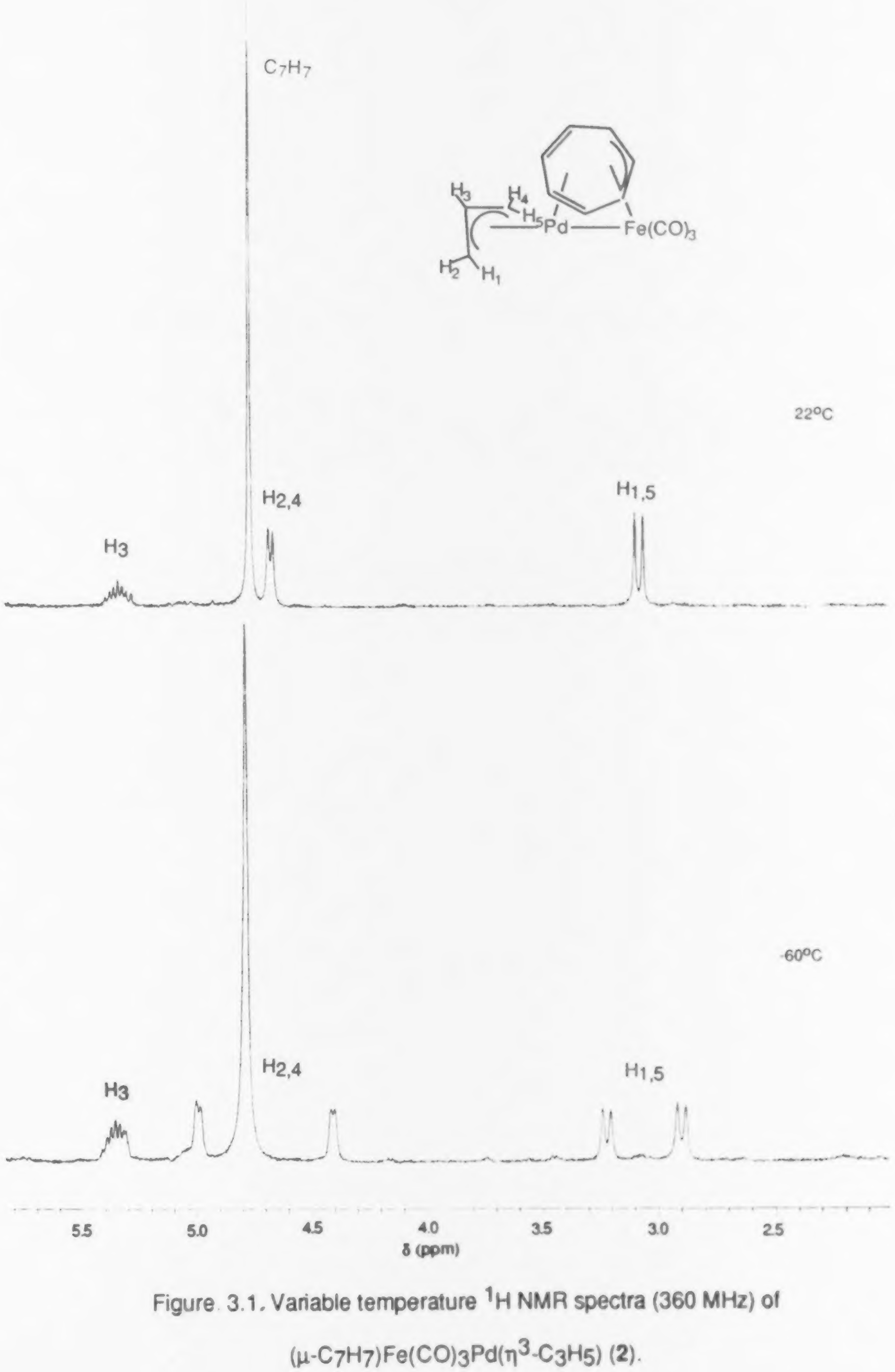

Figure 3.1. Variable temperature ^1H NMR spectra (360 MHz) of

(μ-C_7H_7)$Fe(CO)_3Pd$(η^3-C_3H_5) (**2**).

The simple three-signal pattern of the allyl group undergoes changes as the temperature is lowered. The signals broaden and decoalesce at -30°C. The low temperature limiting ^{1}H NMR spectrum is obtained at -60°C and shows five signals, each corresponding to one proton. At -60°C the central proton, H_3 remains at 5.34 ppm without significant changes, but the signals due to the four terminal protons split into four signals. Based on the coupling constants, the two downfield peaks (5.00 and 4.40 ppm) are assigned to the syn protons, H_2/H_4 and the two upfield signals (3.20 and 2.90 ppm) to the anti protons, H_1/H_5. Clearly, the temperature dependent behavior of these allylic protons indicates that the allyl ligand is fluxional. Also, the observation of five proton signals suggests that in the ground state structure of **2** the allyl group has an asymmetric orientation.

The fluxional allyl group and its asymmetric orientation are confirmed by the variable temperature ^{13}C NMR spectra. At ambient temperature, only two peaks are observed for the allyl ligand, one for the central carbon atom at 113.74 ppm and another for the terminal carbon atoms at 70.51 ppm. At -50°C the latter signal splits into two equal intensity peaks at 70.10 and 71.07 ppm respectively, giving further evidence for the non-equivalence of the two terminal carbon atoms of the allyl ligand at low temperature.

The temperature dependence of the allylic proton resonances can be accounted for by an allyl rotation around the Pd-allyl bond axis. This process exchanges syn-syn (H_1 and H_5) and anti-anti (H_2 and H_4) protons only and results in an AM_2X_2 pattern at the fast exchange limit (Scheme 3.2). Such fluxional motion has been observed in many allyl compounds.[8-12]

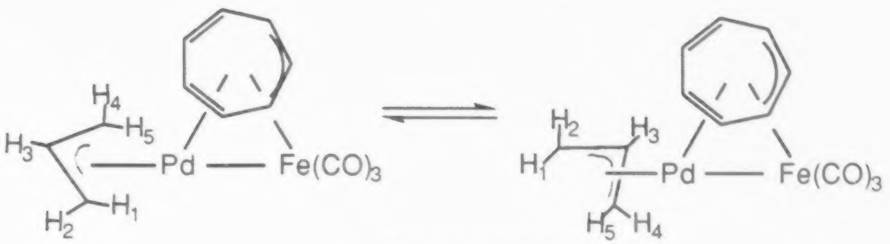
H4
H5
H3
Pd
Fe(CO)3
H2
H1
H2
H3
H1
Pd
Fe(CO)3
H5
H4

(Scheme 3.2)

If the fluxionality of the allyl group proceeded by the other common rearrangement processes, an η^3-η^1-η^3 mechanism (Scheme 3.3),[11] the high temperature limiting ^{1}H NMR spectrum should show an AX_4 peak pattern. This is because the formation of an η^1 intermediate provides a pathway to interchange the syn H_2/H_4 with the anti H_1/H_5 protons. Consequently all four peaks due to the terminal protons would coalesce into a single peak at high temperature, if the exchange rate is faster than the NMR time scale. Obviously, this is not the case for complex **2**.

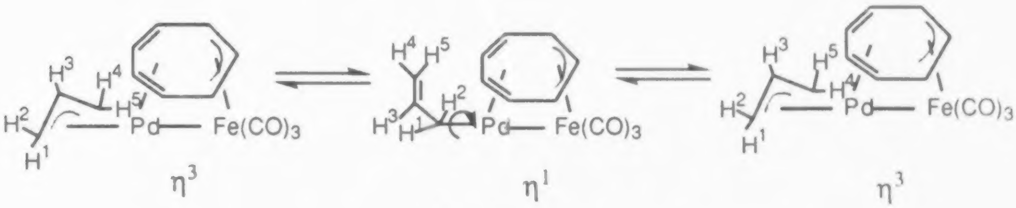
H3
H4
H5
H2
H1
Pd
Fe(CO)3
η3
H4
H5
H2
H3
H1
Pd
Fe(CO)3
η1
H3
H5
H4
H2
H1
Pd
Fe(CO)3
η3

(Scheme 3.3)

In conclusion, the product **2** has a cis-C_7H_7 ring bridged structure. At room temperature both C_7H_7 ring and C_3H_5 ligands are fluxional. But at low temperature (-60°C) the dynamic motion of the allyl group can be stopped and reveals an asymmetrically oriented allyl ligand.

3.2.2. Reaction of $(\eta^3\text{-}C_7H_7)Ru(CO)_3^-$ with $[(\eta^3\text{-}C_3H_5)PdCl]_2$.

The reaction of $(\eta^3\text{-}C_7H_7)Ru(CO)_3^-$ (**1b**) with $[(\eta^3\text{-}C_3H_5)PdCl]_2$ was carried out at -78°C. The work-up, followed by chromatographic separation, gave two products, a red oil **3** and a yellow solid **4**. The red oil **3** is very volatile. At room temperature it can be easily sublimed to a dry ice cooled probe under vacuum (1 mm Hg). The compound is very soluble in hydrocarbon solvents and crystallization can only be achieved in butane at -78°C, the resultant red crystals melt at around 15°C. The other product **4** is an air stable yellow solid which is also soluble in most hydrocarbon solvents. Crystallization of **4** from hexane solution at -20°C gave X-ray quality single crystals.

Surprisingly, elemental analysis and mass spectra of these new compounds revealed that neither of them contained a palladium atom. The mass spectrum of **3**, with a parent ion at m/e=290 followed by successive loss of two CO groups, showed that it contained only one ruthenium atom. From its elemental analysis **3** was formulated as $(C_7H_7)Ru(CO)_2(C_3H_5)$. The mass spectrum of **4** showed a parent ion at m/e=447, followed by successive loss of four CO ligands. The isotope pattern (Figure 3.2) indicated the presence of two ruthenium atoms in this molecule. On the basis of the mass spectrum and elemental analysis, product **4** was formulated as $(C_7H_7)Ru_2(CO)_4(C_3H_5)$. Thus, contrary to what was observed in the reaction of **1a**, the reaction of $(\eta^3\text{-}C_7H_7)Ru(CO)_3^-$ (**1b**) with $[(\eta^3\text{-}C_3H_5)PdCl]_2$ proceeded via an allyl group transfer (Equation. 3.2).

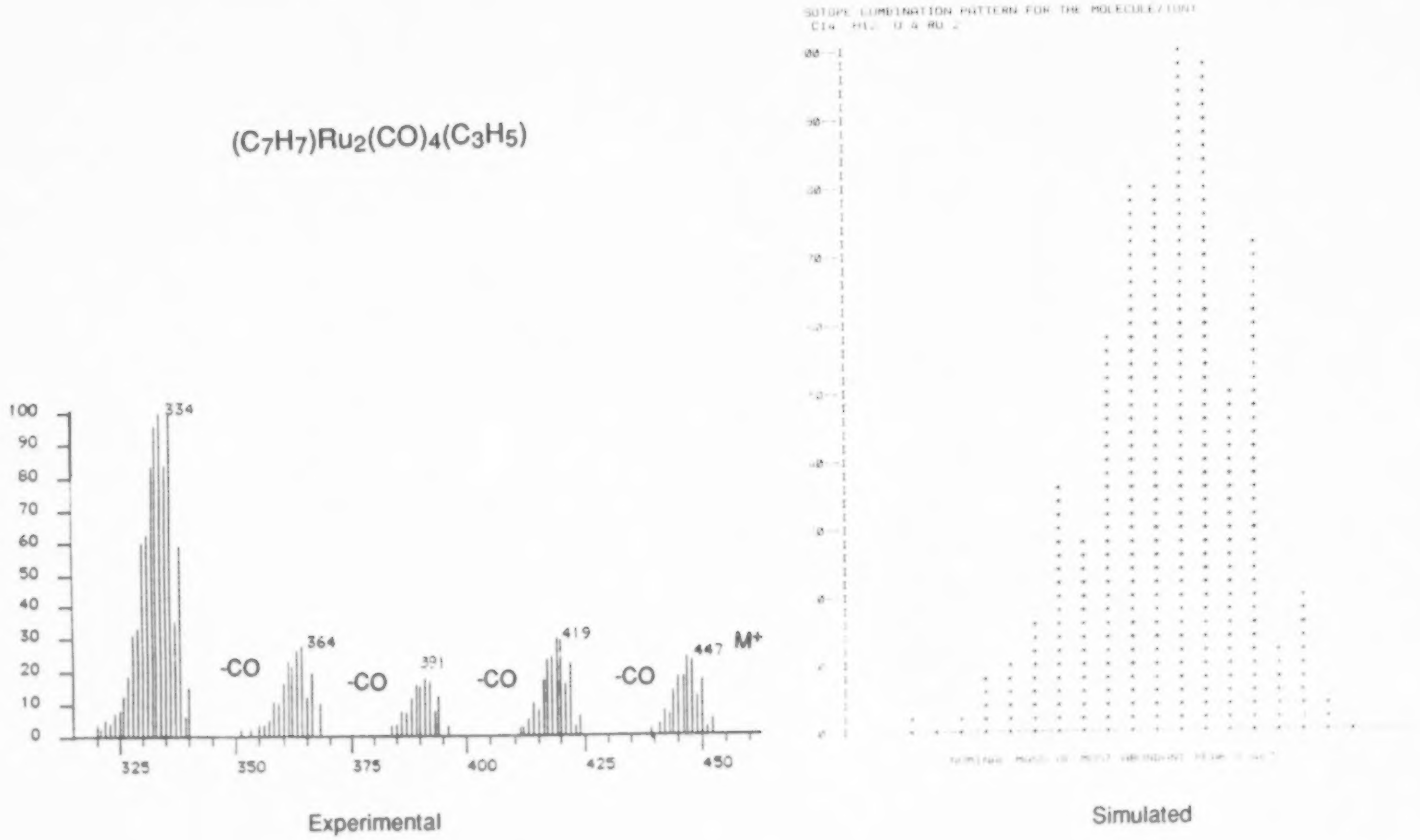

Figure 3.2 Experimental and simulated mass spectra of $(C_7H_7)Ru_2(CO)_5(C_3H_5)$ (**4**).

$$K[(\eta^3\text{-}C_7H_7)Ru(CO)_3] + 1/2\,[Pd(\eta^3\text{-}C_3H_5)Cl]_2 \xrightarrow[-78^oC]{THF} \qquad (3.2)$$

$$(C_7H_7)Ru(CO)_2(C_3H_5) + (C_7H_7)Ru_2(CO)_5(C_3H_5) + Pd + \cdots$$

3.2.2.1 Characterization of $(\eta^3\text{-}C_7H_7)Ru(CO)_2(\eta^3\text{-}C_3H_5)$.

The IR spectrum of **3** shows four terminal CO stretching bands at 2026vs, 2017s, 1975vs and 1966sh cm^{-1}. Based on the above formula, $(C_7H_7)Ru(CO)_2(C_3H_5)$, the very likely explanation for this observation is the presence of two isomeric compounds **3a** and **3b** in solution. The formulation and IR spectrum bring to mind the related ruthenium compound, $(\eta^3\text{-}C_3H_5)_2Ru(CO)_2$, which shows two terminal CO bands at 2024vs, 1971s cm^{-1}.[13] The latter compound has an octahedral geometry with two cis carbonyl ligands. Due to the similarity of the IR spectra it seems clear that **3** has the same structure as $(\eta^3\text{-}C_3H_5)_2Ru(CO)_2$, except that in solution **3** exists as two isomers, the major isomer **3a** shows two bands at 2026vs and 1975vs cm^{-1} and the minor isomer **3b** at 2017s and 1966sh cm^{-1}.

The ^1H NMR spectrum of **3** corroborates the existence of two isomers. At ambient temperature two signals due to the C_7H_7 ring are observed, one broad peak at 4.82 ppm and one sharp resonance at 4.91 ppm with an intensity ratio of roughly 3:1 (Figure 3.3). Therefore, the former is assigned to **3a** and the latter to **3b**. The different width of the two peaks indicates that the fluxionality of the C_7H_7 ring in the two isomers is different. This is confirmed by the variable temperature ^1H NMR spectra of **3** (Figure. 3.3). At -60°C the original single peak due to the C_7H_7 ring of **3a** is replaced by six new peaks, corresponding to seven protons. When the temperature is further decreased to -87°C, six other peaks for the C_7H_7 ring of **3b** are observed as well. The spectra clearly indicate an asymmetric C_7H_7 ring in the ground state structure of **3a** and **3b**.

As expected, the ^1H NMR spectrum also shows two sets of resonances for the allyl protons. Interestingly, the dynamic behavior of the allyl groups are also different for the two isomers. The major isomer **3a** exhibits five broad signals at room temperature which, by -10°C show well resolved coupling patterns. Only two broad peaks at 4.85 and 3.20 ppm in a ratio of 1:2, can be identified at room temperature for the minor isomer **3b**. The peak at 4.85 ppm belongs to the central H_3 and that at 3.20 ppm to two terminal allyl protons, respectively.

That the deceptive ^1H NMR features of the allyl group are due to some rearrangement processes becomes apparent in the -60°C spectrum. Just as for **3a**, the spectrum reveals five one-proton peaks for the allyl moiety of **3b**. On the basis of coupling constants consideration, the resonances at 3.32 and 2.52 ppm are assigned the syn-H_2/H_4 protons and those at 3.08 and 0.35 ppm to the anti-H_1/H_5 protons, respectively. As a result of the large chemical shift separation between the two anti-protons the rate of chemical exchange has only succeeded in coalescing these signals into the base line at room temperature, whereas the signals due to the syn-protons have already emerged as a single averaged peak at 3.20 ppm. Clearly the rearrangement process causing syn-syn and anti-anti exchange is faster in **3b** than in **3a**. Interestingly, the fluxional behavior of the η^3-C_7H_7 ring follows the same trend.

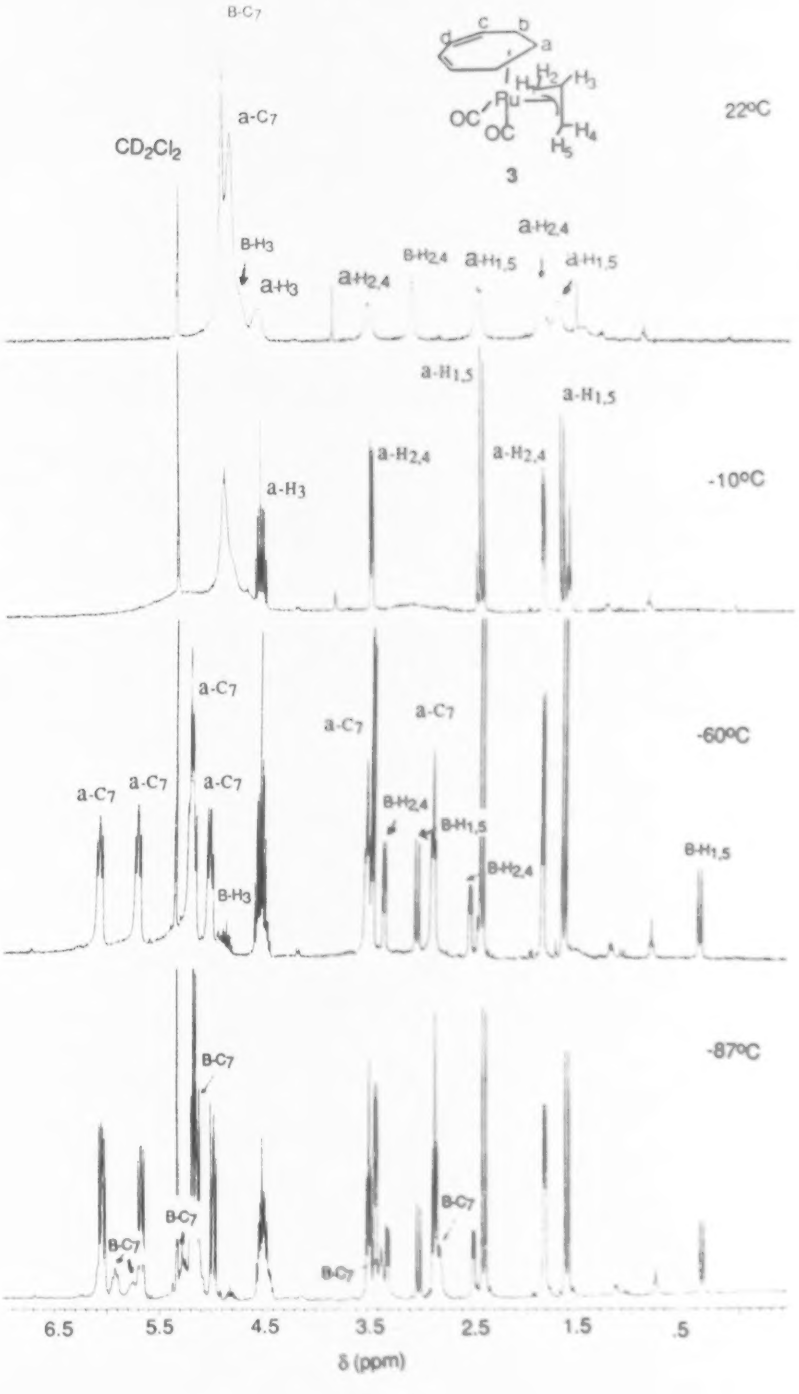

Figure 3.3 Variable temperature ^{1}H NMR spectra (360 MHz) of $(\eta^3\text{-}C_7H_7)Ru(CO)_2(\eta^3\text{-}C_3H_5)$ (**3**).

Thus, at this point, on the basis of the obtained spectroscopic data, we can conclude that compound **3** is $(\eta^3\text{-}C_7H_7)Ru(CO)_2(\eta^3\text{-}C_3H_5)$. In solution it exists as two isomers **3a** and **3b**, both conforming to a cis-octahedral type structure, and both are fluxional, but the rates of rearrangement are different in the isomers.

Any attempt to get a clear picture about the structures of **3a** and **3b** and perhaps to uncover the reasons for the different dynamic behaviors of the two isomers must consider the number of possible isomers for compound **3** and also the possible interconversion pathways. In scheme 3.4 the four isomeric structures of compound **3** are shown. Each of them has cis-octahedral geometry.

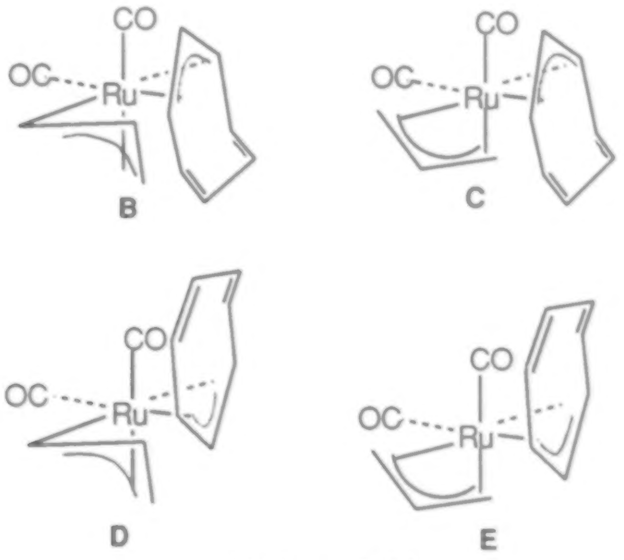

(Scheme 3.4)

The relationship between these structures can be related to the rotation of the cycloheptatrienyl ring or the allyl moieties. Thus pair **B**/**C** and **D**/**E** are related by allyl group rotation, whereas pair **B**/**D** and **C**/**E** by C_7H_7

ring rotation about Ru-C_7 ring bond axis. It is noted that at any time, whether the C_7H_7 ring is static or fluxional, each isomer is asymmetric and should give seven signals for the C_7H_7 and five resonances for the C_3H_5 moieties in the ^1H NMR spectrum. Allyl group rotation, for instance, would only interconvert **B** and **C** or **D** and **E**, but will not result in syn-syn and anti-anti exchange of the allyl protons within one isomer. Therefore simple allyl rotation is not compatible with the ^1H NMR behavior of isomer **3b**.

In order to account for the observation of averaging syn-syn or anti-anti proton peaks in **3b** a fluxional process must exchange the two ends of the asymmetric allyl moiety and yield a time-averaged mirror plane in the molecule. The actual result of this process is racemization of **3b**. Based on this consideration, only a twist process such as the classic Bailar or Ray-Dutt twists for six-coordinate octahedral complexes can meet this requirement. These twist processes for isomers **B** and **D** are illustrated in scheme 3.5. The scheme clearly shows that both processes go through a symmetric, trigonal prismatic intermediate where the presence of a mirror plane renders the two halves of the allyl and C_7H_7 groups equivalent and consequently exchanges the two ends of the allyl group From scheme 3.5 it also appears that the intermediate of the isomer **B** in the Bailar twist process (and for **C** as well) suffers from severe steric congestion between the allyl and C_7H_7 groups, the situation seems to be more favorable for the isomeric pair **D**/**E**. Consequently, the syn-syn and anti-anti exchanges of the allyl protons are more rapid in latter. On this basis we tentatively propose that the minor isomer **3b** has the structure **D** or **E** and the major isomer **3a** has the structure **B** or **C**. It would be tempting to further pursue the actual structures of **3a** and **3b**, but at this stage the conclusion would be speculative at best.

We wish to conclude this section by pointing out that similar twist exchange processes of allyl groups have also been observed in the related $Ru(CO)_2(\eta^3\text{-}C_3H_5)_2$ complex.[25] Finally it is also important to indicate that the fluxional motion of the C_7H_7 ring is distinct from the racemization processes discussed above. The fluxional motion averages the environment of the C_7H_7 ring protons in each individual isomer but does not require any other process to accompany this motion.

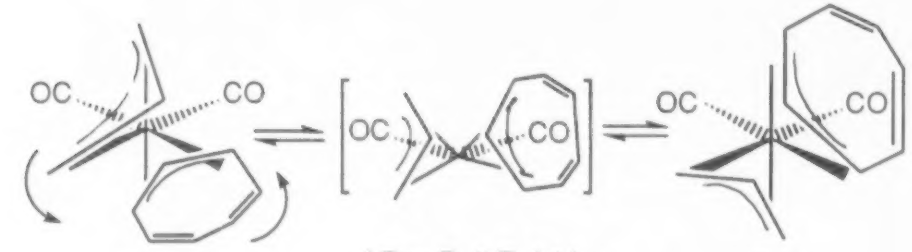

D-Λ (Ray-Dutt Twist) **D-Δ**

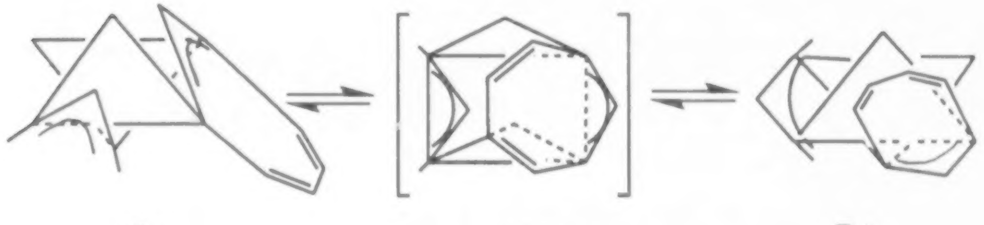

B-Λ (Bailar Twist) **B-Δ**

(Scheme 3.5)

3.2.2.2. Characterization of cis-(μ-C_7H_7)$Ru(CO)_3Ru(CO)(\eta^3\text{-}C_3H_5)$.

At ambient temperature the ^1H NMR spectrum of **4** shows a sharp single peak at 3.84 ppm for the fluxional C_7H_7 ring protons (Figure 3.4). The allyl protons are observed as three peaks in an intensity ratio of 1:2:2. Based

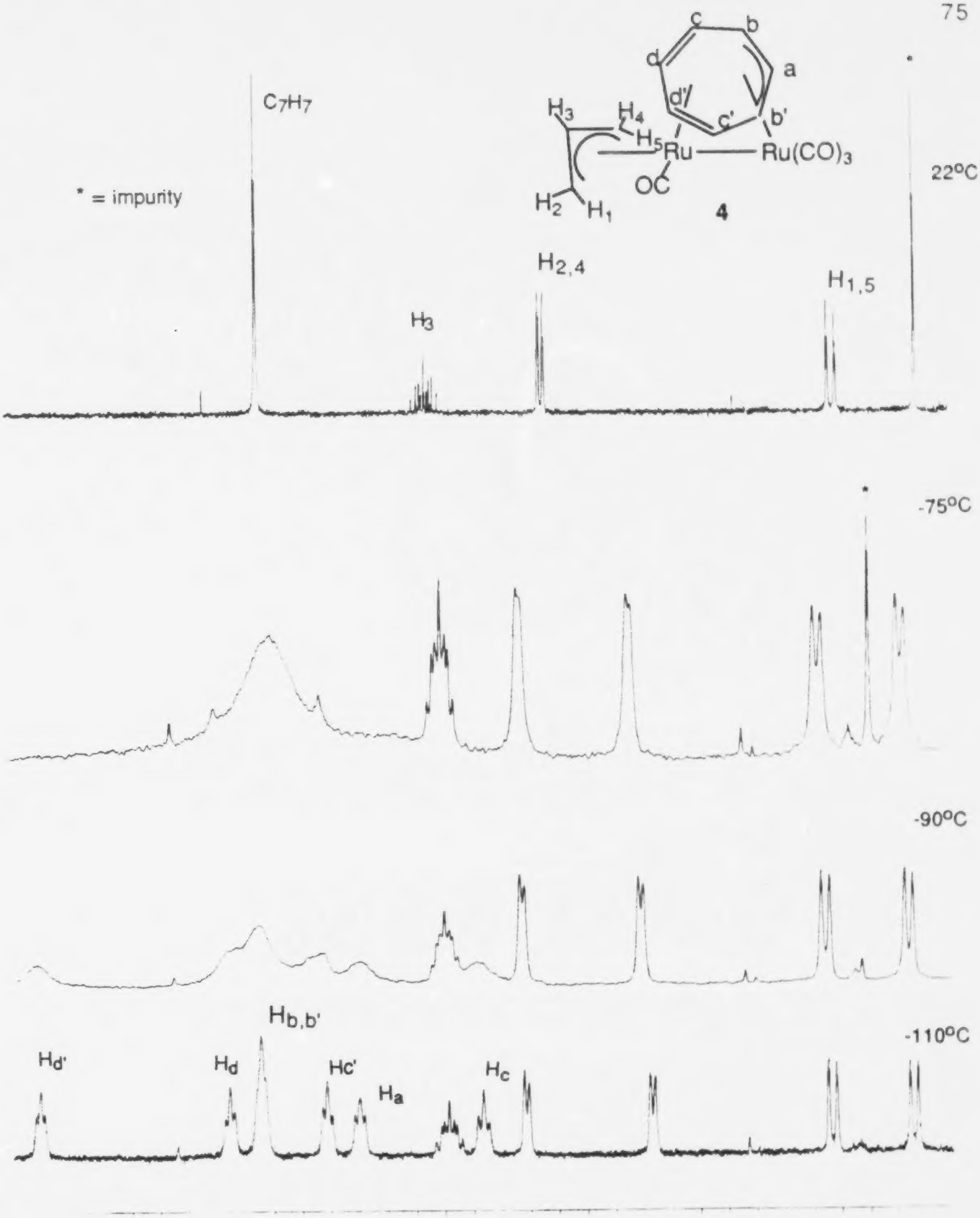

Figure 3.4 Variable temperature ^1H NMR spectra (400 MHz) of $(\mu\text{-}C_7H_7)Ru(CO)_3Ru(CO)(\eta^3\text{-}C_3H_5)$ (**4**) in CD_2Cl_2.

on the intensity and coupling constants it is not difficult to assign the multiplet at 3.26 ppm to the central proton H_3, the doublet at 2.82 ppm (J=6.8 Hz) to the syn protons $H_{2,4}$ and the other doublet at 1.80 ppm (J=11 Hz) to the anti protons $H_{1,5}$.

As the temperature is lowered both the C_7H_7 ring and allyl group resonances undergo line shape changes. By -30°C the allyl signals collapse and at -60°C five well separated signals representing five different allyl protons are seen. The allyl lines continue to sharpen down to -110°C. Allyl group fluxionality was observed in the Fe-Pd complex **2** and therefore the fluxional behavior of the allyl group here is not unexpected. But the process here is different from that of the Fe-Pd compound. It will be discussed in detail later. More interesting is the temperature dependent behavior of the C_7H_7 signal. At -75°C the peak broadens and by -110°C six signals corresponding to the seven different C_7H_7 protons are seen. The assignments appearing on the figure are based on homonuclear decoupling experiments.

The highly fluxional C_7H_7 ring suggests that two metal centers in **4** may be bridged by a C_7H_7 ring in a cis configuration. If this is the case, the stoppage of the fluxional motion is interesting and **4** joins the few, but growing number of cis-(μ-C_7H_7)MM' complexes where ring rotation has been stopped. For example, in cis-(μ-C_7H_7)Ru$(CO)_3$Ir(COD) the low temperature limiting spectrum was reached at -115°C.[14] The low temperature ^1H NMR spectrum clearly shows that the structure of **4** is asymmetric, the environment of the C_7H_7 and C_3H_5 protons are all different.

Also, the ^{13}C NMR spectrum indicates that there are two types of carbonyl ligands in the molecule (198 and 208 ppm). The intensity ratio tentatively suggests that three carbonyls are bonded to one ruthenium and one to the other.

In order to provide unambiguous proof of the structure, to corroborate the disposition of the CO ligands and to deduce the orientation of the allyl ligand, a single crystal X-ray analysis on complex **4** was carried out. A perspective view of the complex **4** shows the cis arrangement of the two Ru centers with respect to the seven membered ring (Figure 3.5). The Ru1 atom is bonded to three carbonyl ligands and to the allylic part (C11, C12, C13) of the C_7 ring. The Ru2 atom is bonded to one carbonyl group, to the η^3-allyl ligand and to the remaining diene part (C14, C15, C16, C17) of the C_7 ring. Both metal centers satisfy the 18 electron rule by formation of a Ru-Ru bond.

The Ru-Ru bond length of 2.8859 (8) Å (Table 3.1) is close to those previously found in complexes containing such bonds $(\mu\text{-}C_8H_8)Ru(CO)_3Ru(CO)_3$, 2.865 Å[15]; $Ru_3(CO)_{12}$, 2.85 Å[16] and $(\mu\text{-}C_8H_8)_2Ru_3(CO)_4$, 2.89 Å[16]. The bond distances of the ruthenium allyl fragment (Ru-C6 2.17 Å, Ru-C7 2.27 Å, Ru-C5 2.24 Å, C5-C6 1.39 Å) are also similar to other Ru-allyl compounds,[19] for instance $(\eta^5\text{-}C_5Me_5)Ru(\eta^3\text{-}C_3H_5)Br_2$, (Ru-$C_c$ 2.175 Å, Ru-C_t 2.164 Å, C_t-C_c 1.439 Å).[19] The bond distances of Ru2 to the diene part of the C_7H_7 ring (Ru2-C14 2.235, Ru2-C15 2.165, Ru2-C16 2.213, Ru2-C17 2.349 Å) are also in the range observed in the related compound $(C_8H_8)_2Ru_3(CO)_4$ (2.37-2.14 Å).[17] As in other bimetallic cis-$(\mu\text{-}C_7H_7)MM'$ complexes the allyl and diene parts of the bridging seven membered ring bend away from the rest of the molecule, resulting in a boat conformation of the C_7 ring. The angle between the two planes (diene plane and allyl plane) is 120°, which is slightly smaller than 124° found in the complex $(\mu\text{-}C_7H_7)Fe(CO)_3Rh(CO)_2$.[4a]

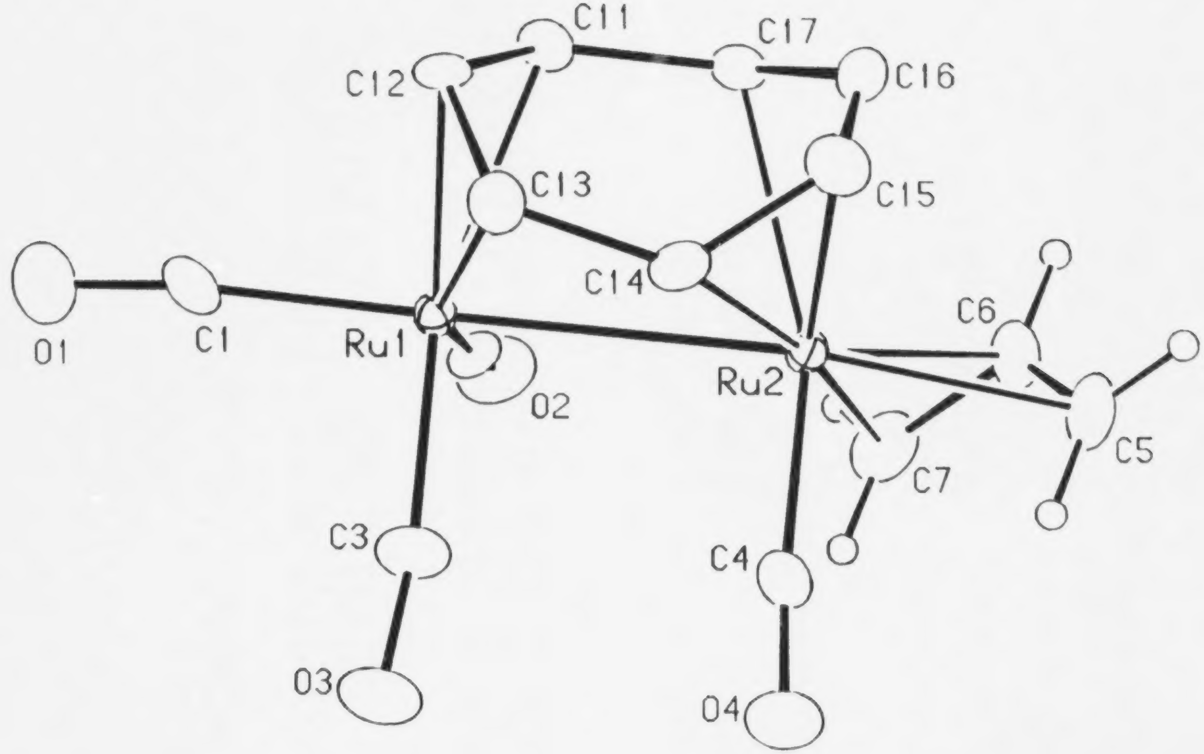
C11
C17
C12
C16
C13
C15
C14
O1
C1
Ru1
C6
Ru2
O2
C5
C7
C3
C4
O3
O4

Figure 3.5 ORTEP diagram of $(\mu\text{-}C_7H_7)Ru(CO)_3Ru(CO)(\eta^3\text{-}C_3H_5)$ (**4**).

Table 3.1 Selected bond distances of (μ-C_7H_7)Ru(CO)$_3$Ru(CO)(η^3-C_3H_5) (**4**).[a]

Atom1	Atom2	Distance (Å)	Atom1	Atom2	Distance (Å)
Ru1	Ru2	2.8859 (8)	Ru2	C17	2.349 (6)
Ru1	C1	1.896 (8)	O1	C1	1.149 (9)
Ru1	C2	1.934 (7)	O2	C2	1.139 (8)
Ru1	C3	1.916 (7)	O3	C3	1.165 (8)
Ru1	C11	2.248 (6)	O4	C4	1.131 (9)
Ru1	C12	2.204 (6)	C5	C6	1.39 (1)
Ru1	C13	2.295 (6)	C6	C7	1.39 (1)
Ru2	C4	1.870 (8)	C11	C12	1.434 (9)
Ru2	C5	2.233 (7)	C11	C17	1.496 (9)
Ru2	C6	2.162 (7)	C12	C13	1.413 (9)
Ru2	C7	2.285 (7)	C13	C14	1.481 (9)
Ru2	C14	2.235 (6)	C14	C15	1.45 (1)
Ru2	C15	2.165 (7)	C15	C16	1.39 (1)
Ru2	C16	2.213 (6)	C16	C17	1.43 (1)

[a] Numbers in parentheses are estimated standard deviations in the least significant digit.

The bond distances of 1.49 (2) Å and 1.48 (2) Å, which are associated with the bonds linking the allyl and diene parts (C11-C17 and C13-C14), are slightly longer than the corresponding value (1.45 Å) found in (μ-C_7H_7)Fe(CO)$_3$Rh(CO)$_2$. These distances are also close to those observed in the complex trans-(η^3-C_5H_5)Mo(CO)$_2$(μ-C_7H_7)Fe(CO)$_3$ (1.50 and 1.49 Å), which has the trans arrangement of the two metals.[18] Both the longer distances separating the two planes and the smaller angle between the two planes indicate that the disruption of π electron delocalization in the C_7H_7 ring is more significant in **4** than in (μ-C_7H_7)$Fe(CO)_3Rh(CO)_2$. This, coupled with the stronger bonding between the metals and the bridging C_7H_7 ring in **4** lead to a higher barrier for metal migration in the latter complex. The NMR behavior of **4** reflects these structural features, the ^1H NMR coalescence temperature of **4** is -80°C, whereas that of FeRh is below -160°C.

Finally, from the ORTEP drawing (Figure 3.5), it is clear that the allyl group is not symmetrically oriented with respect to the C_7H_7 ring. The asymmetrical disposition of the ligand is seen as a consequence of the roughly octahedral geometry of the Ru2 center. The four equatorial positions are occupied by the diene fragment, a carbonyl group and the terminal C7 of the allyl ligand. One axial position is taken up by the C5-C6 bond of the allyl group and the metal-metal bond to Ru1. We should note that the coordination geometry of Ru1 is also octahedral. The allyl part of the ring and two carbonyl ligands occupy the four equatorial positions while another carbonyl group and the metal-metal bond complete the six-coordinate environment of Ru1.

Based on the solid structure of compound **4**, rotation of the allyl group around the Ru-allyl bond axis does not account for the observed changes in the allyl peak pattern over the different temperatures. In such an asymmetrical structure the allyl group should always give rise to five protons signals even at high rotation speed. The fact that only three peaks are observed for the allyl group indicates another type of dynamic process is ocurring. It involves syn-syn or anti-anti proton exchange of the allyl group. A process that could explain this result involves in a fast forward and backward motion of the allyl group with respect to the metal-metal bond. This process produces a time averaged mirror plane in the molecule. Therefore, at the fast exchange limiting an AM_2X_2 pattern is observed for the allyl proton peaks.

3.2.3. Possible Reaction Route of Forming Allyl Transfer Products.

Although we did not attempt to use allylpalladium chloride as an allylating reagent, allyl transfer from Pd has been known for a long time. The first allyl transfer reaction was discovered by two groups.[20,21] They found that reaction of $Fe_2(CO)_9$ with $[(\eta^3\text{-}C_3H_5)PdCl]_2$ resulted in $(\eta^3\text{-}C_3H_5)Fe(CO)_3Cl$. Later, an elegant π-allyl transfer from palladium to cobalt and *vice versa* was reported by Heck.[22] Reaction of $[(\eta^3\text{-}C_3H_5)PdCl]_2$ with sodium tetracarbonylcobaltate in ether solution at ambient temperature afforded the η^3-allylcobalt tricarbonyl complex. The proposed mechanism suggested a series of binuclear intermediates containing a palladium-cobalt bond. The key transfer process involved a cis migration and a 1,2-shift of the allyl group from Pd to Co (Scheme 3.6).[23]

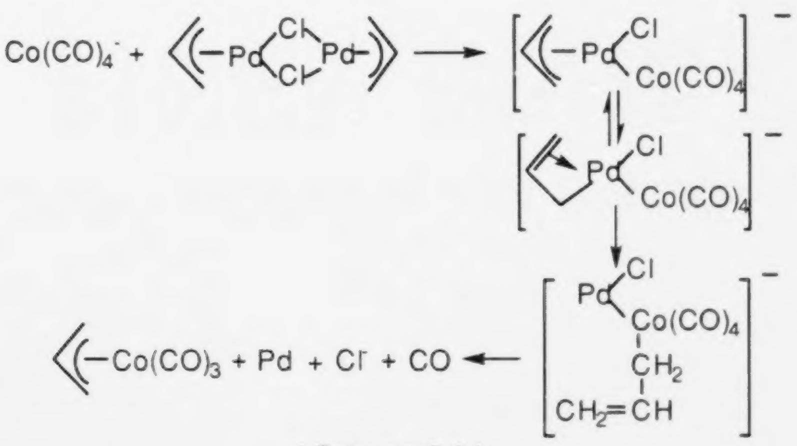

(Scheme 3.6)

On the basis of the above mechanism the transfer process for the reaction of $(\eta^3\text{-}C_7H_7)Ru(CO)_3^-$ with $[(\eta^3\text{-}C_3H_5)PdCl]_2$ could proceed according to scheme 3.7. The first step is ruthenium attack to form the Ru-Pd bimetallic intermediate. This intermediate, by a series of CO elimination accompanied by appropriate hapticity changes of the C_7H_7 ligand, provides a pathway for allyl group transfer from Pd to Ru and gives product **3** and compound **5**. The latter is evidently not stable and further reacts with a $Ru(CO)_3$ unit, which could come from the decomposition of $(\eta^4\text{-}C_7H_8)Ru(CO)_3$ also produced in the reaction, to yield product **4**.

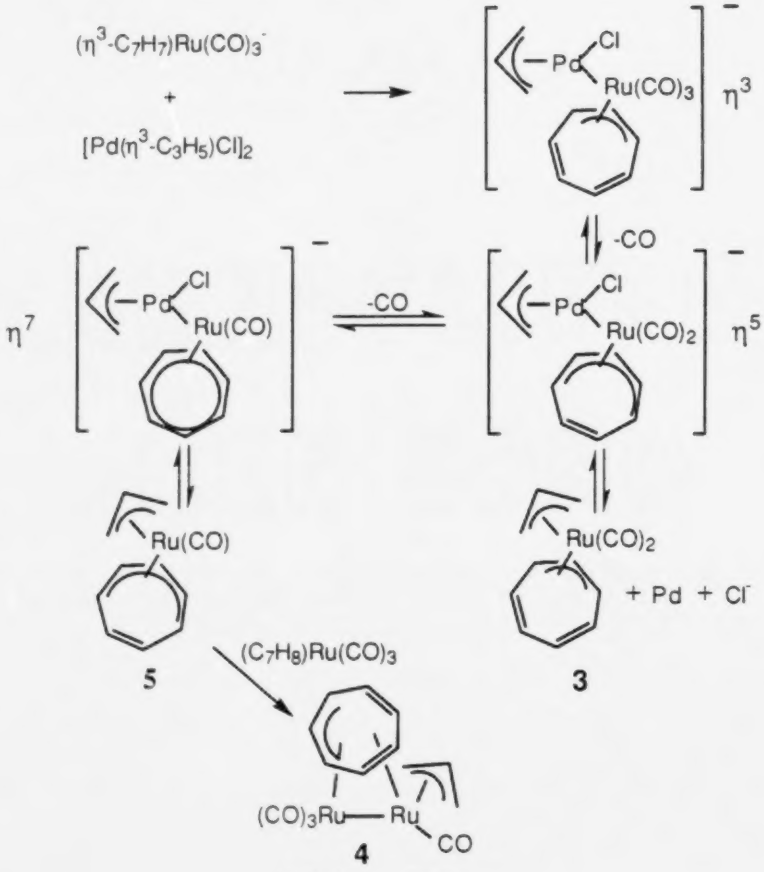
(η3-C7H7)Ru(CO)3-
+
[Pd(η3-C3H5)Cl]2
Pd
Cl
Ru(CO)3
η3
-CO
Pd
Cl
Ru(CO)2
η5
-CO
η7
Pd
Cl
Ru(CO)
Ru(CO)
5
(C7H8)Ru(CO)3
Ru(CO)2
+ Pd + Cl-
3
(CO)3Ru
Ru
CO
4

(Scheme 3.7)

3.2.4. Conclusion.

The very different types of products from reactions of [η^3-C_3H_5)PdCl]$_2$ with the Fe and Ru anions give further evidence of how sensitive the reactivity of these metal nucleophiles is to the nature of the transition metal electrophiles. The prediction of reaction products is difficult, especially for the second (Ru) and third row (Os) transition metals.

3.3. Experimental.

3.3.1. General Techniques and Reagents.

All experimental procedures were performed in standard Schlenk glassware under a static atmosphere of rigorously purified nitrogen. All solvents were dried by refluxing under nitrogen with the appropriate drying agent and distilled just prior to use.

Potassium tertiarybutoxide (KO^{t}Bu) was purchased from Aldrich and sublimed prior to use (150°C, 10^{-3}mmHg). [(η^3-C_3H_5)PdCl]$_2$,[24] (η^4-C_7H_8)Fe(CO)$_3$,[25] (η^4-C_7H_8)Ru(CO)$_3$,[4b] were prepared according to literature methods.

Infrared spectra were obtained with a Nicolet MX-1 Fourier Transform interferometer and a Bomem MB-100 spectrometer. Mass spectra were taken with an A.E.I. MS-12 spectrometer operating at 70eV or 16eV. NMR spectra were recorded on a Bruker WH 200, Bruker WH 360, Bruker AM 400 or Bruker AM 300 spectrometers. Elemental analyses were performed by the Microanalytical Laboratory of this department.

The complete X-ray solid state structure determination on compound **4** was carried out by Dr. Santarsiero and Dr. McDonald of the Structure

Determination Laboratory of this department and MSC Molecular Structure Corporation. A limited amount of pertinent experimental data were extracted from the respective structure reports and included in this thesis for the sake of completeness. Further information including listings of observed and calculated structure factor amplitudes of all reflections may be obtained from Dr. B. McDonald or Dr. J. Takats of this department.

3.3.2. Synthesis of $(\mu\text{-}C_7H_7)Fe(CO)_3Pd(\eta^3\text{-}C_3H_5)$ (2).

Na $[(\eta^3\text{-}C_7H_7)Fe(CO)_3]$ (**1a**) (220mg, 0.87mmol) in THF (20ml) at -10°C was added dropwise to $[(\eta^3\text{-}C_3H_5)PdCl]_2$ (177mg, 0.48mmol) in THF (5ml). After addition was completed the mixture was stirred and was slowly warmed up to room temperature in 2 hr. The IR spectrum showed complete consumption of the anion **1a**. The solvent was removed under vacuum to afford a dark red oil. The residue was extracted with hexane (3x20ml). The combined extracts were concentrated to ~10ml and cooled to -20°C to give a dark red crystalline **2** (115mg, 35%).

Anal. Calcd. for $C_{13}H_{12}O_3FePd$: C, 41.06, H, 3.19. Found: C, 41.07, H, 3.20.

Mass spectrum (70eV, 110°C); M^+ (378), M^+-nCO (n=1-3)

IR (hexane) : υ_{CO} 2003vs, 1945s, 1934s cm^{-1}.

^1H NMR (360 MHz, 22°C, $CDCl_3$): δ 4.76 (s, 7 H, C_7H_7), 5.34 (tt, J_{23}=7Hz, J_{13}=13Hz, H_3), 4.70 (d, J_{23}=7Hz, 2H, $H_{2,4}$), 3.14 (d, J_{13}=13Hz, 2H, $H_{1,5}$). (-60°C, $CDCl_3$): δ 4.78 (s, 7 H, C_7H_7), 5.34 (tt, J_{23}=7Hz, J_{13}=13Hz, H_3), 5.00 (d, J=7Hz, 1H, $H_{2\text{ or }4}$), 4.40 (d, J=7Hz, 1H, $H_{2\text{ or }4}$), 3.20 (d, J=13Hz, 1H, $H_{1\text{ or }5}$), 2.90(d, J=14Hz, 1H, $H_{1\text{ or }5}$),

^{13}C {^1H} NMR (90 MHz, 25°C,CD_2Cl_2): δ 84.86 (s, C_7H_7), 113.74 (s, allyl

CH), 70.51 (s, allyl CH_2) 220.20 (s, CO_{Fe}).

(-50°C, $CDCl_3$): δ 84.19 (s, C_7H_7), 113.74 (s, allyl CH), 70.10 (s, allyl CH_2), 71.07 (s, allyl CH_2), 220.20 (s, CO_{Fe}).

3.3.3. Reaction of $K[(\eta^3\text{-}C_7H_7)Ru(CO)_3]$ with $[(\eta^3\text{-}C_3H_5)PdCl]_2$.

$K[(\eta^3\text{-}C_7H_7)Ru(CO)_3]$ (1.8 mmol) was prepared by the addition of equimolar quantities of KO^tBu in THF (3ml) to $(\eta^4\text{-}C_7H_8)Ru(CO)_3$ (470mg, 1.8 mmol) in THF (20ml) at 23°C. The anion, which was cooled to -78°C, was added dropwise via a canula to a solution of $[(\eta^3\text{-}C_3H_5)PdCl]_2$ (329mg, 0.9 mmol) in THF (5ml) at -78°C. The dark red color of the anion disappeared and some black solid precipitated out from solution. The addition was completed in 25 minutes and resulted in a dark slurry. Evaporation of the solvent under vacuum (the temperature was allowed to warm from -78°C to -10°C) gave a dark residue. The residue was extracted with pentane (2x20ml) at -20°C. Pentane was removed from the resultant red solution and the residue was sublimed to a dry ice cooled probe to give **3** as a red solid (334mg, 42%). The remaining yellow solid residue was identified as **4** (70mg, 9%).

Anal. Calcd. for **3** $C_{12}H_{12}O_2Ru$: C, 49.82, H, 4.18. Found: C, 49.37, H, 4.09.

Mass spectrum (70eV, 22°C); M^+ (289), $M^+\text{-}nCO$ (n=1-2); m.p=15°C.

For **3a**:

IR (hexane): υ_{CO} 2026vs, 1975vs cm^{-1}.

^1H NMR (360 MHz, 23°C, $CDCl_3$): δ 4.82 (s, 7 H, C_7H_7), 4.58 (m, 1H, H_3), 3.50 (d, J=7Hz, 1H, $H_{2 \text{ or } 4}$), 2.50 (d, J=7Hz, 1H, $H_{2 \text{ or } 4}$), 1.85 (d, J=13Hz, 1H,

$H_{1\text{ or }5}$), 1.70 (d, J=14Hz, 1H, $H_{1\text{ or }5}$),

(-60°C, $CDCl_3$): δ 6.05 (t, 1H, C_7H_7), 5.62 (t, 1H, C_7H_7), 5.15 (m, 2H, C_7H_7), 4.95 (t, 1H, C_7H_7), 3.50 (t, 1H, C_7H_7), 2.85 (t, 1H, C_7H_7), 4.50 (m, 1H, H_3), 3.50 (d, J=7Hz, 1H, $H_{2\text{ or }4}$), 2.40 (d, J=13Hz, 1H, $H_{1\text{ or }5}$), 1.85 (d, J=7Hz, 1H, $H_{2\text{ or }4}$), 1.70 (d, J=14Hz, 1H, $H_{1\text{ or }5}$),

For **3b**:

IR (hexane): υ_{CO} 2017s, 1966sh cm^{-1}.

^1H NMR (360 MHz, 23°C, $CDCl_3$): δ 4.91 (s, 7 H, C_7H_7), 4.85 (s br, 1H, H_3), 3.20 (s br, 2H).

(-87°C, CD_2Cl_2): δ 5.92 (t, 1H, C_7H_7), 5.74 (t, 1H, C_7H_7), 5.24 (m, 2H, C_7H_7), 5.15 (m, 1H, C_7H_7), 3.35 (t, 1H, C_7H_7), 2.80 (t, 1H, C_7H_7), 4.80 (m, 1H, H_3), 3.32 (d, J=7Hz, 1H, $H_{2\text{ or }4}$), 3.08 (d, J=7Hz, 1H, $H_{2\text{ or }4}$), 2.52 (d, J=13Hz, 1H, $H_{1\text{ or }5}$), 0.35 (d, J=14Hz, 1H, $H_{1\text{ or }5}$),

For **4**:

Anal. Calcd. $C_{14}H_{12}O_4Ru_2$: C, 37.67, H, 2.71. Found: C, 37.99, H, 2.79.

Mass spectrum (16eV, 140°C); M^+ (447), M^+-nCO (n=1-4).

IR (hexane): υ_{CO} 2050s, 1994s, 1979m, 1953m, 1954w, sh cm^{-1}.

^1H NMR (400 MHz, 22°C, CD_2Cl_2): δ 3.84 (s, 7 H, C_7H_7), 3.26 (tt, J_{23}=7Hz, J_{13}=13Hz, H_3), 2.82 (d, J_{23}=7Hz, 2H, $H_{2,4}$), 1.80 (d, J_{13}=13Hz, 2H, $H_{1,5}$).

(-110°C, CD_2Cl_2): δ 4.62 (m, 1H, $H_{d'}$), 3.95 (m, 1H, H_d), 3.84 (m, 2H, $H_{b,b'}$), 3.61 (m, 1H, $H_{c'}$), 3.50 (t, 1H, H_a), 3.06 (m, 1H, H_c), 3.18 (m, 1H, H_3), 2.90 (d, J=7Hz, 1H, $H_{2\text{ or }4}$), 2.48 (d, J=7Hz, 1H, $H_{2\text{ or }4}$), 1.84 (d, J=13Hz, 1H, $H_{1\text{ or }5}$), 1.52 (d, J=14Hz, 1H, $H_{1\text{ or }5}$),

^{13}C {^1H} NMR (90 MHz, 22°C,CD_2Cl_2): δ 64.43 (s, C_7H_7), 83.17 (s, allyl CH), 43.56 (s, allyl CH_2) 198.07 (s, CO_{Ru1}), 208.38 (s, CO_{Ru2}).

3.3.4. X-ray Structure Determination of 4.

X-ray quality crystals of **4** were grown from hexane solution at -20°C. The structure was solved by Dr. B. D. Santarsiero of the Structure Determination Laboratory of this department. The following information was obtained from the structure report (File number SDL:TAK9111). A bright yellow crystal of **4** with the dimensions of 0.29 x 0.12 x 0.1 mm was selected and mounted on a glass fiber with epoxy, and optically centered in the X-ray beam of an Enraf-Nonius CAD4 automated diffractometer. The automatic peak search and reflection indexing programs generated a triclinic cell. The space group $P\bar{1}$ (No. 2) was chosen, and confirmed as the correct choice by the successful solution and refinement of the structure.

The cell constants and orientation matrix were obtained from a least-squares refinement of the setting angles of 24 reflections in the range $18.2^{\circ}<2\theta<39.6^{\circ}$.

The intensity data were collected at room temperature (23°C) with θ-2θ scans at 6.7-1.8° min^{-1} (in θ). The scan range and aperture width were varied as a function of θ to compensate for the $\alpha 1$-$\alpha 2$ wavelength dispersion: ω scan width = $0.60 + 0.347\tan\theta$ and aperture width $=(3.00 + \tan\theta)$ mm.

The backgrounds for the peaks were measured by extending the scan by 25% on either side of the calculated range; this gave a peak-to-background counting time ratio of 2:1. Intensity measurements were made out to a maximum 2θ of 56.0°. Three reflections were chosen as intensity and orientation standards, and these were remeasured after every 120 min of exposure time to check on crystal and electronic stability over the course of data collection; no appreciable decay was evident.

Table 3.2 Crystallographic data of $(\mu\text{-}C_7H_7)Ru(CO)_3Ru(CO)(\eta^3\text{-}C_3H_5)$ (**4**).

A. Crystal Data

$C_{14}H_{12}O_4Ru_2$; FW = 446.39

Crystal dimensions: 0.29 × 0.12 × 0.10 mm

triclinic space group $P\bar{1}$ (No. 2)

$a = 7.0336\ (8)$, $b = 8.9436\ (9)$, $c = 11.642\ (1)$ Å

$\alpha = 88.457\ (8)^\circ$, $\beta = 87.602\ (8)^\circ$, $\gamma = 74.554\ (2)^\circ$

$V = 705.2$ Å^3; $Z = 2$; $D_c = 2.102$ g cm^{-3}; $\mu = 10.97$ cm^{-1}

B. Data Collection and Refinement Conditions

Radiation:	Mo K_α ($\lambda = 0.71073$ Å)
Monochromator:	incident beam, graphite crystal
Take-off angle:	3.0°
Detector aperture:	$(3.00 + \tan\theta)$ mm horiz × 4.00 mm vert
Crystal-to-detector distance:	173 mm
Scan type:	$\theta{-}2\theta$
Scan rate:	6.7–1.8° min^{-1}
Scan width:	$0.60 + 0.347\tan\theta^\circ$
Data collection 2θ limit:	56.0°
Data collection index range:	$h, \pm k, \pm \ell$
Reflections measured:	3395 total, averaged; 2766 with $I > 3\sigma(I)$
Observations:variables ratio:	2766:181
Agreement factors R_1, R_2, GOF:	0.076, 0.133, 3.926
Corrections applied:	absorption correction

Table 3.3 Fractional coordinates and equivalent isotropic thermal parameters of $(\mu\text{-}C_7H_7)Ru(CO)_3Ru(CO)(\eta^3\text{-}C_3H_5)$ (**4**).

Atom	x	y	z	U_{eq}
Ru1	426.2(1)	65.9(1)	716.37(9)	2.77(3)*
Ru2	196.9(1)	365.0(1)	796.02(9)	2.84(3)*
O1	664(2)	-256(1)	645(1)	7.9(5)*
O2	663(1)	226(1)	549(1)	6.6(3)*
O3	686(2)	33(1)	926.5(9)	7.3(4)*
O4	412(2)	349(1)	1015(1)	8.3(4)*
C1	564(2)	-137(1)	670(1)	5.0(4)*
C2	578(2)	167(1)	614(1)	4.4(4)*
C3	583(2)	56(2)	849(1)	5.3(4)*
C4	336(2)	348(2)	931(1)	5.8(5)*
C5	88(2)	618(1)	833(1)	6.3(5)*
C6	179(2)	594(1)	724(1)	6.0(5)*
C7	379(2)	517(1)	710(2)	6.3(5)*
C11	153(2)	129(1)	612(1)	4.6(4)*
C12	146(2)	6(1)	692(1)	4.1(3)*
C13	146(2)	35(1)	811(1)	4.4(4)*
C14	65(1)	182(1)	872(1)	4.2(3)*
C15	-84(2)	312(2)	826(1)	5.2(4)*
C16	-80(2)	365(1)	713(1)	4.9(4)*
C17	68(2)	300(1)	627(1)	4.3(4)*

*Indicates atom refined anisotropically.

The equivalent isotropic displacement parameter U is $1/3\sum_{i=1}^{3} r_i^2$, where r_i are the root-mean-square amplitudes of vibration.

3.4. References.

1. Smidt, J.; Hafner, W.; Jira, R.; Sedlmeier, J.; Sieber, R.; Ruttinger, R.; Kojer, H., *Angew. Chem.* **1959**, *71*, 176

2. Jira, R.; Sedlmeier, J.; Smidt, J., *Justus Liebigs Ann. Chem.* **1966**, *693*, 99

3. (a). Bäckvall, Jan-E.; *Acc. Chem. Res.* **1983**, *16*, 335

   (b). Maitlis, P. M., *"The Organic Chemistry of Palladium"* Aademic Press, New York, **1971**, Vol. *1* and 2.

4. (a). Bennett, M. J.; Pratt, J. L.; Simpson, K. A.; LiShingMan, L. K. K.; Takats, J., *J. Am. Chem. Soc.* **1976**, *98*, 4810

   (b). Edelmann, F.; Kiel, G. Y.; Takats, J.; Vasudevamurthy, A.; Yeung, M. Y., *J. Chem. Soc. Chem. Commun.* **1988**, 296

   (c). LiShingMan, L. K. K.; Reuvers, J. G. A.; Takats, J.; Deganello,G., *Organometallics* **1983**, *2*, 28

   (d). Reuvers, J. G. A.; Takats, J., *Organometallics* **1990**, *9*, 578

5. Astley, S.; Takats, J., manuscripts in preparation

6. (a). Ball, R. G.; Edelmann, F.; Kiel, G.-Y.; Takats, J.; Drews, R., *Organometallics* **1986**, *5*, 829

   (b). Vasudevamurthy, A.; Takats, J., *Organometallics* **1987**, *6*, 2005

   (c). Lin, G. Y.; Takats, J., *J. Organomet. Chem.* **1984**, *269*, C4

7. Salzer, A.; Egolf, T.; Philipsborn, W. von, *Helv. Chim. Acta* , **1982**, *65*,1145

8. King, R. B., *Inorg. Chem.* **1966**, *5*, 2242

9. Horton, A. D.; Kemball, A. C.; Mays, M. J., *J. Chem. Soc. Dalton Trans* **1988**, 2953

10. Horton, A. D.; Mays, M. J., *J. Chem. Soc. Dalton Trans* **1990**, 155

11. Vrieze, K., in" *Dynamic Nuclear Magnetic Resonance Spectroscopy*" (Jackman, L. M. and Cotton, F. A., eds.), Academic Press, New York, **1975**, p. 441

12. Faller, J. W., *Adv. Organomet. Chem.* **1977**, *16*, 211

13. Cooke, M.; Goodfellow, R. J.; Green, M.; Parker, G., *J. Chem. Soc. (A)* **1971**, 16

14. Astley, S. T.; Takats, J., *J. Organomet. Chem.* **1989**, *363*, 167

15. Cotton, F. A.; Edwards, W. T., *J. Am. Chem. Soc.* **1967**, *90*, 5412

16. Churchill, M. R.; Hollander, F. J.; Hutchinson, J. P., *Inorg. Chem.* **1977**, *16*, 2655

17. Bennett, M. J.; Cotton, F. A.; Legzdins, P., *J. Am. Chem. Soc.* **1968**, *90*, 6335

18. Cotton, F. A.; Reich, C. R., *J. Am. Chem. Soc.*, **1969**, *91*, 847

19.(a). Nagashima, H.; Mukai, K.; Shiota, Y.; Yamaguchi, K.; Ara, K.; Fukahori, T.; Suzuki, H.; Akita, M.; Moro-oka, Y.; Itoh, K., *Organometallics* **1990**, *9*, 799

(b). Marsh, R. A.; Howard, J.; Woodward, P., *J. Chem. Soc. Dalton Trans* **1972**, 778

(c). Smith, A. E.; *Inorg. Chem.* **1972**, *11*, 2306

20. Nesmeyanov, A. N.; Kritskaya, I. I., *J. Organomet. Chem.* **1968**, *14*, 387

21. Grindred, C.; Dissertation, MacMaster University, Hamilton, Ontario, Canada, 1966

22. Heck, R. F., *J. Am. Chem. Soc.* **1968**, *90*, 317

23. Efraty, A., *J. Organomet. Chem.* **1973**, *57*, 1

24. Tatsuno, Y.; Yoshida, T.; Otsuka, S., *Inorg. Synth.* **1979**, *19*, 220

25. Burton, R.; Pratt, L; Wilkinson, G., *J. Chem. Soc.* **1961**, 594

Chapter 4.

Synthesis and Characterization of Cycloheptatrienyl Bridged Heterobimetallic Complexes, $(\mu\text{-}C_7H_7)M(CO)_3Mo(CO)_2(L)$ (M=Fe, Ru, Os) $(L=\eta^5\text{-}C_9H_7, \eta^5\text{-}C_5H_5)$

4.1. Introduction.

The ability of the anionic complexes, $(\eta^3\text{-}C_7H_7)M(CO)_3^-$ (M=Fe **1a**, Ru **1b**, Os **1c**) as precursors for the preparation of cycloheptatrienyl bridged bimetallic complexes has been clearly demonstrated.[1-6] However the obtained results revealed a perplexing picture of their ambident reactivity. Reactions of $(\eta^3\text{-}C_7H_7)Fe(CO)_3^-$ (**1a**) with group 14 halides (R_3EX, E=Si, Ge, Sn, Pb) gave evidence of electrophilic discrimination. Depending on the electrophiles (R_3EX) two distinct products, ring (E=Si, Ge) or metal substituted products (E=Sn, Pb), were obtained (Scheme 4.1).[4a,b] On the other hand, metal-dependent nucleophilicity of anions **1** was displayed in their reactions with $[M''(COD)Cl]_2$ (M"=Rh, Ir). The Fe and Ru anions gave metal substituted cis-$(\mu\text{-}C_7H_7)M(CO)_3M''(COD)$ (M=Fe, Ru; M"=Rh, Ir) (Scheme 4.1),[1,2] whereas the Os anion initially afforded ring substituted trans compounds which further converted to thermodynamically more stable cis compounds (Scheme 4.1).[3] But, as has been seen in chapter two, the alteration of the metal center in anions **1** had no significant effect on the type of bimetallic compounds that were obtained in reactions with $[M'(CO)_4X]_2$ (M'=Mn, Re; X=Cl, Br) (Scheme 4.1). Clearly, besides the anions themselves, the nature of the electrophiles also plays an important role in determining the outcome of these reactions.

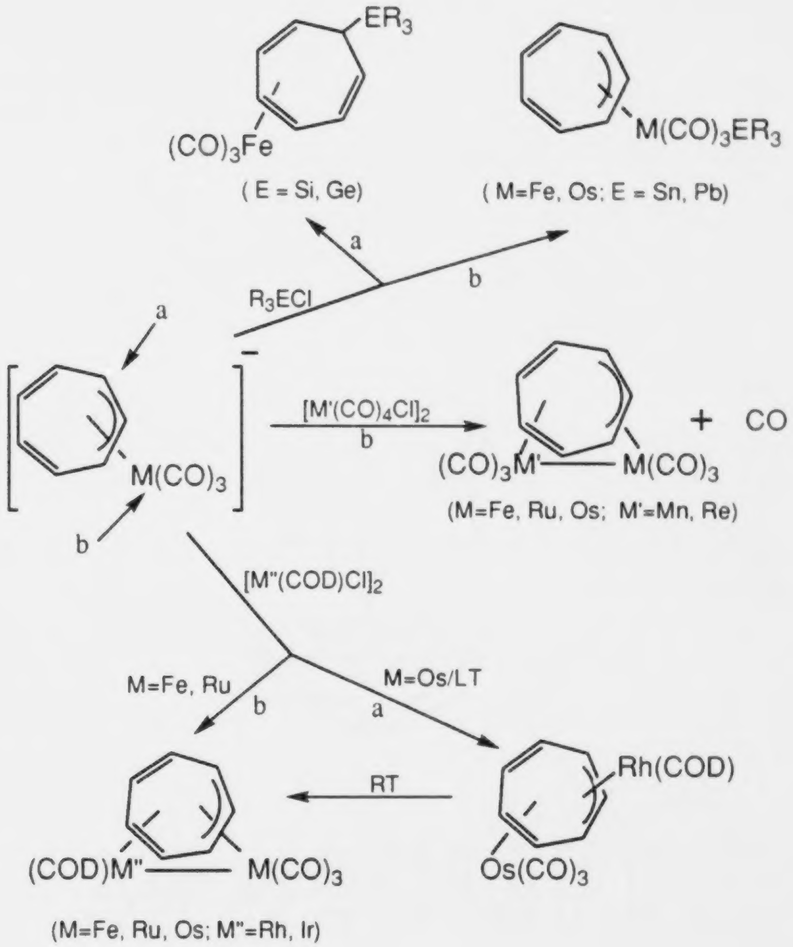
ER$_3$
(CO)$_3$Fe
(E = Si, Ge)
M(CO)$_3$ER$_3$
(M=Fe, Os; E = Sn, Pb)
a
b
R$_3$ECl
a
M(CO)$_3$
b
−
[M'(CO)$_4$Cl]$_2$
b
(CO)$_3$M'
M(CO)$_3$
+ CO
(M=Fe, Ru, Os; M'=Mn, Re)
[M"(COD)Cl]$_2$
M=Fe, Ru
b
M=Os/LT
a
RT
Rh(COD)
Os(CO)$_3$
(COD)M"
M(CO)$_3$
(M=Fe, Ru, Os; M"=Rh, Ir)

(Scheme 4.1)

In order to obtain more information about this electrophilic effect it is necessary to carry out reactions of anions **1** with other transition metal electrophiles. In this chapter we describe the reactions of **1** with the cationic complex $[(\eta^5\text{-}C_9H_7)Mo(CO)_2(CH_3CN)_2]^+$ (**2a**) (η^5-C_9H_7=Indenyl). To explore possible ligand effect caused by the indenyl group, reactions with $[(\eta^5\text{-}C_5H_5)Mo(CO)_2(CH_3CN)_2]^+$ (**2b**) (η^5-C_5H_5=cyclopentadienyl) were also carried out. Surprisingly, the reactions of the Fe and Ru anions resulted in exclusive formation of trans-(μ-η^4,η^3-C_7H_7)M(CO)$_3$Mo(CO)$_2$(η^5-C_9H_7) (M=Fe **3a**, Ru **3b**) and trans-(μ-η^4,η^3-C_7H_7)M(CO)$_3$Mo(CO)$_2$(η^5-C_5H_5) (M=Fe **4a**, Ru **4b**). Furthermore, the reactions of the Os anion **1c** yielded two types of products. The major products were still the trans compounds (**3c** and **4c**). The minor products proved to be the cis compounds, but **without** a metal-metal bond, cis-(μ-η^4,η^3-C_7H_7)Os(CO)$_3$Mo(CO)$_2$(L) (L=η^5-C_9H_7 **5c**, η^5-C_5H_5 **6c**). The nature of these products were studied by spectroscopic methods and in some cases (**3a**, **3c** and **5c**) the solid state structures were determined by the X-ray crystallography. Since the products are fluxional, the migration mechanisms of the metal moieties around the C_7H_7 ring were probed by the multisite magnetization transfer method.

4.2. Results and Discussion.

4.2.1. Preparation and Characterization of (μ-η^4,η^3-C_7H_7)M(CO)$_3$Mo(CO)$_2$(η^5-C_9H_7) (M=Fe, Ru, Os).

The reactions of the cationic complex, [(η^5-C_9H_7)Mo(CO)$_2$(CH_3CN)$_2$]$^+$ (**2a**) with (η^3-C_7H_7)M(CO)$_3^-$ (M=Fe **1a**, Ru **1b**, Os **1c**) were carried out at low temperature. Work-up and crystallization from CH_2Cl_2-hexane solution gave modest yields of the bimetallic products FeMo (**3a**), RuMo (**3b**) and OsMo (**3c**), respectively (Equation 4.1). From the osmium reaction a second bimetallic product **5c** was also isolated. Compound **5c** will be discussed in section 4.2.5.

$$\underset{\mathbf{1}}{K[(\eta^3\text{-}C_7H_7)M(CO)_3]} + \underset{\mathbf{2a}}{[(\eta^5\text{-}C_9H_7)Mo(CO)_2(CH_3CN)_2]BF_4} \xrightarrow[LT]{THF} \qquad (4.1)$$

$$(\,M{=}Fe,\ Ru,\ Os\,) \qquad (\mu\text{-}C_7H_7)MMo(CO)_5(C_9H_7) + (C_7H_8)M(CO)_3$$

The FeMo compound **3a** appears as dark red crystals and is soluble in most common organic solvents. Although solid **3a** can be stored in air for several days without apparent decomposition, its solution is air-sensitive. The RuMo compound **3b** is also red, but it is less stable than the corresponding FeMo **3a**. Column chromatography on silica gel caused rapid decomposition of **3b** to $(\eta^4\text{-}C_7H_8)Ru(CO)_3$ and another mononuclear compound **7**. The nature of **7** will be described in the section 4.2.4. Work-up of the osmium reaction mixture was carried out at low temperature and provided two major products **3c** and **5c** in a ratio of 2:1, in addition to small amounts of $(\eta^4\text{-}C_7H_8)Os(CO)_3$. Both **3c**, orange-red crystals and **5c**, yellow crystals are moderately soluble in common organic solvents. Solutions of the products, especially that of **5c**, are air sensitive. Both **3c** and **5c** also rapidly decomposed on silica gel columns.

Elemental analysis indicated a composition of $C_{21}H_{14}O_5MoM$ (M=Fe, Ru, Os) for the corresponding compounds **3a-c**. This was further corroborated and refined by the mass spectra of the compounds which, in all cases, showed parent molecular ion peaks, followed by successive loss of five carbonyl groups and fragments of C_9H_7 and C_7H_7. These results suggested that the formula of compounds **3a-c** was $(C_7H_7)MMo(CO)_5(C_9H_7)$ (M=Fe, Ru, Os).

In principle, there are three possible structures that could satisfy the above molecular formula and give the favored 18 electron configuration at each metal center, cis-(μ-η^3,η^4-C_7H_7)M(CO)$_3$Mo(CO)$_2$(η^3-C_9H_7) (**A**), cis-(μ-η^3,η^2-C_7H_7)M(CO)$_3$Mo(CO)$_2$(η^5-C_9H_7) (**B**) and trans-(μ-η^4,η^3-C_7H_7)M(CO)$_3$Mo(CO)$_2$(η^5-C_9H_7) (**C**) (Scheme 4.2). The last structure has been observed in the analogous cyclopentadienyl compound (μ-η^4,η^3-C_7H_7)Fe(CO)$_3$Mo(CO)$_2$(η^5-C_5H_5), which was prepared by a totally different route via photolysis of Fe(CO)$_5$ in the presence of (η^3-C_7H_7)Mo(CO)$_2$(η^5-C_5H_5).[7]

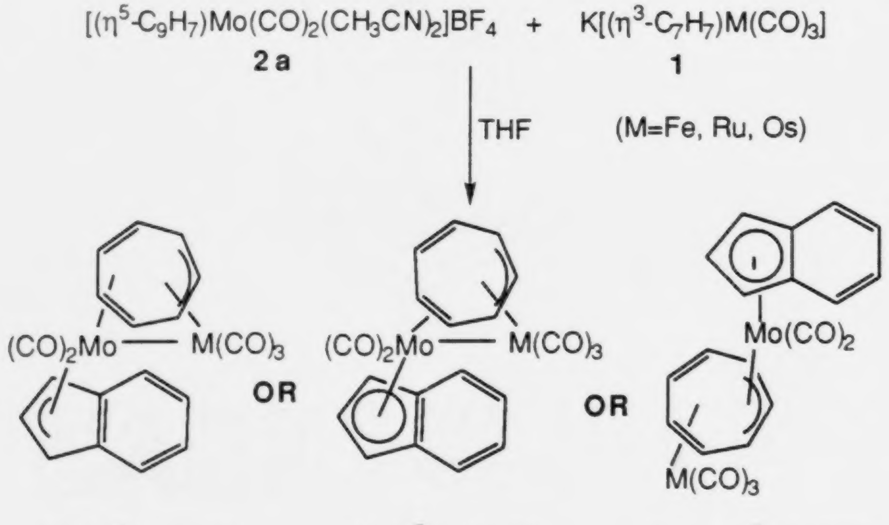
[(η^5-C_9H_7)Mo(CO)$_2$(CH_3CN)$_2$]BF_4 + K[(η^3-C_7H_7)M(CO)$_3$]
2a
1
THF
(M=Fe, Ru, Os)
(CO)$_2$Mo
M(CO)$_3$
OR
(CO)$_2$Mo
M(CO)$_3$
OR
Mo(CO)$_2$
M(CO)$_3$

cis-(η^3-indenyl) (**A**)

cis-(η^5-indenyl) (**B**)

trans-(η^5-indenyl) (**C**)

(Scheme 4.2)

On this basis it is perhaps tempting to conclude that compounds **3a-c** all contain the trans arrangement of the metal fragments. However the other structural formulations can not be dismissed without due consideration. Indeed, so far the reactions of the Fe and Ru anions have not given any trans-type products. Also, there are documented examples of compounds with the η^3-indenyl moiety,[8] and the cis-(μ-η^3,η^2-C_7H_7) bonding mode has been identified in two separate occasions, in Deganello's work (cis-(μ-η^3,η^2-C_7H_7)Fe(CO)$_3$Pd(η^5-C_5H_5))[6] and in chapter 2 (cis-(μ-η^2,η^3-C_7H_7)Re(CO)$_4$Os(CO)$_3$).

The spectroscopic data of products **3a-c** should provide clues as to their actual structures. It was noted that the different arrangements of metal moieties (trans or cis) require different bonding modes for the indenyl ligand (η^3 or η^5) and the C_7H_7 ring. This should result in distinct IR and especially NMR features and the fluxional behavior of the C_7H_7 ring in these different structures will be different as well.

The infrared spectra of compounds **3a**, **3b**, and **3c** (Table 4.1) displayed five well-separated absorption bands in the terminal carbonyl region (for FeMo **3a**; υ_{CO}=2044vs, 1982vs, 1973s, 1952s, 1882m cm^{-1}). The first three, with two closely spaced bands are the typical IR band pattern for (η^4-diene)M(CO)$_3$ complexes (cf. (η^4-C_7H_8)Fe(CO)$_3$; υ_{CO}=2050s, 1989s, 1975m cm^{-1})[9] and suggests a trans-type structure for the compounds **3a-c**. Indeed the IR spectrum of **3a** greatly resembles that of the known compound, trans-(μ-C_7H_7)Fe(CO)$_3$Mo(CO)$_2$(η^5-C_5H_5).[7]

NMR spectroscopic studies further supported the trans structure. The room temperature ^{1}H NMR spectra of compounds **3a**, **3b** and **3c** showed a very similar four-peak pattern in an intensity ratio of 2:2:2:1 for their indenyl ligands (c.f. **3a**, Figure 4.1). Based on the homonuclear decoupling experiments the four peaks could be unambiguously assigned (Table 4.1). It was previously noted that the chemical shifts for the $H_{1,3}$ protons and $C_{4,9}$ carbons of the indenyl ligand occurs at very different region depending on the bonding modes, η^3-C_9H_7 or η^5-C_9H_7. For instance, the $H_{1,3}$ resonance in (η^5-C_9H_7)Ir(PEt$_3$)$_2$ occurs at 4.91 ppm, but in (η^3-C_9H_7)Ir(PMe$_3$)$_3$ the

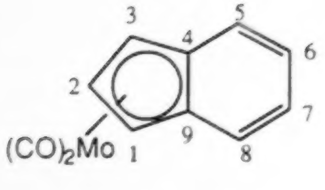

trans- (η^5-C_9H_7)

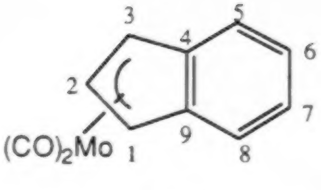

cis-(η^3-C_9H_7)

same $H_{1,3}$ peak has shifted upfield to 2.78 ppm.[8] The resonances of the $H_{1,3}$ protons in compounds **3a-c** are at about 5.2 ppm and indicate that the indenyl ligand in these compounds is very likely η^5-coordinated. This indication is further supported by the ^{13}C NMR spectrum. The $C_{4,9}$ peaks of compounds **3a-c** appear at around 113 ppm, a position that is much closer to 121.15 ppm observed in (η^5-C_9H_7)Ir(PEt_3)$_2$ and far from 156.7 ppm of (η^3-C_9H_7)Ir(PMe_3)$_3$.[8] Actually, in the known complex, (η^5-C_9H_7)Mo(CO)$_2$(η^3-C_3H_5),[10] the $H_{1,3}$ signal is at 5.87 ppm, which corroborate the presence of an η^5-indenyl ligand in our products.

Further evidence for the trans-(η^5-indenyl) structure came from the fluxionality of the products. It was found that metal migration around the C_7H_7 ring in compounds **3a-c** is a slow process. For instance, in the FeMo compound **3a**, no signal for the C_7H_7 ring was observed at room temperature (Figure 4.1). Increasing the temperature to +70°C resulted in the appearance of a broad singlet at 3.98 ppm. Upon lowering the temperature, four peaks started to appear at -5°C. The low temperature limiting spectrum was obtained at -40°C. For the corresponding Ru and Os compounds the low temperature limiting spectra were reached at even higher temperatures (-20°C and 10°C) which suggested slower rotation of the C_7H_7 ring in these molecules. As mentioned in previous chapters, a typical characteristic of cis-C_7H_7 ring bridged compounds is the fast whizzing of the C_7H_7 ring, even at low temperature.[1a] In contrast, in the known trans compounds the process is much slower. In trans-(μ-C_7H_7)Fe(CO)$_3$Mo(CO)$_2$(η^5-C_5H_5)[7] the whizzing of the C_7H_7 ring is totally frozen out at -50°C.

Table 4.1. Infrared, ^{1}H and ^{13}C NMR data of **3a-c** and **5c**.

	IR (cm^{-1})[b]	^{1}H NMR (ppm)							
		Indenyl (C_9H_7)[c]				C_7H_7[c]			
		$H_{6,7}$	$H_{5,8}$	$H_{1,3}$	H_2	H_d	H_c	H_b	H_a
3a[d]	2044vs 1982vs 1973s 1952s 1882m	6.44	6.18	5.18	4.62	4.68	3.41	3.60	-0.72
3b[e]	2061vs 1997vs 1989s 1948s 1877m	6.48	6.25	5.22	4.75	4.95	3.55	3.65	-0.90
3c[f]	2062vs 1990vs 1982s 1947s 1876m	6.52	6.32	5.28	4.92	5.10	3.45	3.65	-0.70
5c[f]	2072vs 2006vs 1985vs 1943m 1879s	6.52	6.32	5.38	5.01	4.78	3.20	3.35	-1.25

^{13}C NMR (ppm)[g]										
	Indenyl (C_9H_7)					C_7H_7				
	$C_{6,7}$	$C_{5,8}$	$C_{4,9}$	C_2	$C_{1,3}$	C_d	C_c	C_b	C_a	average
3a[h]	125.54	123.53	112.84	87.57	79.60					68.00
3b[h]	125.52	123.71	112.95	87.82	79.90					
3c[h]	125.24	123.41	112.79	87.68	79.85	86.80	68.68	47.85	1.15	
5c[h]	124.72	123.27	112.79	89.83	80.69	88.61	71.44	45.86	-0.80	

[a] Chemical shifts (d) in ppm from Me_4Si. [b] In hexane. [c] Assignment based on homonuclear spin-decoupling experiments. [d] In toluene-d_8 at -40°C. [e] In toluene-d_8 at -18°C. [f] In toluene-d_8 at 23°C. [g] Assignment based on heteronuclear decoupling experiments. [h] In CD_2Cl_2 at 23°C.

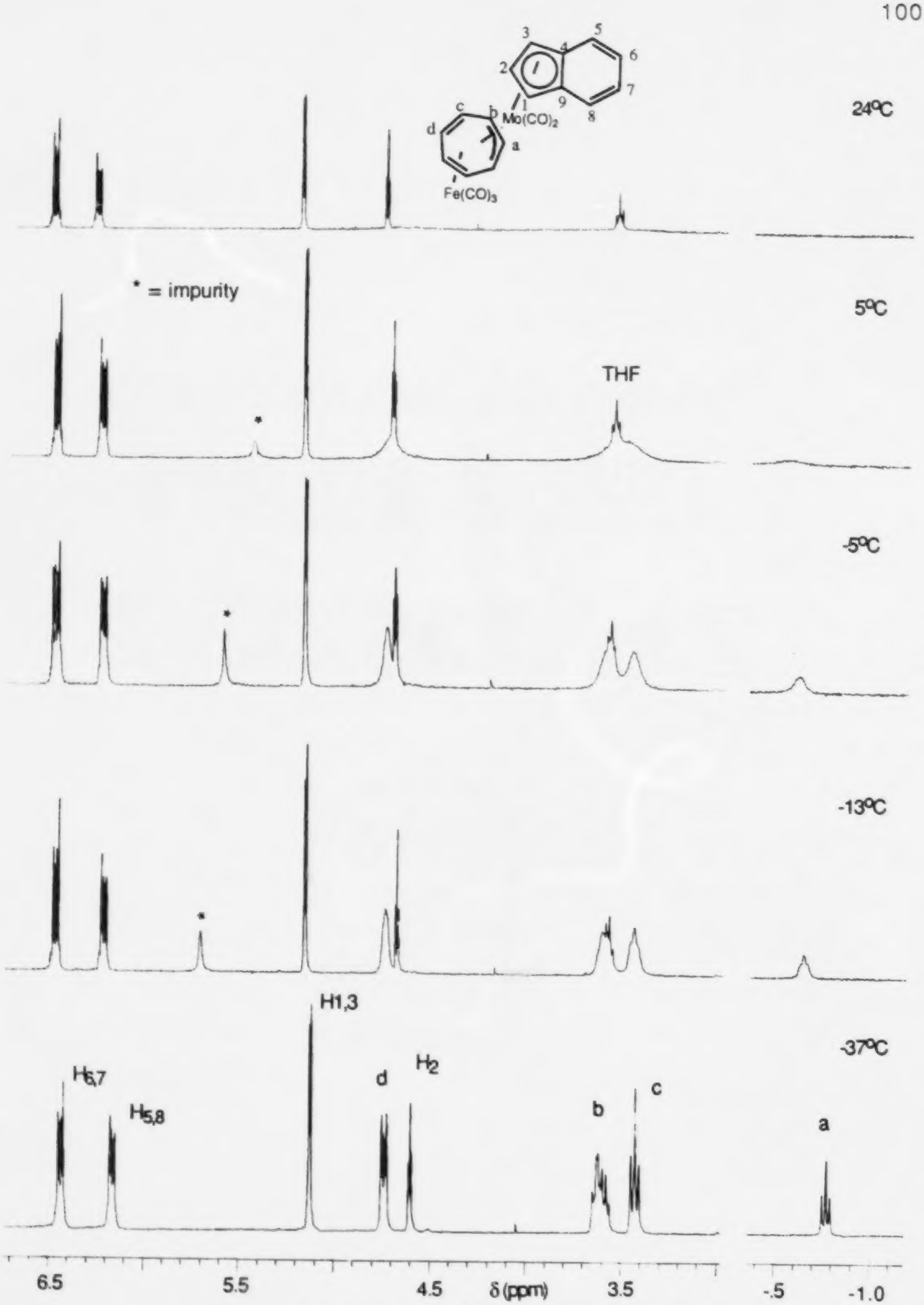

Figure 4.1 Variable temperature ^{1}H NMR spectra (360 MHz) of (μ-C_7H_7)Fe(CO)$_3$Mo(CO)$_2$(η^5-C_9H_7) (**3a**) in toluene-d_8.

At this point it seemed clear that compounds **3a-c** have the trans structure. A comparison of their low temperature ^{1}H NMR spectra (for FeMo **3a**, H_d 4.68, H_c 3.41, H_b 3.60, H_a -0.72 ppm) with the analogous complex trans-(μ-C_7H_7)Fe(CO)$_3$Mo(CO)$_2$(η^5-C_5H_5) (H_d 5.40, H_c 3.83, H_b 4.50, H_a 4.98 ppm),[7] shows obvious similarities . Both have four peaks for the C_7H_7 ring in a ratio of 2:2:2:1 which is expected for the C_s symmetry of the trans structure. The upfield shifts in the indenyl compounds is due to the shielding effect of the indenyl ligand. Such shielding appears especially strong for the H_a proton which moves ca. 6 ppm upfield from its position in the Cp complex. Similar observations have been reported in other indenyl compounds. For instance, in *exo*-(η^5-C_9H_7)Mo(CO)$_2$(η^3-C_3H_5) the central proton of the allyl ligand appears at 0.15 ppm, but the corresponding Cp compound displays the same proton peak at 3.61 ppm.[11] The similarity between the mononuclear and binuclear compounds is clear in the following scheme 4.3.

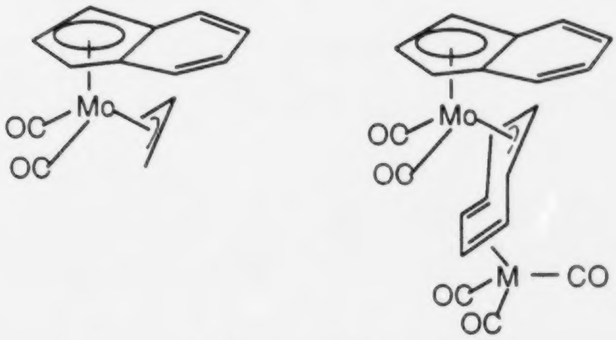

(Scheme 4.3)

4.2.2. Solid State Structures of $(\mu\text{-}C_7H_7)M(CO)_3Mo(CO)_2(\eta^5\text{-}C_9H_7)$ (M=Fe, Os).

The final proof of the trans structure came from X-ray crystallographic studies. Perspective views of compounds **3a** and **3c** are shown in Figure 4.2 which also establishes the numbering system. It is clear that the two metal moieties occupy opposite faces of the bridging C_7H_7 ring, i.e. trans-(μ-C_7H_7) bonding arrangement. This trans structure is the same as that of the analogous Cp compound. For comparison, a perspective view of the Cp complex is also shown in Figure 4.3.[12] Important bond distances and angles of **3a** and **3c**, together with that of the Cp compound, are listed in Table 4.2 and 4.3. A quick overview of the tables shows that the bonding in **3a**, **3c** and the Cp compound is very similar.

In these compounds the Mo atom is η^3 bonded to the C_7H_7 ring and η^5 bonded to the indenyl ring. The distances of Mo to the η^3-C_7H_7 ring in compounds **3a** and **3c** range from 2.20 Å to 2.42 Å which is the same as in the Cp compound (2.22-2.42 Å). The shorter Mo-C15 distance (2.20 Å) compared to Mo-C14 (2.42 Å) is typical for η^3-allyl compounds (cf. $[PhB(pz)_3]Mo(CO)_2(\eta^3\text{-}C_3H_5)$,[13] Mo-$C_c$ 2.22 Å, Mo-C_t 2.37 Å). The carbon-carbon bond distances of the allyl part in the C_7H_7 ring are also typical. These observations suggest that replacement of the Cp ring by the indenyl ligand does not change the bonding situation between molybdenum and the C_7H_7 ring. The distances of Mo to indenyl ligand in compounds **3a** and **3c** are ca. 2.30-2.47 Å, similar to 2.27-2.39 Å found for η^5-C_9H_7-W bonds in $(\eta^5\text{-}C_9H_7)W(CO)_2(\eta^3\text{-}C_9H_7)$.[14] The bonds from Mo to the ring junction carbons (C29 and C24) (average 2.43 Å) are much shorter than the corresponding metal-carbon distances (3.12 Å) to the η^3-indenyl ligand in

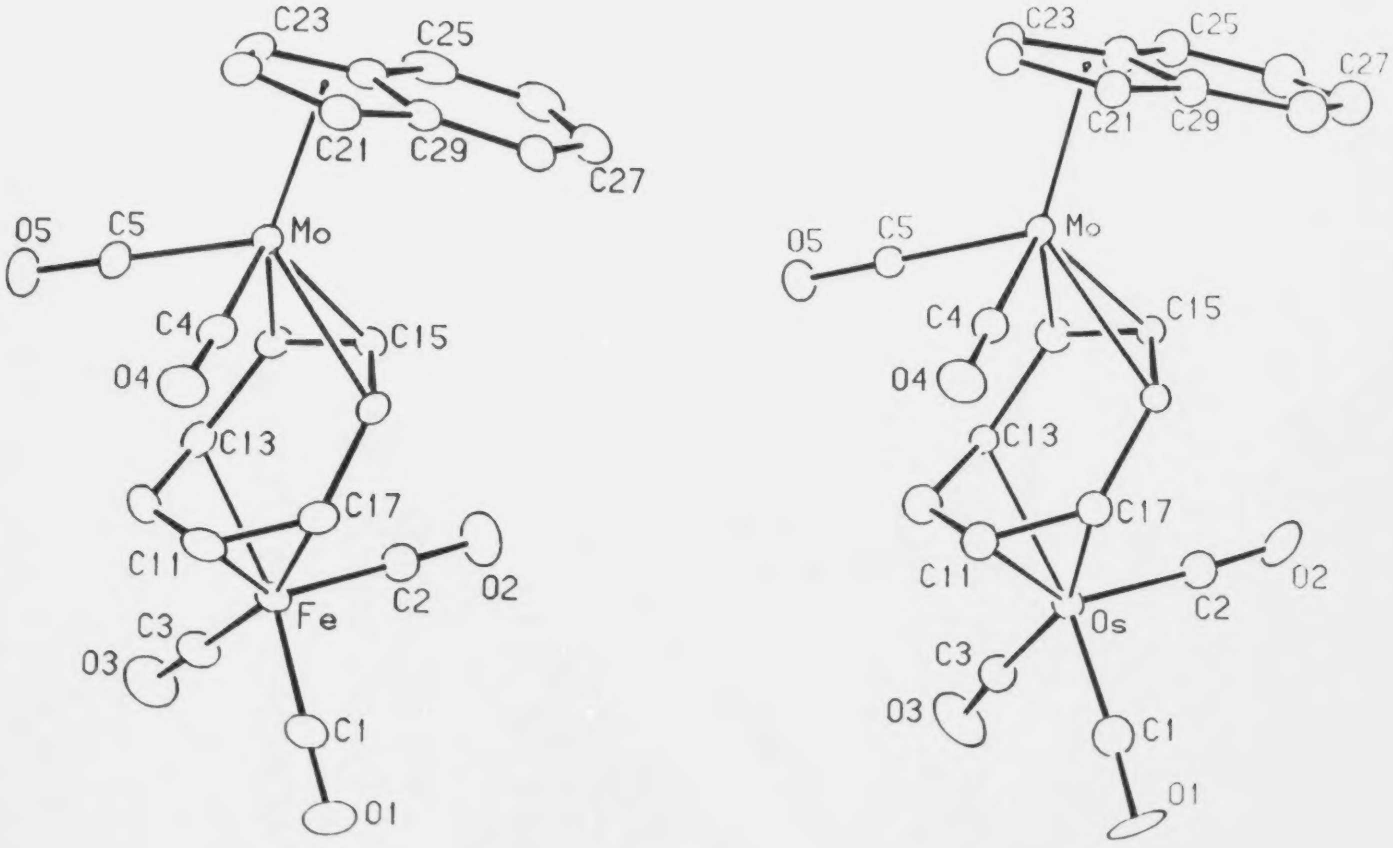
C23
C25
C21
C29
C27
O5
C5
Mo
C4
C15
O4
C13
C17
C11
O2
C2
Fe
C3
O3
C1
O1
C23
C25
C27
C21
C29
O5
C5
Mo
C4
C15
O4
C13
C17
C11
O2
C2
Os
C3
O3
C1
O1

Figure 4.2 Perspective views of (μ-C_7H_7)M(CO)$_3$Mo(CO)$_2$(η^5-C_9H_7) (M=Fe **3a**, Os **3c**).

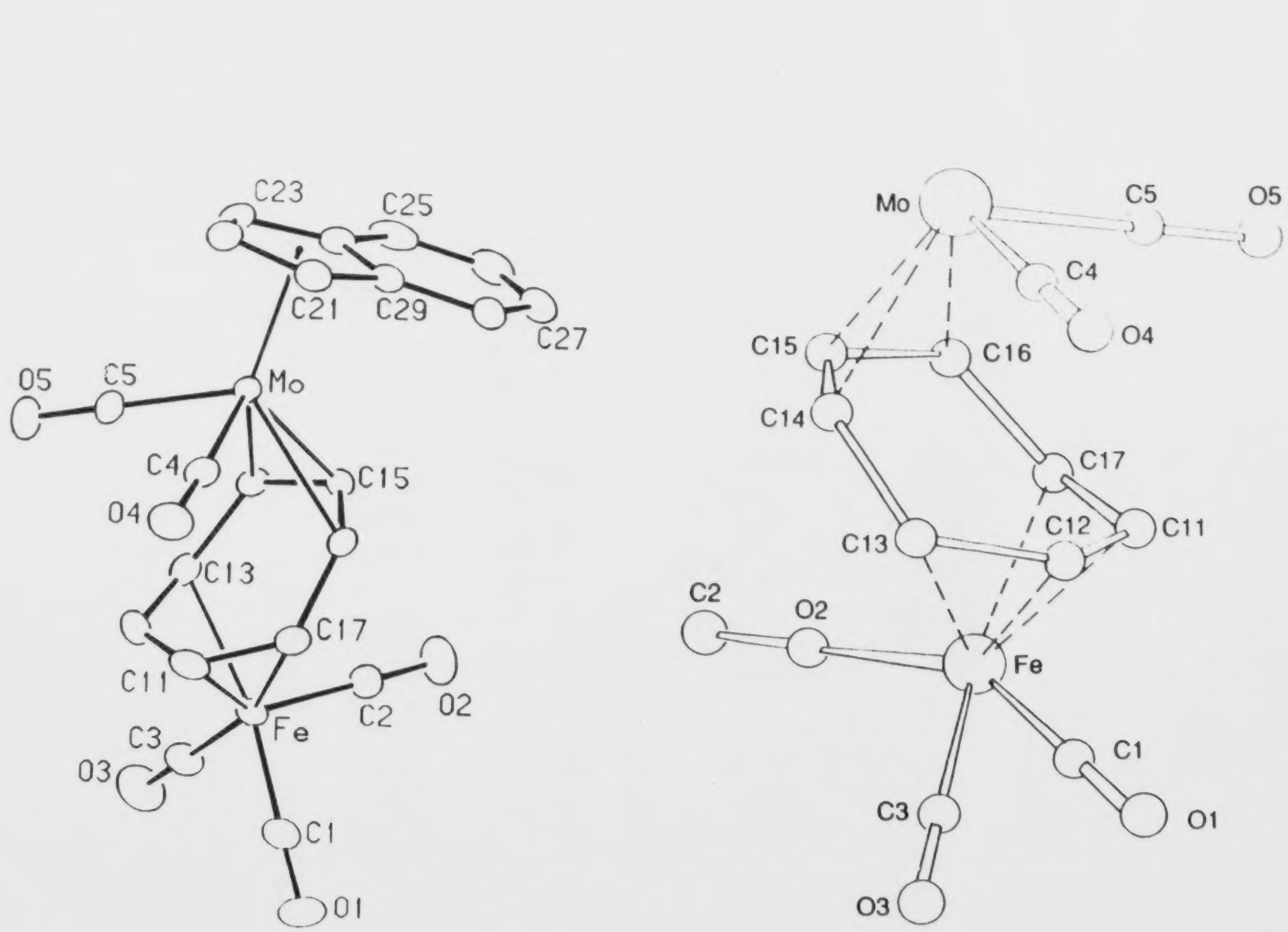
C23
C25
C21
C29
C27
O5
C5
Mo
C4
C15
O4
C13
C17
C11
C2
O2
Fe
C3
O3
C1
O1
Mo
C5
O5
C4
O4
C15
C16
C14
C17
C12
C11
C13
C2
O2
Fe
C1
C3
O1
O3

Figure 4.3 Perspective views of trans-(μ-C_7H_7)Fe$(CO)_3$Mo$(CO)_2$(η^5-C_9H_7) (**3a**) and trans-(μ–C_7H_7)Fe$(CO)_3$Mo$(CO)_2$(η^5-C_5H_5) (C_5H_5 ring not shown)

Table 4.2. Selected bond distances of (μ–C_7H_7)M$(CO)_3$Mo$(CO)_2$(η^5-C_9H_7) (**3**) (M=Fe **a**, Os **c**) and (μ–C_7H_7)Fe$(CO)_3$Mo$(CO)_2$(η^5-C_5H_5).

		FeMo 3a	**OsMo 3c**	**FeMoCp**
Atom1	Atom2	Length (Å)		
Fe/Os	C1	1.791 (4)	1.83 (3)	1.800 (9)
Fe/Os	C2	1.790 (4)	1.88 (2)	1.799 (9)
Fe/Os	C3	1.787 (4)	1.89 (2)	1.766(11)
Fe/Os	C11	2.042 (4)	2.20 (2)	2.059 (7)
Fe/Os	C12	2.036 (4)	2.21 (2)	2.024(10)
Fe/Os	C13	2.139 (3)	2.25 (2)	2.171 (9)
Fe/Os	C17	2.183 (3)	2.27 (3)	2.158 (8)
C11	C12	1.395 (6)	1.41 (2)	1.36 (1)
C11	C17	1.423 (5)	1.43 (3)	1.42 (1)
C12	C13	1.413 (5)	1.46 (2)	1.41 (1)
C13	C14	1.500 (5)	1.53 (2)	1.49 (1)
C14	C15	1.395 (4)	1.40 (2)	1.38 (1)
C15	C16	1.401 (4)	1.39 (2)	1.41 (1)
C16	C17	1.480 (5)	1.53 (2)	1.50 (1)
Mo	C4	1.930 (3)	1.98 (2)	1.941 (9)
Mo	C5	1.924 (4)	1.92 (2)	1.929(10)
Mo	C14	2.424 (3)	2.40 (2)	2.426 (8)
Mo	C15	2.204 (3)	2.18 (2)	2.222 (8)
Mo	C16	2.410 (3)	2.42 (2)	2.397(10)
Mo	C21	2.322 (3)	2.33 (2)	
Mo	C22	2.307 (4)	2.30 (2)	
Mo	C23	2.332 (3)	2.33 (2)	
Mo	C24	2.439 (3)	2.44 (2)	
Mo	C29	2.430 (3)	2.47 (2)	

Table 4.3. Selected bond angles of (μ–C_7H_7)M(CO)$_3$Mo(CO)$_2$(η^5-C_9H_7) (**3**) (M=Fe **a**, Os **c**) and (μ–C_7H_7)Fe(CO)$_3$Mo(CO)$_2$(η^5-C_5H_5).

			FeMo 3a	**OsMo 3c**	**FeMoCp**
Atom1	Atom2	Atom3	Angle (degree)[a]		
C1	Fe/Os	C2	99.9 (2)	98 (1)	101.5 (4)
C1	Fe/Os	C3	92.4 (2)	94 (1)	91.4 (4)
C2	Fe/Os	C3	100.3 (2)	95 (1)	100.9 (4)
C4	Mo	C5	80.8 (2)	81.7 (9)	80.5 (3)
C13	C14	C15	124.0 (3)	124 (2)	125.7 (8)
C14	C15	C16	117.8 (3)	118 (2)	116.8 (9)
C15	C16	C17	124.6 (3)	125 (2)	123.7 (10)
C11	C17	C16	129.6 (3)	132 (2)	129.1 (8)
C12	C11	C17	119.5 (3)	119 (2)	118.1 (7)
C11	C12	C13	119.4 (3)	119 (2)	122.5 (9)
C12	C13	C14	130.2 (3)	127 (2)	128.4 (8)

[a] Number in parentheses are estimated standard deviations in the least significant digit.

$(\eta^3\text{-}C_9H_7)W(CO)_2(\eta^5\text{-}C_9H_7)$.[14] This strongly supports the simple η^5-indenyl ligand in these compounds The local geometry of the Mo moiety can be viewed as the classical "piano-stool" with two carbonyl groups and two terminal allyl carbons of the C_7H_7 ring forming the "four legs". The same geometry was observed in the Cp compound.

The $M(CO)_3$ fragment is η^4 coordinated to the diene part of the C_7H_7 ring. The distances of the metal to the inner diene carbons (C11 and C12) are shorter than to the outer diene carbons (C13 and C17) which, together with the similar carbon-carbon bond distances in the coordinated diene (for FeMo: 1.40-1.42 Å; for OsMo: 1.41-1.46 Å) indicate strong interaction between the metal and the diene part of the ring.[15] In the free, uncoordinated diene an obvious short-long-short pattern for these bond distances is observed. The geometry of the metal center can be viewed as an approximate square-pyramid with two CO ligands and two olefin bonds in the basal plane and the remaining CO at the apical position. The same geometry is observed in the Cp complex.[12]

Finally, the C_7H_7 ring in compounds **3a** and **3c** exists in a chair conformation which is the same as in all known trans compounds.[3,12] This is another distinctive difference from the cis compounds which normally appear in a boat conformation for their C_7H_7 ring. The different geometries between trans and cis compounds appear to have significant effect on the dynamic behavior of these compounds which will be discussed later.

4.2.3. Fluxional Behavior of trans-$(\mu\text{-}C_7H_7)M(CO)_3Mo(CO)_2(\eta^5\text{-}C_9H_7)$ (M=Fe, Ru, Os).

Cotton's objective for the preparation of the trans compound

$(\mu\text{-}C_7H_7)Fe(CO)_3Mo(CO)_2(\eta^5\text{-}C_5H_5)$ was to investigate how the simultaneous attachment of two metal moieties without a metal-metal bond would affect the whizzing rate of the cycloheptatrienyl ring, as compared to the rates in mononuclear systems and in dinuclear compounds with a metal-metal bond. The mechanism for metal migration in the trans compound was also of interest. A line-shape analysis of the variable temperature ^1H NMR spectra indicated that the predominant rearrangement process in the Cp compound was either a 1,2- or a mixture of 1,2- and 1,3-metal shifts.[7] With a series of similar trans compounds at hand, it was clearly worthwhile to determine and compare the fluxional behavior of **3a-c** with the Cp analogue.

The room temperature ^1H NMR spectrum of FeMo **3a** shows no peak for the C_7H_7 ring protons (Figure 4.1). Upon lowering the temperature to 0°C three broad peaks appear. At -40°C the low temperature limiting spectrum is obtained and gives four well-separated peaks in a ratio of 2:2:2:1. The line shape changes in compounds **3b** and **3c** were similar except that the low temperature limiting spectra were reached at higher temperatures (-20°C for RuMo, 10°C for OsMo, respectively).

Since Cotton's experience with the analogous Cp compound showed that line shape analysis does not lead to an unambiguous identification of the mechanism of metal migration, a more sensitive probe was sought for this purpose. The multisite magnetization transfer (MMT) method is particularly useful in this regard, and has been used by McClung et al. to analysize complex fluxional processes of related organometallic systems containing the C_7H_7 ring ligand.[16] The experiment involves in irradiating one of the exchanging sites by selective inversion of the magnetization. The exchange process transfers the label to other exchanging sites in the molecule, where it can be detected by measuring the magnetization from the time of inversion until thermal equilibrium is retained. Since all sites are monitored, very precise information about the dynamic pathway and mechanism can be obtained.

Based on the experiments it was determined that for compounds **3a-c** the metal moieties migrated around the C_7H_7 ring with a series of intramolecular 1,2 shifts. The 1,2-shift is the common process elucidated for organometallic compounds with an η^3-C_7H_7 ligand.[17,18] Such a shift can be achieved by rotation of the ML_n fragment as it moves from a site to next, in effect accompanied by another ligand movement such as carbonyl scrambling. Another possibility is a sliding motion of the ML_n fragment with no relationship to other ligand movement. The identification of the two processes can rely on the activation energies of the two related processes, metal migration and ligand scrambling. If the two movements have identical activation energies the metal migration with rotation is indicated. Unfortunately, in our case, the unavailability of ^{13}C enriched samples made it impossible to gain information on the carbonyl scrambling process. But based on the ligand size we postulate that the process may go through a 1,2-slide motion with the least movement of the indenyl ligand. In fact, a similar 1,2-slide mechanism has been deduced for the Rh(COD) fragment in trans-(μ-C_7H_7)$Os(CO)_3$Rh(COD).[3] A possible pathway for 1,2-slide motion of the $M(CO)_3$ and $Mo(CO)_2(\eta^5\text{-}C_9H_7)$ groups is depicted in scheme 4.4. The formation of the 3-center 2-electron intermediate is achieved by bonding to the terminal carbon atoms of the diene part from the 16 electron $Mo(CO)_2(\eta^3\text{-}C_9H_7)$ fragment.[19] Similar 3-center 2-electron bonding has been observed in coordinatively unsaturated Rh complex and has been postulated in the related trans-(μ-C_7H_7)$Os(CO)_3$Rh(COD).[3]

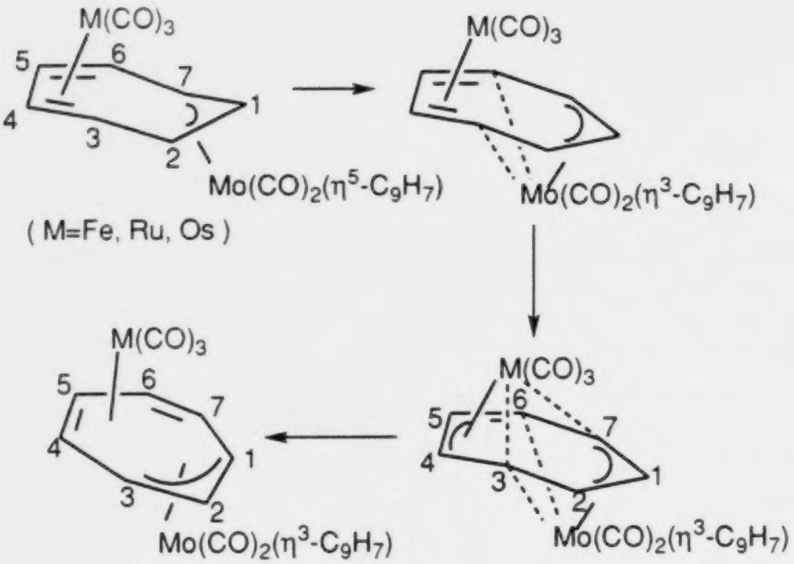

(Scheme 4.4)

The rate constants and activation parameters of the 1,2 shift process are recorded in Table 4.4 and 4.5. The free energies of activation at 298 K are 55 kJ mol^{-1} for **3a**, 60 kJ mol^{-1} for **3b** and 73 kJ mol^{-1} for **3c**, respectively. The value for **3a** is similar to the analogous Cp compound, trans-(μ-C_7H_7)Fe(CO)$_3$Mo(CO)$_2$(η^5-C_5H_5). The activation energies are significantly higher than in related cis-compounds. For instance in cis-(μ-C_7H_7)Os(CO)Rh(COD), a molecule which also contains Os and a second row metal, $\Delta G^{\ddagger}$ is 43 kJ mol^{-1} some 30 kJ mol^{-1} lower than in **3c**.

The differences in fluxional behavior between cis- and trans compounds can be supported by the X-ray structural data. The conformation of the bridging C_7H_7 ring is different in the two classes, boat form in cis- and chair form in trans compounds. Comparison of the two conformations indicates that the allyl and diene parts are further separated in the trans compounds. The distances between the two parts are longer in trans compounds (1.48~1.53 Å in **3a** and **3c**) than in cis compounds (1.45-1.46 Å).[1,3] Also, the torsional angles (φ) between two π systems is different. The values of 57° and 64° in **3a** and **3c** are much larger than those in cis compounds (23° and 21°C).[1,3] and imply that the delocalization of the π electrons in the C_7H_7 ring is more limited in trans compounds. Consequently metal migration in the latter is more difficult than in cis-(μ-C_7H_7)MM' derivatives.

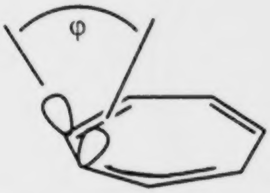

Table 4.4. Rate constants of metal migration in (μ–C_7H_7)M$(CO)_3$Mo$(CO)_2$(η^5-C_9H_7) (**3**) (M=Fe **a**, Ru **b**, Os **c**).

FeMo		RuMo		OsMo	
Temp[a]	Rate[b]	Temp[a]	Rate[b]	Temp[a]	Rate[b]
251.6	6.625	275.2	16.90	324.0	9.010
244.7	2.834	262.4	4.010	320.0	6.165
237.2	0.950	251.2	0.866	312.7	3.460
230.2	0.284	249.8	0.700	308.2	2.400
227.5	0.325	238.8	0.094		

[a]Units for temperature are degree of Kelvin. [b]Units for rate constant are s^{-1}.

Table 4.5. Activation parameters of metal migration in $(\mu-C_7H_7)M(CO)_3Mo(CO)_2(\eta^5-C_9H_7)$ (**3**) (M=Fe **a**, Ru **b**, Os **c**) (kJ mol^{-1}).[a,b].

Compound	$\Delta H^\ddagger$	St.D	$\Delta S^\ddagger$	St.D	$\Delta G^\ddagger$	Error[c]
FeMo	67.24	2.88	39.7	11.8	55.41	6.4
RuMo	70.25	2.18	35.0	8.6	59.86	4.7
OsMo	67.48	1.48	-19.2	4.7	73.00	2.9

[a] At 298 K. [b]Activation parameters $\Delta H^\ddagger$ and $\Delta S^\ddagger$ calculated from the rate constants using a non-linear least squares fitting procedure. Units for $\Delta S^\ddagger$ are J/mole K.[c] Errors calculated by summation of one standard deviation for $\Delta H^\ddagger$ and $\Delta S^\ddagger$.

The somewhat larger separation between the allyl and diene parts in **3c** (1.53 Å) than in **3a** (average 1.49 Å) is in the right direction for the observed activation energy for metal migration. Also the trend in $\Delta G^\ddagger$ (FeMo≤RuMo<OsMo) is consistent with the well-known increase in metal-ligand bond strength while descending a transition metal triad.

4.2.4. Characterization of the Byproduct, $(\eta^3-C_7H_7)Mo(CO)_2(\eta^5-C_9H_7)$ from Decomposition of $(\mu-C_7H_7)Ru(CO)_3Mo(CO)_2(\eta^5-C_9H_7)$ on the Silica Gel Column.

Purification of compound **3b** was initially attempted via silica gel column chromatography. The effort failed to afford the pure product. Instead, compound **3b** decomposed and two mononuclear compounds were obtained. The first major component proved to be $(\eta^4-C_7H_8)Ru(CO)_3$. The second compound was isolated as red-brown crystals **7**.

Based on the mass spectrum and element analysis, compound **7** was formulated as $(C_7H_7)Mo(CO)_2(C_9H_7)$. The IR spectrum of **7** showed two carbonyl bands in the terminal CO region (υ_{CO}=1959, 1896 cm^{-1}) which was consistent with the above formula. The ^1H NMR spectrum at room temperature displayed a broad time averaged signal at 4.15 ppm due to the C_7H_7 ring, in addition to the typical resonances from an η^5-indenyl group. The molecule is highly fluxional, the rotation of the C_7H_7 ring could be frozen out only at -80°C. At this temperature four peaks in the ratio of 2:2:2:1 were observed (Figure 4.4). According to ^1H-^1H decoupling experiments at -95°C, where the better resolution of the proton coupling was observed, the upfield triplet at -2.78 ppm was assigned to H_a, the triplet at 3.82 ppm to H_b, the multiplet at 6.12 ppm to H_c, the multiplet at 5.20 ppm to H_d.

Comparison of the IR and NMR spectral data of **7** with the analogous Cp compound, $(\eta^3-C_7H_7)Mo(CO)_2(\eta^5-C_5H_5)$,[22] shows very similar features. The low temperature (-110°C) ^1H NMR spectrum of the C_7H_7 ring for the Cp compound (H_c 6.12, H_d 4.95, H_b 3.76 and H_a 1.13 ppm) is similar to that of compound **7**, except for the position of H_a (Figure. 4.4). Based on arguments presented before, the about 4 ppm upfield shift of the H_a resonance is attributed to the shielding effect of the indenyl ring. Therefore the structure of **7** is $(\eta^3-C_7H_7)Mo(CO)_2(\eta^5-C_9H_7)$.

Interestingly, only two bands are observed in the IR spectrum of **7**, which indicates the presence of one compound in solution. This is different from the analogous Cp compound, $(\eta^3-C_7H_7)Mo(CO)_2(\eta^5-C_5H_5)$[22] and the related $(\eta^5-C_9H_7)Mo(CO)_2(\eta^3-C_3H_5)$ complex,[12] where an equilibrium between two conformers (*endo* and *exo*) of the C_7H_7/C_3H_5 ligands exist in solution (Scheme 4.5).

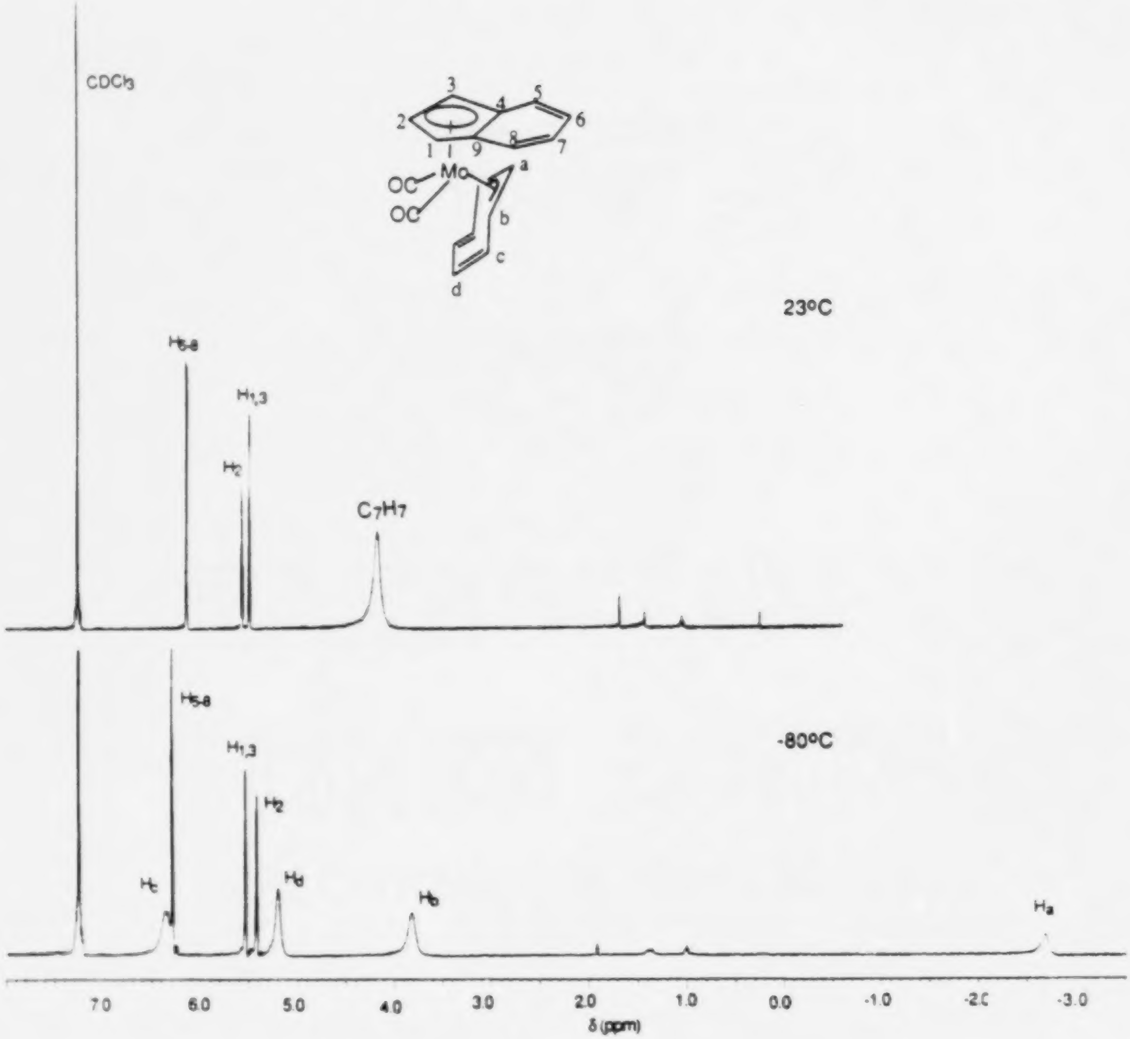

Figure 4.4 ^1H NMR spectra (360 MHz) of $(\eta^5\text{-}C_9H_7)Mo(CO)_2(\eta^3\text{-}C_7H_7)$ (**7**).

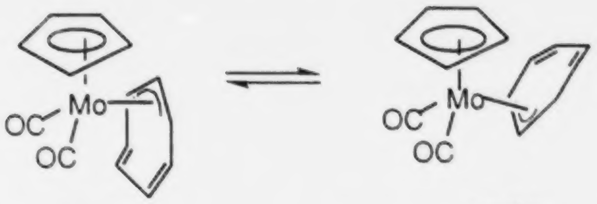

exo **endo**

(Scheme 4.5)

Based on the chemical shift argument, **7** appears to have an *exo* conformation for its C_7H_7 ring. Only in the *exo* form H_a experiences the strong shielding effect of the indenyl ring. The observation of only one rotamer for **7** may be explained by the steric interaction between indenyl ligand with the C_7H_7 ring.

4.2.5. Characterization of the Minor Product from Reaction of $(\eta^3\text{-}C_7H_7)Os(CO)_3^-$ with $[(\eta^5\text{-}C_9H_7)Mo(CO)_2(CH_3CN)_2]^+$.

As mentioned at the beginning of this chapter, two bimetallic complexes were obtained from the osmium reaction. Unexpectedly, the mass spectrum and elemental analysis of the second product **5c** were identical to those of trans-$(\mu\text{-}C_7H_7)Os(CO)_3Mo(CO)_2(\eta^5\text{-}C_9H_7)$ (**3c**), but subtle differences in their spectroscopic features clearly indicated that the structures of **3c** and **5c** were different.

As with compound **3c** the IR spectrum of **5c** showed five well separated CO bands in the terminal carbonyl region (υ_{CO}=2072s, 2006s, 1985s, 1943m, 1879s cm^{-1}) (Figure 4.5). Most of the bands in **5c** were at slightly higher frequency than in **3c** (υ_{CO}=2062s, 1990s, 1982s, 1947m, 1876s cm^{-1}). But, the most notable differences between them were the larger separation between the second and the third band (21 cm^{-1} in **5c**, only

8 cm^{-1} in **3c**) and the reversal of the relatively intensity of the two lowest frequency bands. Since the three highest frequency bands could confidently be assigned to the Os(CO)$_3$ moiety, the larger splitting between the second and third bands in **5c** was indicative of a greater distortion from local C_{3v} symmetry of the Os(CO)$_3$ moiety in this compound. A distortion of the Mo(CO)$_2$ unit was also indicated by the calculated (OC)Mo(CO) angle, based on the relative band intensities (Scheme 4.6).[23] The estimated angle in **3c** was 82°, in good agreement with the X-ray determinated value of 81.7°, whereas the value for compound **5c** was 108°. The bigger angle is presumably due to some sort of steric interaction in **5c**.

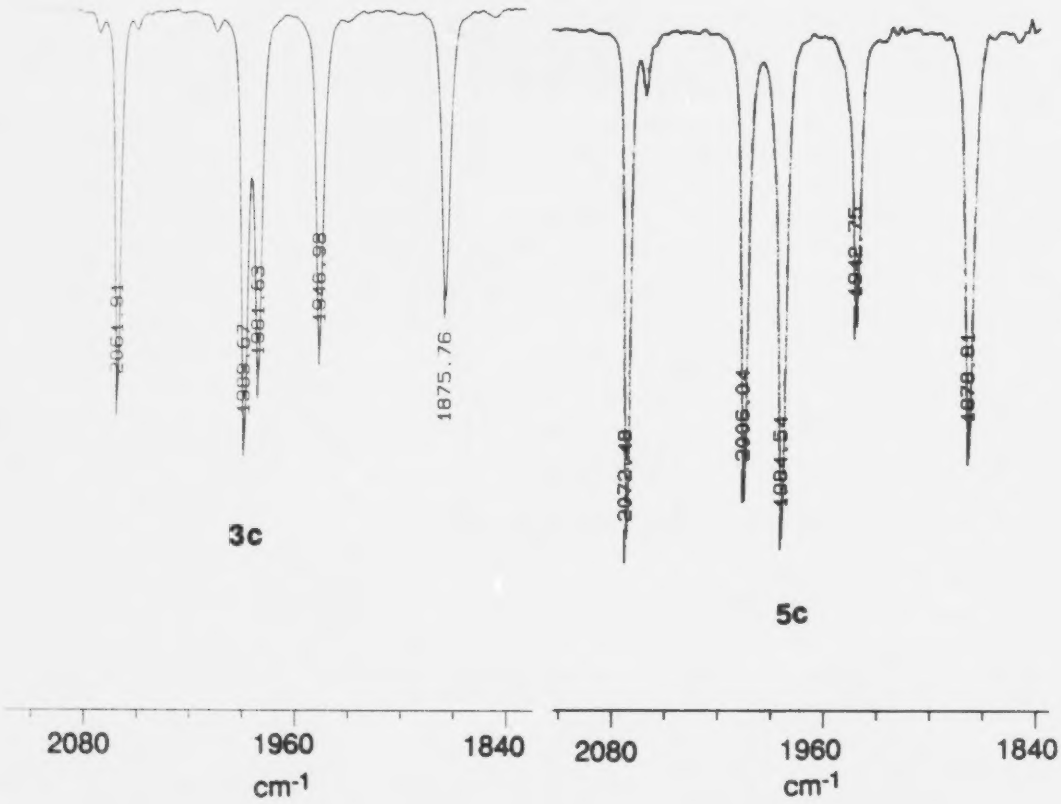

Figure 4.5 Infrared spectra of trans-**3c** and cis-(μ-C_7H_7)Os(CO)$_3$Mo(CO)$_2$(η^5-C_9H_7) (**5c**).

$$\frac{\mathbf{I}(1)}{\mathbf{I}(2)} = \frac{\mathbf{R}^2_{sym}}{\mathbf{R}^2_{asym}} = \text{cotan}^2\theta$$

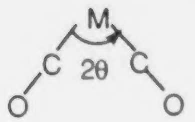

I = intensity of CO band
R = vector dipole

(Scheme 4.6)

The room temperature ^1H NMR spectra of two products **3c** and **5c** (Figure 4.6) were very similar, except for the significant upfield shift (-1.25 ppm) of the central allyl proton in **5c**. As argued before, the upfield shift of a resonance is suggestive of greater shielding from the indenyl ring.

The simplest explanation of the obtained data could be the existence of two isomers which are related by rotation of the C_7H_7 ring (Scheme 4.7). Indeed, it was already mentioned that at room temperature $(\eta^5\text{-}C_5H_5)Mo(CO)_2(\eta^3\text{-}C_7H_7)$ exhibited an equilibrium between *exo* and *endo* isomers, although the analogous indenyl compounds discussed in the previous section did not have the same equilibrium.

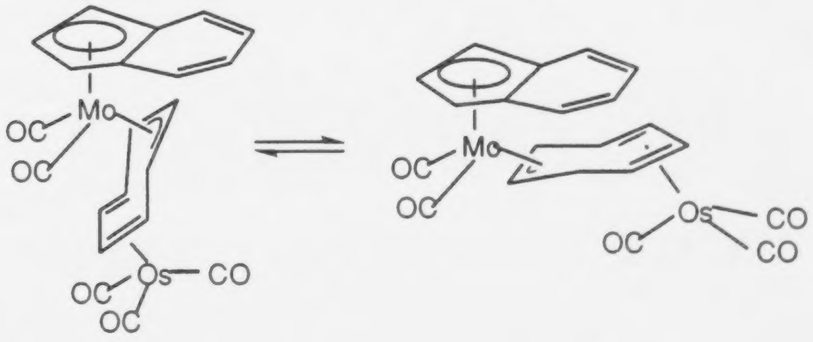

(*exo*) (*endo*)

(Scheme 4.7)

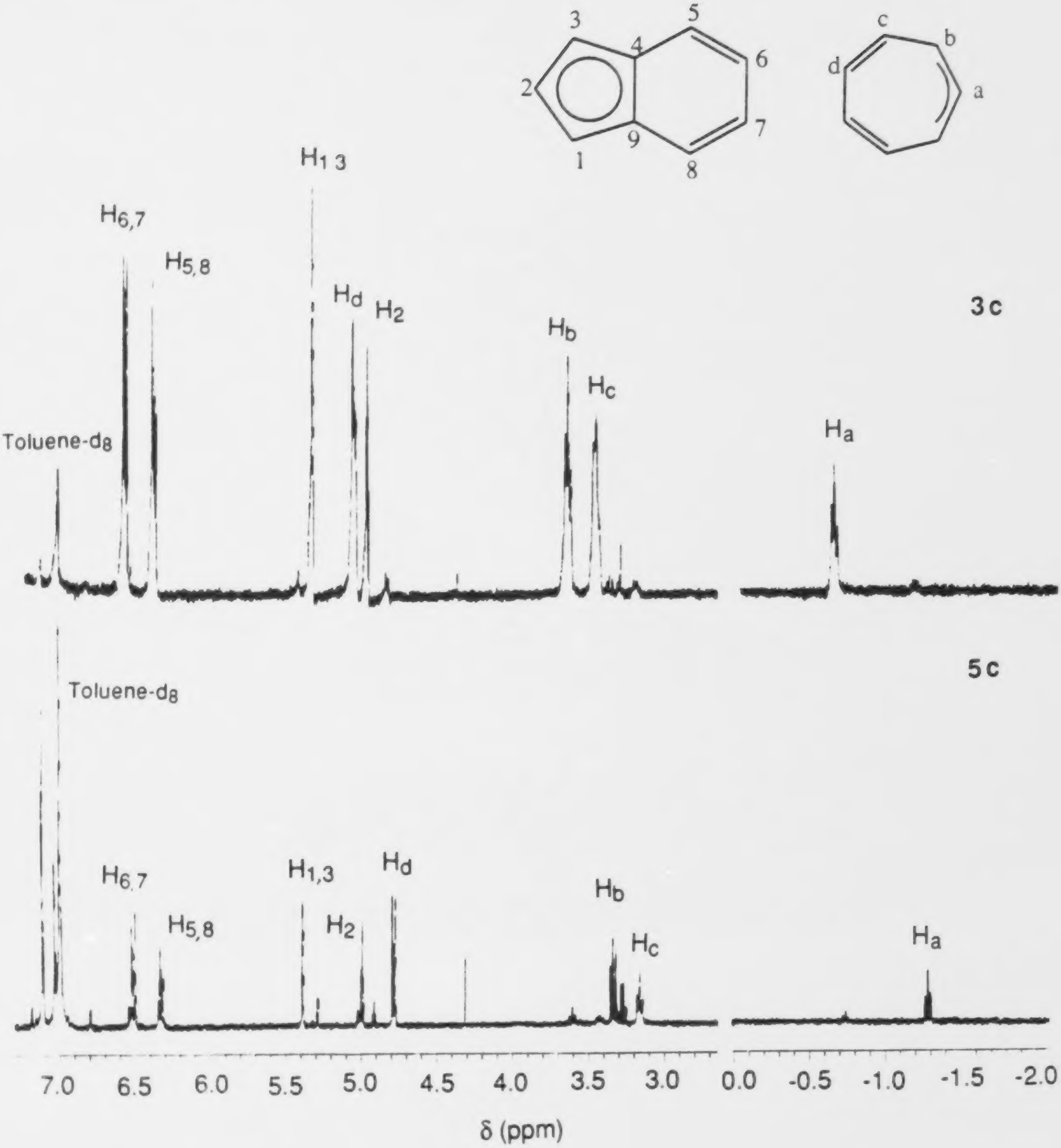

Figure 4.6 ^{1}H NMR spectra (400 MHz) of **3c** and **5c**

X-ray crystallography had clearly established that compound **3c** had the *exo* arrangement, this then would imply that compound **5c** had an *endo* configuration. However, this is contrary to the shielding arguments presented above. Therefore the possibility of simple rotameric relationship between **3c** and **5c** was ruled out at this point.

There were of course other isomeric structures that could have been proposed for **5c**. In fact, two possible cis-type structures, cis-$(\mu\text{-}\eta^3,\eta^4\text{-}C_7H_7)M(CO)_3Mo(CO)_2(\eta^3\text{-}C_9H_7)$ and cis-$(\mu\text{-}\eta^3,\eta^2\text{-}C_7H_7)M(CO)_3Mo(CO)_2(\eta^5\text{-}C_9H_7)$ were shown at the beginning of this chapter. However, the fluxionality of the cis-type compounds should be higher than that shown by **5c** in which the C_7H_7 ring is static at room temperature. Also, the high field of H_a signal was still best accommodated by an *exo* orientation the C_7H_7 ring towards the indenyl ring in which the H_a proton is under the shielding region of the indenyl ligand. It was difficult to see how the above mentioned cis structures could yield such an arrangement.

Another possible structure for **5c** is to change the conformation of the C_7H_7 ring from the chair form to the boat form, but still keeping the trans arrangement of two metal moieties (Scheme 4.8). In this structure the bonding modes for both C_7H_7 ring and the indenyl ring would be same as in **3c**. The only difference is the conformation of the C_7H_7 ring. To account for the presence of **3c** and **5c** it must be assumed that the conformational exchange between the chair and boat forms is stopped. This appears unlikely, but it may be possible as a result of strong Os-C bonds.

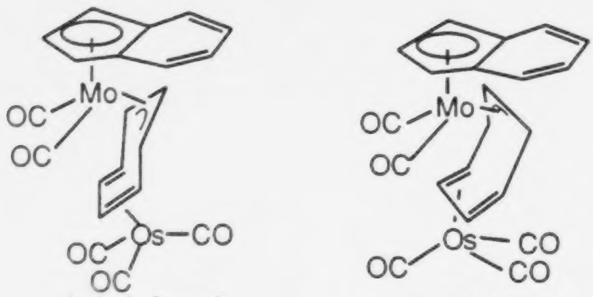

(chair form) (boat form)

(Scheme 4.8)

Since the above possibility for the structure of **5c** represents a highly unusual form and no other obvious structure can accommodate all the spectroscopic data, the molecular structure of **5c** was determined by X-ray crystallography. The perspective view of **5c** is shown in Figure 4.7.

Surprisingly, the figure shows that two metal fragments occupy the same face of the C_7H_7 ring. The molecule adopts a cis-type structure but with important differences from the typical cis-(μ-C_7H_7)MM' structures.[1] Although the conformation of the bridging C_7H_7 ring in **5c** is still the boat form, now the $Os(CO)_3$ moiety is bonded to the diene part in an η^4-fashion and the (indenyl)$Mo(CO)_2$ group via an η^3-fashion. Both metal centers achieve their 18 electron configurations and consequently there is **no** metal-metal bond between the two metal moieties. The very long distance between the two metal atoms (3.94 Å) agrees with this. Thus two components differ only by the location of the two metal fragments with respect to the bridging C_7H_7 ring.

Unfortunately, due to poor crystal quality and extensive decomposition during the data collection, the structure of **5c** could not be properly refined and the resulting structural parameters are not accurate.

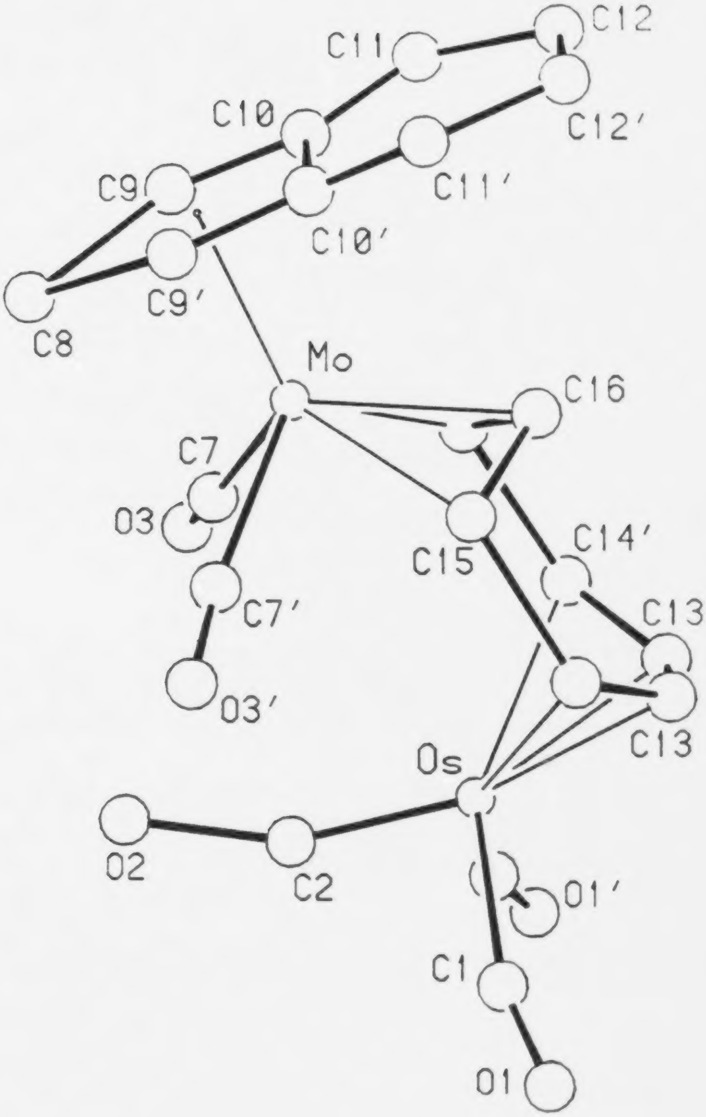
C12
C11
C10
C12'
C9
C11'
C10'
C9'
C8
Mo
C16
C7
O3
C14'
C15
C13'
C7'
O3'
C13
Os
O2
C2
O1'
C1
O1

Figure 4.7 Perspective view of cis-(μ-C_7H_7)Os$(CO)_3$Mo$(CO)_2$(η^5-C_9H_7) (**5c**).

Thus a comparison between the structures of cis-**5c** and trans-**3c** is not possible. Nevertheless, it is still clear from figure 4.6 that the orientation of the C_7H_7 ring is exo with respect to the indenyl ligand and that H_a of **5c** is indeed in the shielding region of the indenyl ring. Furthermore, the cis arrangement of the two metal fragments without the metal-metal bond results in severe congestion between the carbonyl ligands and causes structural distortions. The most evident is the opening up of the (OC)Mo(CO) angle to accommodate the apical Os(CO) ligand. A result which was predicted from the IR spectrum of this molecule.

4.2.6. Reactions of $(\eta^3\text{-}C_7H_7)M(CO)_3^-$ (M=Fe, Ru, Os) with $[(\eta^5\text{-}C_5H_5)Mo(CO)_2(CH_3CN)_2]^+$.

Finally, in order to examine the possible effect caused by the indenyl ligand, especially whether its presence was responsible for the formation of trans-**3c** and cis-**5c** in the osmium reaction, the reactions of **1** with $[(\eta^5\text{-}C_5H_5)Mo(CO)_2(CH_3CN)_2]^+$ were also carried out. The experimental conditions and work-up were similar to the indenyl reactions. In all cases the same type of products were obtained, and this was the same in the osmium reactions as well where both trans and cis isomers were isolated. The spectral features of these Cp compounds were very similar to those of indenyl compounds, with the exception of the H_a proton of the bridging C_7H_7 ring which, as expected, occured some 4.5 ppm to low field and gave solid foundation to the argument concerning the shielding effect from the indenyl ligand. Therefore we can conclude that the change of ligand in the electrophile did not alter this reaction pathway.

4.3. Conclusion.

The formation of trans compounds **3** and **4** was unexpected, but interesting. It again demonstrates the variable reactivity of the anion **1**. Based on the results obtained, it seems that although the η^3-C_7H_7 form **A** is the only bonding form for anion **1** (Scheme 4.9),[24] the distribution of the negative charge is not only concentrated on the metal atoms. Calculations[25] have shown that actually, in the η^3 form **A**, a substantial amount of electron density is distributed to the C_7H_7 ring by an Fe-C_{allyl} dπ-back donation. It was further found that the electron density on the η^3-C_7H_7 ring is even higher than in the η^4 form **B**. The latter has been considered as containing a free anionic allyl fragment in the C_7H_7 ring.

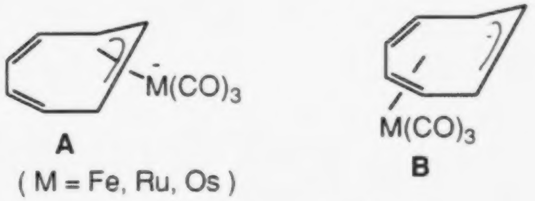

(Scheme 4.9)

Thus "active" electrophiles such as $[(\eta^5\text{-}C_9H_7)Mo(CO)_2(CH_3CN)_2][BF_4]$, R_3GeCl, R_3SiCl can attack to the C_7H_7 ring to form ring substituted trans compounds.

Increased M-C back bonding in the order of Fe<Ru<Os leads to higher electron density localized on the C_7H_7 ring in the Os anion (**1c**) than in the corresponding Fe and Ru anions. In consequence, the the C_7H_7 ring of **1c** is more nucleophilic than the Fe and Ru anions. Therefore "less active"

electrophiles ([M"(COD)Cl]$_2$ M"=Rh, Ir) only with the Os anion lead to ring attacked compounds, such as trans-(μ-C_7H_7)Os(CO)$_3$M(COD) (M=Rh, Ir).

There is no a priori reason why the C_7H_7 ring could not be attacked by electrophiles on both sides (Scheme 4.10). The trans compound could be formed by path a and the cis type compound is obtained by path b. Loss of a ligand from the latter will result in the formation of a metal-metal bond and yields the "normal" cis-(μ-C_7H_7)MM' product. The detection of the OsMo compound **5c** is important since it shows that under certain conditions this hitherto unobserved "intermediate" can be trapped (Scheme 4.10).

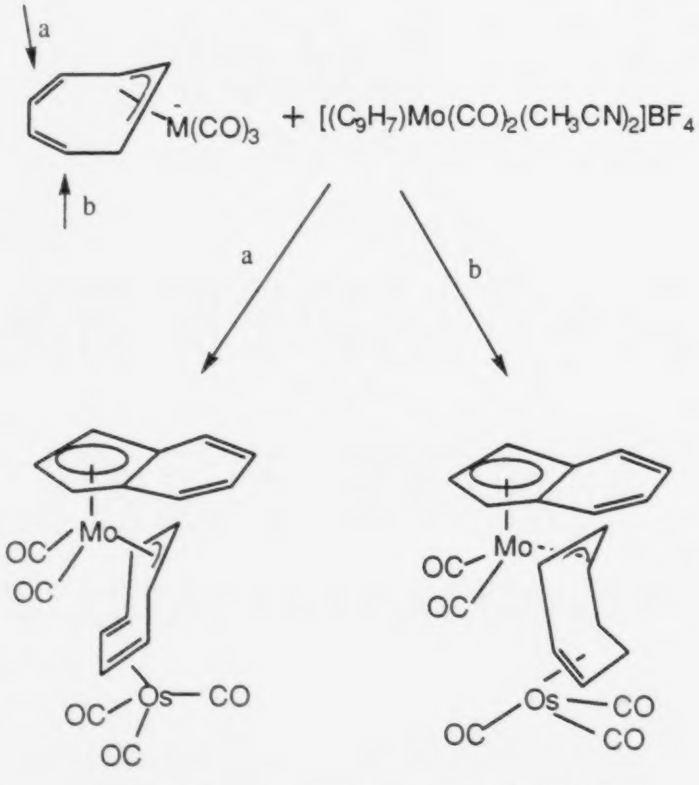

(trans-**3c**)

(cis-**5c**)

(Scheme 4.10)

4.4. Experimental.

4.4.1. Techniques and Reagents

All experimental procedures were performed by using standard Schlenk glassware under a static atmosphere of rigorously purified nitrogen. All solvents were dried by refluxing under nitrogen with the appropriate drying agent and distilled just prior to use.

$Mo(CO)_6$ was purchased from the Ventron Company. Potassium tertiarybutoxide (KO^tBu), Indene, dicyclopentadiene, $HBF_4\cdot$Diethyl ether complex (85%) and CH_3CN were purchased from the Aldrich Chemical Company. KO^tBu was sublimed prior to use (180°C, 10^{-3} mmHg). Indene was distilled prior to use. Dicyclopentadiene was cracked at 180°C in the presence of Fe powder and cyclopentadiene distilled at 45°C. CH_3CN was treated with potassium metal before usage. The following reagents $Li[(\eta^5\text{-}C_9H_7)Mo(CO)_3]$,[26] $(\eta^5\text{-}C_9H_7)Mo(CO)_3CH_3$,[26] $[(\eta^5\text{-}C_9H_7)Mo(CO)_2(CH_3CN)_2]BF_4$,[27] $Li[(\eta^5\text{-}C_5H_5)Mo(CO)_3]$,[26] $(\eta^5\text{-}C_5H_5)Mo(CO)_3(CH_3)$,[26] $[(\eta^5\text{-}C_5H_5)Mo(CO)_2(CH_3CN)_2]BF_4$,[28] $(\eta^4\text{-}C_7H_8)Fe(CO)_3$,[10] $(\eta^4\text{-}C_7H_8)Ru(CO)_3$[2] and $(\eta^4\text{-}C_7H_8)Os(CO)_3$[3] were prepared according to literature methods.

Infrared spectra were obtained with a Nicolet MX-1 Fourier Transform interferometer and a Bomem MB-100 spectrometer. Mass spectra were taken with an A.E.I. MS-12 spectrometer operating at 16eV or 70eV. NMR spectra were recorded on Bruker WH 200, Bruker WH 360, Bruker AM 400 or Bruker AM 300 spectrometers. Elemental analyses were performed by the Microanalytical Laboratory of this department.

The mechanism of the metal migrations in compounds **3a**, **3b** and **3c** was deduced from selective ^{1}H spin inversion recovery experiments.[16b] These were performed by Ms Gerdy Aarts. Analysis of the data and calculation of the activation parameters from the deduced rate constant were carried out by Ms Gerdy Aarts and Professor R. E. D. McClung using a non-linear least squares fitting procedure.

The solid state X-ray structure determinations of compounds **3a**, **3c** and **5c** were carried out by Dr. Santarsiero of the Structure Determination Laboratory of this department and MSC Molecular Structure Corporation. A limited amount of pertinent experimental data has been extracted from the respective structure reports and are included in this thesis for sake of completeness. Further information including listings of observed and calculated structure factor amplitudes of all reflections may be obtained from Dr. B. McDonald or Dr. J. Takats of this department.

4.4.2. Synthesis of trans-(μ-C_7H_7)$Fe(CO)_3Mo(CO)_2$(η^5-C_9H_7) (3a).

A THF solution (10 ml) of Na(η^3-C_7H_7)$Fe(CO)_3$ (200 mg, 0.78 mmol) was added to a cold (-78° C) suspension of [(η^5-C_9H_7)$Mo(CO)_2(CH_3CN)_2$]BF_4 (358 mg, 0.86 mmol) in THF (5 ml). The addition was completed in 10 minutes and gave a dark red solution. The reaction mixture was allowed to warm up slowly to room temperature. The solvent was removed under vacuum to give a dark red oil. The residue was dissolved in CH_2Cl_2 (2 ml) and the solution was applied to a freshly prepared silica gel column (1x10cm). Elution with hexane gave some (η^4-C_7H_8)$Fe(CO)_3$. Changing to hexane-CH_2Cl_2 (2:1) resulted in the development of a red band which was collected to give a clear red solution.

The solution was concentrated to 3 ml and kept at -20°C overnight to give dark red crystals (112 mg, 30%).

Anal. Calcd. for $C_{21}H_{14}O_5FeMo$: C, 50.64, H, 2.83. Found: C, 50.68, H, 2.83.

Mass Spectrum (16 eV, 200°C); M^+ (498), M^+-*n*CO (*n* = 1 - 5).

IR (hexane): υ_{CO} 2044vs 1982vs 1973s 1952s 1882s cm^{-1}.

^1H NMR (200 MHz, 90°C, toluene-d_8): δ 6.58 (m, 2H, $H_{6,7}$), 6.40 (m, 2H, $H_{5,8}$), 5.23 (d, 2H, $H_{1,3}$), 4.84 (t, 1H, H_2), 3.40 (s, 7H,C_7H_7); (360 MHz, -40°C): 6.44 (m, 2H, $H_{6,7}$), 6.18 (m, 2H, $H_{5,8}$), 5.18 (d, 2H, $H_{1,3}$), 4.62 (t, 1H, H_2), 4.68 (m, 2H, H_d), 3.60 (m, 2H, H_b), 3.41 (t, 2H, H_c), -0.72 (t, 1H, H_a).

^{13}C {^1H} NMR (90 MHz, 25°C, CD_2Cl_2): δ 241.95 (s, MoCO), 211.80 (s, FeCO), 125.54 (s, $C_{6,7}$), 123.53 (s, $C_{5,8}$), 112.84 (s, $C_{4,9}$), 87.57 (s, C_2), 79.60 (s, $C_{1,3}$), 68.00 (s br, C_7).

4.4.3. Synthesis of trans-(μ-C_7H_7)Ru(CO)$_3$Mo(CO)$_2$(η^5-C_9H_7) (3b).

A freshly prepared THF solution (20 ml) of K[(η^3-C_7H_7)Ru(CO)$_3$] (1.8 mmol) was added to a slurry of [(η^5-C_9H_7)Mo(CO)$_2$(CH_3CN)$_2$]BF_4 (785 mg, 1.8 mmol) in THF (10 ml) at -78°C. The addition was completed in 30 minutes and resulted in a dark red solution with a precipitate. The precipitate was filtered off and the solvent was removed at low temperature (-40 to -20°C) under vacuum to give an orange-brown residue. The residue was washed with pentane (3 x 25 ml) at low temperature to remove the byproduct (η^4-C_7H_8)Ru(CO)$_3$. The remaining solid was redissolved in a mixture of CH_2Cl_2-hexane (2:1) (5ml). After one week at -78°C red solids were obtained (826 mg, 48%) which can be further recrystallized to give red crystals.

Anal. Calcd. for $C_{21}H_{14}O_5RuMo$: C, 41.39, H, 2.45. Found: C, 41.23, H, 3.02.

Mass Spectrum (70 eV, 100°C); M^+ (533), M^+-nCO (n = 1 - 5).

IR (hexane): υ_{CO} 2061vs 1997vs 1989s 1948s 1877s cm^{-1}.

^{1}H NMR (360 MHz, -20°C, toluene-d_8): δ 6.48 (m, 2H, $H_{6,7}$), 6.25 (m, 2H, $H_{5,8}$), 5.22 (d, 2H, $H_{1,3}$), 4.75 (t, 1H, H_2), 4.95 (m, 2H, H_d), 3.65 (m, 2H, H_b), 3.55 (t, 2H, H_c), -0.90 (t, 1H, H_a).

$^{13}C\{^1H\}$ NMR (90 MHz, 25°C, CD_2Cl_2): δ 125.52 (s, $C_{6,7}$), 123.71 (s, $C_{5,8}$), 112.95 (s, C4,9), 87.82 (s, C_2), 79.9 (s, $C_{1,3}$).

4.4.4. Isolation of $(\eta^3\text{-}C_7H_7)Mo(CO)_2(\eta^5\text{-}C_9H_7)$ (7).

As in the previous preparation, the reaction of $K[(\eta^3\text{-}C_7H_7)Ru(CO)_3]$ (0.54 mmol) with $[(\eta^5\text{-}C_9H_7)Mo(CO)_2(CH_3CN)_2]BF_4$ (255 mg 0.58 mmol) gave a dark oily residue after the usual work-up. The residue was redissolved in CH_2Cl_2 (2ml) and the solution was applied to a freshly prepared silica gel column (0.7x5cm). Elution with hexane gave a large amount of $(\eta^4\text{-}C_7H_8)Ru(CO)_3$ and a clear red brown solution. The red brown solution was concentrated to about 2 ml. The solution was cooled at -20°C overnight to give **5** as red brown crystals (26mg, 13%).

Anal. Calcd. for $C_{18}H_{14}O_2Mo$: C, 60.35, H, 3.94. Found: C, 59.71, H, 3.80.

Mass Spectrum (70 eV, 160 °C); M^+ (318), M^+-nCO (n = 2).

IR (hexane): υ_{co} 1959s, 1896s cm^{-1}.

^{1}H NMR (360 MHz, 22°C, $CDCl_3$): δ 6.15 (m, 4H, $H_{5\text{-}8}$), 5.49 (d, 2H, $H_{1,3}$), 5.55 (t, 1H, H_2), 4.15 (s, 7H, C_7H_7); (-80°C): 6.20 (m, 4H, $H_{5\text{-}8}$), 5.50 (d, 2H, $H_{1,3}$), 5.42 (t, 1H, H_2), 6.35 (m, 2H, H_c), 5.20 (m, 2H, H_d), 3.82 (t, 2H, H_b), -2.78 (t, 1H, H_a).

^{13}C {^1H} NMR (90 MHz, 25°C, CD_2Cl_2): δ 236.11 (s, MoCO), 125.12 (s, $C_{6,7}$), 123.81 (s, $C_{5,8}$), 111.89 (s, C4,9), 90.16 (s, C_2), 81.30 (s, $C_{1,3}$), 100.54 (s, C_7)

4.4.5. Synthesis of trans-(μ-C_7H_7)$Os(CO)_3Mo(CO)_2$(η^5-C_9H_7) (3c) and cis-(μ-C_7H_7)$Os(CO)_3Mo(CO)_2$(η^5-C_9H_7) (5c).

A freshly prepared THF solution (20 ml) of K[(η^3-C_7H_7)$Os(CO)_3$] (0.55 mmol) was added to a slurry of [(η^5-C_9H_7)$Mo(CO)_2(CH_3CN)_2$]BF_4 (233 mg, 0.55 mmol) in THF (5 ml) at -78°C. The addition was completed in 10 minutes and gave a dark red solution. IR spectrum of the resulting dark red reaction mixture showed complete consumption of the anion and indicated the formation of two new compounds. The mixture was allowed to warm up to -20°C and filtered at low temperature. The solvent was then removed under vacuum between -40 and -20°C to give a brown, oily residue. The residue was redissolved in CH_2Cl_2 and concentrated to ca. 3 ml. Pentane solution (3ml) was added. The mixture was kept at -78°C overnight to give a brown solid which proved to be a mixture of **3c** and **5c** (208 mg, 60% for **3c** and **5c** together). The mixture was redissolved in pentane-CH_2Cl_2 (2:1) solution (10 ml) and kept at -10°C for crystallization. After several fractional crystallizations **3c** and **5c** could be separated, but the procedure is inefficient.

Anal. Calcd. for $C_{21}H_{14}O_5OsMo$ (**3c** and **5c** together): C, 39.88, H, 2.23. Found: C, 39.20, H, 2.51.

Data for 3c, yellow crystals.

Mass Spectrum (16 eV, 210°C); M^+ (632), M^+-*n*CO (*n* = 1 - 5).

IR (hexane): υ_{CO} 2062vs 1990vs 1982s 1947s 1876s cm^{-1}.

^1H NMR (400 MHz, 23°C, toluene-d_8): δ 6.52 (m, 2H, $H_{6,7}$), 6.32 (m, 2H, $H_{5,8}$), 5.28 (d, 2H, $H_{1,3}$), 4.92 (t, 1H, H_2), 5.10 (m, 2H, H_d), 3.65 (m, 2H, H_b), 3.45 (m, 2H, H_c), -0.70 (t, 1H, H_a).

^{13}C {^1H} NMR (90 MHz, 25°C, CD_2Cl_2): δ 241.98 (s, MoCO), 125.24 (s, $C_{6,7}$), 123.41 (s, $C_{5,8}$), 112.79 (s, C4,9), 87.68 (s, C_2), 79.85 (s, $C_{1,3}$), 86.80 (s, C_d), 68.68 (s, C_b), 47.85 (s, C_c), 1.15 (s,C_a).

Data for 5c, red crystals

IR (hexane): υ_{CO} 2072vs 2006vs 1985vs 1943m 1879s cm^{-1}.

^1H NMR (400 MHz, 23°C, toluene-d_8): δ 6.52 (m, 2H, $H_{6,7}$), 6.32 (m, 2H, $H_{5,8}$), 5.38 (d, 2H, $H_{1,3}$), 5.01 (t, 1H, H_2), 4.78 (m, 2H, H_d), 3.35 (t, 2H, H_b), 3.20 (m, 2H, H_c), -1.25 (t, 1H, H_a).

^{13}C {^1H} NMR (90 MHz, 25°C, CD_2Cl_2): δ 241.98 (s, MoCO), 124.72 (s, $C_{6,7}$), 123.27 (s, $C_{5,8}$), 112.79 (s, C4,9), 89.83 (s, C_2), 80.69 (s, $C_{1,3}$), 88.61 (s, C_d), 71.44 (s, C_b), 45.86 (s, C_c), -0.80 (s,C_a).

4.4.6. Synthesis of trans-(μ-C_7H_7)M(CO)$_3$Mo(CO)$_2$(η^5-C_5H_5) (M=Fe 4a, Ru 4b, Os 4c) and cis-(μ-C_7H_7)Os(CO)$_3$Mo(CO)$_2$(η^5-C_5H_5) (6c)

The compounds **4a-4c** and **6c** were prepared according to the procedure outlined above for analogous indenyl derivatives except that column chromatography on silica gel column was used for the separation and isolation of pure products.

Data for 4a, dark red crystals (50 mg, 20%).

Mass Spectrum (70 eV, 200°C); M^+ (448), M^+-*n*CO (*n* = 1 - 5).

IR (hexane): υ_{CO} 2045vs 1982vs 1974s 1952s 1882s cm^{-1}.

^1H NMR (360 MHz, 48°C, Toluene-d_8): δ 4.41 (s, 5H, Cp), 4.17 (s br, 7H, C_7H_7); (-40°C): 4.15 (s, 5H, Cp), 4.87 (m, 2H, H_d), 4.04 (t, 1H, H_a), 3.77 (t, 2H, H_b), 3.53 (m, 2H, H_c).

^{13}C {^1H} NMR (90 MHz, -40°C, $CDCl_3$): δ 242.38 (s, MoCO), 93.43 (s, Cp), 90.02 (s, C_d), 66.19 (s, C_b), 65.12 (s, C_c), 75.43 (s,C_a).

Data for 4b, red orange crystals (10 mg, 4%).

Mass Spectrum (16 eV, 180°C); no M^+ (483) is observed.

IR (hexane): υ_{CO} 2061vs 1997vs 1990s 1949s 1877s cm^{-1}.

^1H NMR (360 MHz, 25°C, $CDCl_3$): δ 5.20 (s, 5H, Cp), 4.91 (s, 7H, C_7H_7); (-40°C): 5.25 (s, 5H, Cp), 5.40 (m, 2H, H_d), 4.47 (m, 3H, $H_{a,b}$), 3.59 (m, 2H, H_c).

Data for 4c. yellow crystals (10mg, 8%)

Mass Spectrum (16 eV, 100°C); no M^+(582) is observed.

IR (hexane): υ_{CO} 2062vs 1989vs 1983s 1947s 1875s cm^{-1}.

^1H NMR (360 MHz, 25°C, Toluene-d_8): δ 4.43 (s, 5H, Cp), 5.18 (m, 2H, H_d), 4.05 (t, 2H, H_b), 3.88 (t, 1H, H_a), 3.40 (m, 2H, H_c).

Data for 6c. orange crystals (5 mg, 4%)

IR (hexane): υ_{CO} 2072s 2006s 1984s 1944m 1877s cm^{-1}.

^{1}H NMR (360 MHz, 25^{o}C, CDCl$_3$): δ 4.43 (s, 5H, Cp), 5.52 (m, 2H, H$_d$), 4.10 (m, 3H, H$_{a,b}$), 3.38 (m, 2H, H$_c$).

4.4.7. X-ray Structure Determination of 3a.

X-ray quality crystals of **3a** were obtained from CH$_2$Cl$_2$/hexane over 2 days at -20 ^{o}C. The structure was solved by Dr. B. D. Santarsiero of the Structure Determination Laboratory of this department. The following information was obtained from the structure report (File number SDL:TAK9002). An orange crystal of **3a** with the approximate dimensions of 0.56 x 0.53 x 0.15 mm, was mounted on a glass fiber with epoxy, and optically centred in the X-ray beam of an Enraf-Nonius CAD4 automated diffractometer. All intensity measurements were performed using Zr-filtered MoK$_\alpha$ radiation (λ = 0.71073 Å).

The automatic peak search and reflection indexing programs generated a monoclinic cell. The systematic absences (h0l, l odd; 0k0, k odd) led to the choice of space group as P2$_1$/c.

The cell constants and orientation matrix were obtained from a least-squres refinement of the setting angles of 24 reflections in the range 16.6^o<2θ<25.4^o.

The intensity data were collected at room temperature (23 ^{o}C) with ω-2θ scans at 4.0-1.2^o min^{-1} (in θ). The scan range was varied as a function of θ to compensate for the α_1-α_2 wavelength dispersion: ω scan width=0.50+0.347tanθ.

The backgrounds for the peaks were measured by extending the scan by 25% on either side of the calculated range; this gave a peak-to-background counting time ratio of 2:1. Intensity measurements were made out to a maximum 2θ of 56°. Three reflections were chosen as intensity and orientation standards, and these were remeasured after every 120 min of exposure time to check on the crystal and electronic stability over the course of data collection; no appreciable decay was evident. A summary of the crystallographic data is presented in Table 4.6 Positional and equivalent isotropic parameters for the non-hydrogen atoms are given in Table 4.7.

4.4.8. X-ray Structure Determination of 3c.

X-ray quality crystals of **3c** were grown by slow evaporation of a pentane solution of **3c** The structure was solved by Dr. B. D. Santarsiero of the Structure Determination Laboratory of this department. The following information was obtained from the structure report (File number SDL:TAK9108). A bright yellow crystal of **3c** with the dimensions of 0.30 x 0.14 x 0.06 mm, was mounted on a glass fiber with epoxy, and optically centred in the X-ray beam of an Enraf-Nonius CAD4 automated diffractometer. All intensity measurements were performed using Zr-filtered MoK_{α} radiation (λ = 0.71073 Å).

The automatic peak search and reflection indexing programs generated a monoclinic cell. The systematic absences (h0l, l odd; 0k0, k odd) led to the choice of space group as $P2_1/n$, a non-standard setting of $P2_1/c$.

The cell constants and orientation matrix were obtained from a least-squres refinement of the setting angles of 24 reflections in the range $16.4^{o}<2\theta<19.4^{o}$.

The intensity data were collected at room temperature (23 ^{o}C) with θ-2θ scans at 5.0-2.2^{o} min^{-1} (in θ). The scan range was varied as a function of θ to compensate for the α_1-α_2 wavelength dispersion: ω scan width=0.80+0.347tanθ.

The backgrounds for the peaks were measured by extending the scan by 25% on either side of the calculated range; this gave a peak-to-background counting time ratio of 2:1. Intensity measurements were made out to a maximum 2θ of 56^{o}. Three reflections were chosen as intensity and orientation standards, and these were remeasured after every 120 min of exposure time to check on the crystal and electronic stability over the course of data collection; no appreciable decay was evident. A summary of the crystallographic data is presented in Table 4.8. Positional and equivalent isotropic parameters for the non-hydrogen atoms are given in Table 4.9.

4.4.9. X-ray Structure Determination of 5c.

X-ray quality crystals of **5c** were grown by slow evaporation of a pentane solution of **5c**. The structure was solved by Dr. B. D. Santarsiero of the Structure Determination Laboratory of this department. The following information is the brief crystal data of **5c**: Pnma (No. 62), a=7.463Å, b=12.169Å, c=21.375Å, V=1941Å^3, z=4, ρ_{calc}=2.274 g cm^{-3}, μ=72.232 cm-1, T=-130^{o}C, radiation=MoK$_{\alpha}$(0.717073Å), R=0.178, R$_w$=0.180, GOF=7.162.

Table 4.6. Crystallographic data of (μ-C_7H_7)Fe(CO)$_3$Mo(CO)$_2$(η^5-C_9H_7) (**3a**)

A. Crystal Data

$C_{21}H_{14}FeMoO_5$; FW = 498.13

Crystal dimensions: 0.56 × 0.53 × 0.15 mm

monoclinic space group $P2_1/c$ (No. 14)

$a = 10.250\ (4)$, $b = 6.810\ (1)$, $c = 28.516\ (10)$ Å

$\beta = 106.93\ (3)°$

$V = 1904.5$ Å^3; $Z = 4$; $D_c = 1.737$ g cm^{-3}; $\mu = 14.33$ cm^{-1}

B. Data Collection and Refinement Conditions

Radiation:	Mo K_α ($\lambda = 0.71073$ Å)
Take-off angle:	3.0°
Detector aperture:	2.40 mm horiz × 4.00 mm vert
Crystal-to-detector distance:	173 mm
Scan type:	$\omega - 2\theta$
Scan rate:	4.0–1.2° min^{-1}
Scan width:	$0.50 + 0.347\tan\theta°$
Data collection 2θ limit:	56.0°
Data collection index range:	$h, \pm k, \pm \ell$
Reflections measured:	4956 total, averaged; 3493 with $I > 3\sigma(I)$
Observations:variables ratio:	3493:254
Agreement factors R_1, R_2, GOF:	0.045, 0.060, 2.071
Corrections applied:	absorption correction

Table 4.7. Fractional coordinates and equivalent isotropic thermal parameters for (μ-C_7H_7)Fe(CO)$_3$Mo(CO)$_2$(η^5-C_9H_7) (**3a**).

Atom	x	y	z	U
Mo	246.0 (3)	263.94(5)	320.40(1)	3.137(9)*
Fe	215.16(6)	149.6(1)	480.77(2)	3.94(2)*
O1	85.1(4)	350.9(7)	546.2(1)	7.8(1)*
O2	492.6(4)	301.7(7)	519.5(2)	7.6(2)*
O3	237.2(5)	-218.2(7)	535.9(2)	9.1(2)*
O4	-49.0(3)	392.9(6)	312.1(1)	6.3(1)*
O5	104.7(4)	-141.3(5)	309.7(1)	6.5(1)*
C1	133.0(5)	273.5(8)	519.8(2)	5.3(2)*
C2	384.9(5)	242.3(7)	505.1(2)	4.8(2)*
C3	228.4(5)	-74.3(9)	514.6(2)	5.7(2)*
C4	62.8(4)	347.8(7)	315.8(2)	4.4(1)*
C5	158.3(5)	11.4(7)	313.7(2)	4.4(1)*
C11	65.7(4)	210.7(9)	417.4(2)	5.2(2)*
C12	115.7(5)	21.0(8)	415.7(2)	5.1(2)*
C13	256.1(5)	-6.8(7)	421.6(2)	4.3(1)*
C14	348.7(4)	93.9(6)	397.0(1)	3.7(1)*
C15	369.0(4)	296.4(7)	397.5(1)	3.8(1)*
C16	258.3(4)	418.3(6)	397.6(1)	3.7(1)*
C17	156.3(4)	373.3(7)	423.6(2)	4.4(1)*
C21	251.3(5)	487.2(7)	259.4(2)	4.6(1)*
C22	232.1(5)	301.5(8)	238.7(2)	5.1(2)*
C23	349.9(5)	186.5(8)	260.1(2)	4.9(1)*
C24	447.9(4)	310.0(8)	292.8(2)	4.5(1)*
C25	585.3(5)	279.4(9)	323.7(2)	6.1(2)*
C26	651.1(5)	434(1)	352.2(2)	6.7(2)*
C27	588.5(5)	613(1)	352.6(2)	6.4(2)*
C28	458.2(5)	651.2(8)	324.4(2)	5.3(2)*
C29	385.6(4)	499.8(7)	292.8(2)	4.0(1)*

*Indicates an atom refined anisotropically.
The equivalent isotropic displacement parameter U is $1/3\sum_{i=1}^{3} r_i^2$, where r_i are the root-mean-square amplitudes of vibration.

Table 4.8. Crystallographic data of (μ-C_7H_7)Os(CO)$_3$Mo(CO)$_2$(η^5-C_9H_7) (**3c**).

A. Crystal Data

$C_{21}H_{14}MoO_5Os$: FW = 632.48

Crystal dimensions: 0.30 × 0.14 × 0.06 mm

monoclinic space group $P2_1/n$ (a non-standard setting of $P2_1/c$ [No. 14])

$a = 10.245\ (3)$, $b = 6.804\ (2)$, $c = 27.940\ (6)$ Å

$\beta = 93.70\ (2)°$

$V = 1943.6$ Å^3; $Z = 4$; $D_c = 2.161$ g cm^{-3}; $\mu = 71.99$ cm^{-1}

B. Data Collection and Refinement Conditions

Radiation:	Mo K_α ($\lambda = 0.71073$ Å)
Take-off angle:	3.0°
Detector aperture:	2.40 mm horiz × 4.00 mm vert
Crystal-to-detector distance:	173 mm
Scan type:	$\theta-2\theta$
Scan rate:	5.0–2.2° min^{-1}
Scan width:	$0.80 + 0.347 \tan\theta°$
Data collection 2θ limit:	56.0°
Data collection index range:	$h, \pm k, \pm \ell$
Reflections measured:	5043 total, averaged; 1926 with $I > 3\sigma(I)$
Observations:variables ratio:	1926:149
Agreement factors R_1, R_2, GOF:	0.064, 0.086, 2.091
Corrections applied:	absorption correction

Table 4.9. Fractional coordinates and equivalent isotropic thermal parameters for (μ-C_7H_7)Os$(CO)_3$Mo$(CO)_2$(η^5-C_9H_7) (**3c**).

Atom	*x*	*y*	*z*	*U*
Os	264.5(1)	144.4(2)	980.38(4)	3.30(3)*
Mo	74.5(2)	261.7(4)	818.75(8)	2.75(6)*
O1	296(3)	-234(4)	1037.1(7)	8.3(9)*
O2	25(2)	307(3)	1023.9(7)	6.4(8)*
O3	469(2)	353(4)	1046.2(9)	8.2(9)*
O4	206(2)	-148(3)	808.3(7)	5.6(7)*
O5	358(2)	395(3)	812.4(7)	5.5(8)*
C1	279(3)	-85(5)	1015(1)	5.6(9)
C2	121(3)	253(5)	1010(1)	4.5(8)
C3	393(3)	277(4)	1020(1)	4.6(8)
C4	158(3)	1(4)	811.6(9)	4.0(7)
C5	251(2)	349(4)	815.3(8)	3.1(6)
C11	301(3)	11(5)	911(1)	4.5(8)
C12	355(3)	201(4)	912(1)	4.9(8)
C13	269(2)	367(4)	921.0(8)	2.7(6)
C14	138(3)	415(4)	894(1)	4.2(8)
C15	27(2)	295(4)	893.4(8)	2.7(6)
C16	46(2)	92(4)	893.6(8)	2.7(6)
C17	165(2)	-12(4)	916.1(9)	4.0(7)
C21	-89(3)	192(4)	759(1)	4.2(8)
C22	9(3)	301(4)	739(1)	4.1(8)
C23	9(2)	489(4)	759.8(9)	3.1(6)
C24	-92(3)	500(5)	792(1)	4.3(7)
C25	-137(3)	641(5)	820.4(9)	4.4(7)
C26	-237(3)	614(5)	852(1)	6.0(9)
C27	-300(3)	432(5)	851(1)	7(1)
C28	-263(3)	285(5)	823(1)	5.8(9)
C29	-158(3)	302(4)	791(1)	4.3(8)

*Indicates an atom refined anisotropically.
The equivalent isotropic displacement parameter *U* is $1/3\sum_{i=1}^{3} r_i^2$, where r_i are the root-mean-square amplitudes of vibration.

4.5. References

1. (a).Bennett, M. J.; Pratt, J. L.; Simpson, K. A.; LishingMan, L. K. K.; Takats, J., *J. Am. Chem. Soc.*, **1976**, *98*, 4810

   (b).Edelmann; F.; Takats, J.; *J. Organomet. Chem.*, **1988**, *344*, 351

2. (a).Edelmann, F.; Kiel, G. Y.; Takats, J.; Vasudevamurthy, A.; Yeung, M. Y., *J. Chem. Soc.,Chem. Commun.* **1988**, 296

   (b).Astley, S. T.; Takats, J., *J. Organomet. Chem.,* **1989**, *363*, 167

3. Astley, S., *Ph. D. Thesis,* University of Alberta, **1989**, chapter *4*

4. (a).LiShingMan, L.K.K.; Reuvers, J. G. A.; Takats,J.; Deganello, G., *Organometallics* **1983**, *2*, 28

   (b).Reuvers, J. G. A.; Takats, J., *Organometallics* **1990**, *9*, 578

5. Salzer, A.; Egolf, T.; Philipsborn, W. von, *Helv. Chim. Acta* **1982**, *65*,1145

6. Arioldi, M.; Deganello, G.; Gennaro, G.; Moret, M.; Sironi, A., *J. Chem. Soc. Chem. Commun.* **1992**, 850

7. Cotton, F. A.; Reich, C. R., *J. Am. Chem. Soc.* **1969**, *91*, 847

8. Merola, J. S.; Kacmarcik, R. T.; Engen, D. Van., *J. Am. Chem. Soc.* **1986**, *108*, 329

9. Burton, R.; Pratt, L.; Wilkinson, G., *J. Chem. Soc.* **1961**, 594

10. King, R. B.; Bisnette, M. B., *Inorg. Chem.*, **1965**, *4*, 475

11. Faller, J. W.; Chen, C. C.; Mattina, M. J.; Jakubowski, A., *J. Organomet. Chem.*, **1973**, *52*, 361

12. Cotton, F. A.; DeBoer, B. G.; LaPrade, M. D., *Abstract of the XXIIIrd IUPAC Conference,* Boston, **1971**, Vol.*3*, 1

13. Cotton, F. A.; Murillo, C. A.; Stults, B. R., *Inorg. Chim. Acta,* **1977**, *22*, 75

14. Nesmeyanov, A. N.; Ustynyuk, N. A.; Makarova, L. G.; Andrianov, V. G.; Struchkov, Yu. T.; Steffen, A.; Ustynyuk, Tu. A.; Malyugina, S. G., *J. Organomet. Chem.*, **1978**, *159*, 189

15. Cotton, F. A.; Wilkinson, G., *"Advanced Inorganic Chemistry"* Wiley, NewYork, **1972**, third edition, p. 728

16.(a).Mann, B. E., *Adv. Organomet. Chem.*, **1988**, *28*, 397

(b).Muhandiram, D. R.; McClung, R. E. D., *J. Magn. Reson.*, **1987**, *71*, 187

17. Kiel, G. Y.; Takats, J., *Organometallics* **1987**, *6*, 2009

18. Mann, B. E. *"Comprehensive Organonetallic Chemisty"*, (Edited by Wilkinson, G.; Stone, F. G. A.; Abel, E. W.), Pergamon Press, Oxford, **1982**, Vol. *3*, p. 132.

19. O'Connor, J.; Casey, C. P., *Chem. Rev.* **1987**, *87*, 307

20. Ceccon, A.; Gambaro, A.; Santi, S.; Valle, G.; Venzo, A.,J. *Chem. Soc. Chem. Comm.* **1989**, 51.

21. Bleeke, J. R.; Donaldson, A. J.,*Organometallics* **1986**, *5*, 2401.

22. Faller, J. W., *Inorg. Chem.*, **1969**, *8*, 767

23. Cotton, F. A.; Wilkinson, G., *"Advanced Inorganic Chemistry"* Wiley, NewYork, **1988**, fifth edition, p. 1035

24. Astley, S. T.; Takats, J., *Organometallics* **1990**, *9*, 184

25. Hofmann, P., *Z. Naturforsch.*, **1978**, *33b*, 251

26. Jolly, W. L., *Inorg. Synth.* **1968**, *11*, 116

27. Allen, S. R.; Beevor, R. G.; Green, M.; Orpen, A. G.; Paddick, K. E.; Williams, L. D., *J. Chem. Soc. Dalton Trans,* **1987**, 591

28. Treichel, P. M.; Barnett, K. W.; Shubkin, R. L., *J. Organomet. Chem.* **1967**, *7*, 449

Chapter 5

Synthesis, Characterization and Reactivity of the (Formylcycloheptatrienyl)tricarbonyliron Anion

$[(CHOC_7H_6)Fe(CO)_3]^-$

5.1. Introduction

Due to its antiaromatic nature the free cycloheptatrienide anion is unstable and difficult to prepare.[1] It has , therefore, been little used in organic synthesis. In contrast, as has been shown in previous chapters, the metal stabilized derivatives $[(\eta^3\text{-}C_7H_7)M(CO)_3]^-$ (M=Fe **1a**, Ru **1b**, Os **1c**) are more easily prepared[2] and their versatile reactivities have been demonstrated by the preparation of different cycloheptatrienyl bridged bimetallic complexes.[3] This raises the possibility that through the reactions of $[(\eta^3\text{-}C_7H_7)M(CO)_3]^-$ (**1**) with organic electrophiles carbon-carbon bond formation and elaboration of the C_7H_7 ring could be achieved. Recent reports of acylation of the C_7H_7 ring by Williams et al.,[4] reactions of the anion **1a** with alkyl chloroformates by Airoldi et al.[5] and nucleophilic addition of the anion **1a** to 2-chlorotropone by Nitta et al.[6] are efforts in this direction (Scheme 5.1).

Until recently, very little information on the behavior of ring substituted C_7H_7 metal derivatives were available,[4a,b,5] although the unsubstituted metal anions **1** have been studied extensively.[2c,7,8] To continue our systematic investigation of cycloheptatrienyl complexes and to add to the efforts of utilizing them in organic synthesis it was decided to study the deprotonation of $[\eta^4\text{-}6\text{-}(CHO)C_7H_7]Fe(CO)_3$ (**2**) to give the formyl-substituted cycloheptatrienyl anion $[(CHOC_7H_6)Fe(CO)_3]^-$ (**3**). This chapter describes the preparation, characterization and preliminary reactivity study of anion **3**.

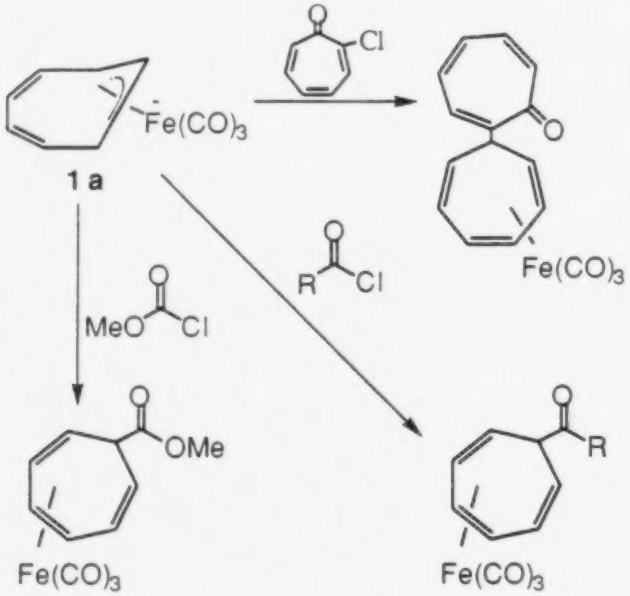

(Scheme 5.1)

5.2. Results and Discussion.

5.2.1. Preparation and Characterization of $[(CHOC_7H_6)Fe(CO)_3]^-$.

Deprotonation of the readily available aldehyde derivative $[\eta^4\text{-}6\text{-}(CHO)C_7H_7]Fe(CO)_3$ (**2**) by $NaN(SiMe_3)_2$ in benzene solution at ambient temperature gave the sodium salt of the anion, **3a**. Under these conditions pure **3a** precipitated directly from the reaction mixture and was isolated in the form of a pyrophoric orange-red powder in 90% yield (Scheme 5.2). Other strong bases, such as KO^tBu, can also be used to deprotonate **2**. The presence of the electron withdrawing CHO group renders anion **3a** less reactive than the unsubstituted anions **1**. Anion **3a** can be stored in a Schlenk tube under N_2 atmosphere at room temperature for several months without apparent decomposition.

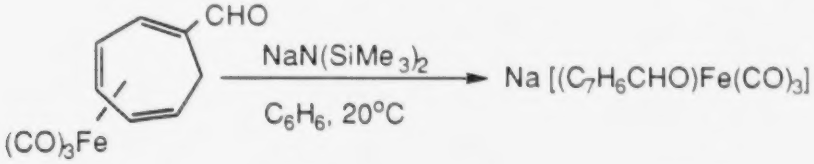

2 (Scheme 5.2) **3a**

The IR spectrum of **3a** (in a THF solution) displayed two broad bands at 1985 and 1910 cm^{-1} in the carbonyl stretching region. The shift of the two bands to lower frequencies with respect to that of the neutral compound **2** was expected and indicated the formation of a negatively charged complex. The fact, that the bands appeared at higher frequencies than in the related unsubstituted anion, $Na[(\eta^3\text{-}C_7H_7)Fe(CO)_3]$ (also in THF, υ_{CO}: 1944, 1869, 1847, 1823 cm^{-1}), was also consistent with the presence of the electron withdrawing formyl substituent on the ring. With possible delocalization onto the CHO group there is more electron density on the C_7H_7 ring and thereby weaker back-bonding to the carbonyl ligands, as observed. Surprisingly, but still in line with the above arguments about the electron delocalization onto the formyl group, the spectrum of **3a** did not show the expected aldehyde band (υ_{CO}, 1684 cm^{-1} in **2**).

The ^1H NMR spectrum at room temperature (Figure 5.1) showed five broad signals, one in the formyl CHO region at 7.92 ppm. The broadness of the resonances was an indication that the molecule was experiencing some sort of rearrangement. This would not be unexpected since $[(\eta^3\text{-}C_7H_7)Fe(CO)_3]^-$ (**1a**) is highly fluxional. Also, it was noted by Airoldi et al. that at room temperature $[(COOEtC_7H_6)Fe(CO)_3]^-$ rapidly rearranges in solution.[5] The non-rigid structure of **3a** was confirmed by variable temperature ^1H NMR studies. The low temperature (-100°C) spectrum (Figure 5.1) shows two sets of resonances, which indicates the presence of two isomers. This is most clearly seen by the appearance of two formyl signals. The isomer ratio is ca. 3:1. This observation is totally different from the unsubstituted anion **1** where only one structure is detected in solution at low temperature.[2c]

Based on the 18 electron rule, there are several possible structures that can be drawn for anion **3a**. Some of these are shown in scheme 5.3. The following comments are intended to tentatively relate the observed spectral data with the possible structures.

First, it is easy to see that in some structures the negative charge can be delocalized onto the formyl oxygen atom with concomitant reduction in HC=O bond order to form an enolate like structure. Therefore the disappearance of the normal υ_{CHO} band in the IR spectrum is not surprising. Second, the temperature dependent behavior of the ^1H NMR spectra indicated that there is a rearrangement between the species. The rearrangement appears to be different from the process observed by Deganallo et. al for $[(COOEtC_7H_6)Fe(CO)_3]^-$. In that case rapid metal migration around the C_7 ring is accompanied by facile rotation about the C_7-COOEt bond. The combination of the two processes results in a time-averaged mirror plane through the C_7 ring and gives a symmetrical room temperature spectrum which consists of three peaks in the ratio of 2:2:2 ($H_{1,6}$:$H_{2,5}$:$H_{3,4}$) (Scheme 5.3). The observation of four peaks in a ratio of

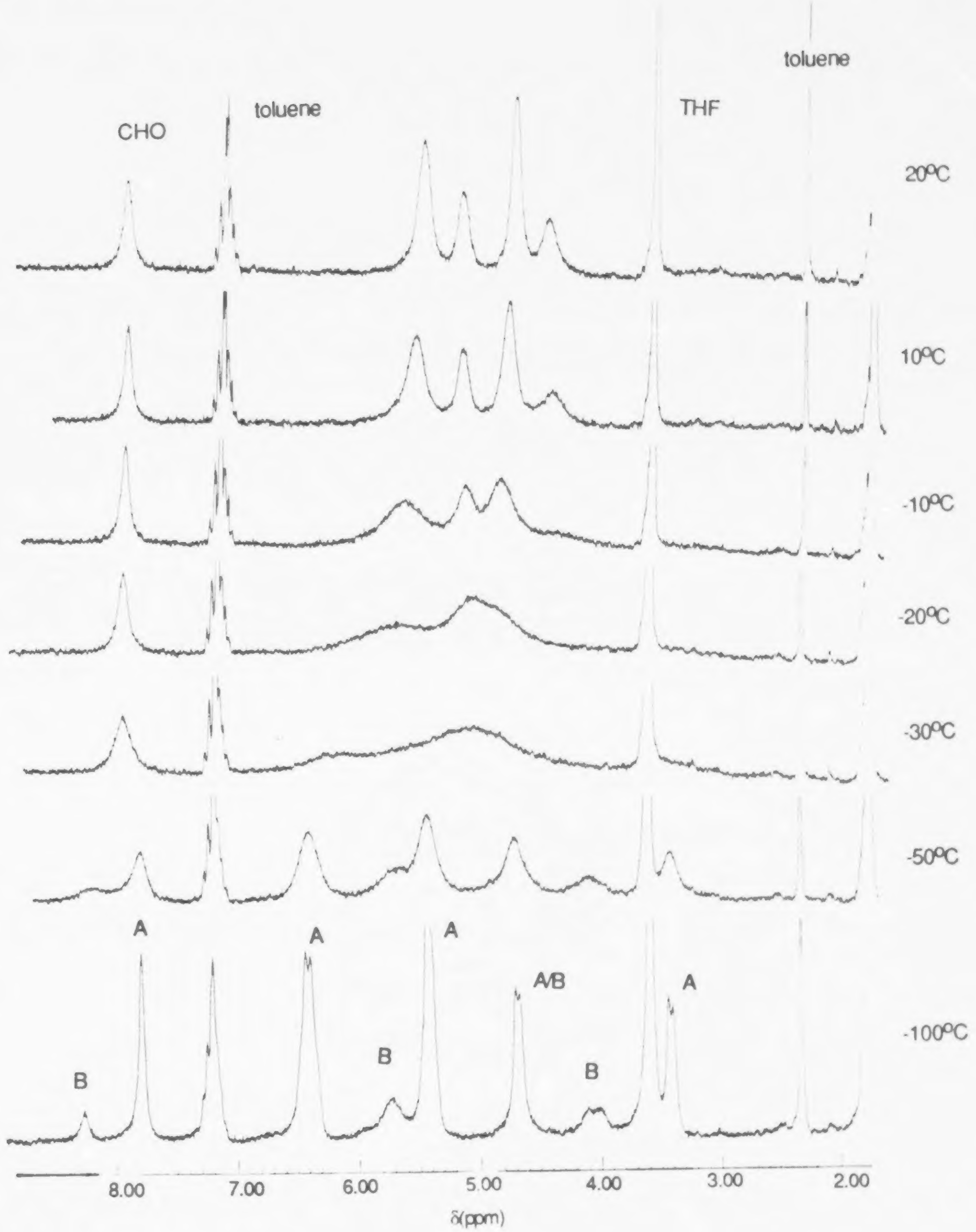

Figure 5.1 Variable temperature ^{1}H NMR spectra (200 MHz) of $(CHOC_7H_6)Fe(CO)_3^-$ (**3a**) in THF-d_8

2:1:2:1 at room temperature for compound **3a** is not in accord with such a process.

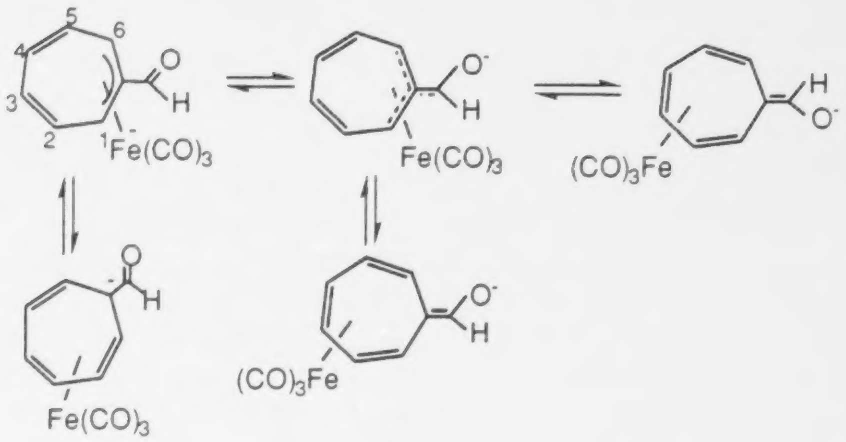

(Scheme 5.3)

Unfortunately, the low temperature ^{1}H NMR spectra provided insufficient information as to the nature of the isomers present. In particular, poor resolution of the signals made it impossible to determine the relationship of the ring hydrogens by homonuclear decoupling experiments. With the hope of aiding the assignment and establishing how the nature of the anion is dependent on the counter ion, different salts (Ph_4As^+, R_4N^+) of anion **3** were prepared. The variable temperature ^{1}H NMR spectra of these anions were also similar to the sodium salt and the low temperature spectra were not well resolved.

Attempts to grow single crystals of the sodium salt from various solvents proved unsuccessful, but single crystals in the presence of 18-crown-6 ether could be obtained. A perspective view of complex **3a** is shown in figure 5.2. During refinement it was discovered that the crown-ether molecule is disordered and attempts to deal with the disorder failed. Consequently the precision of the determination is low, nevertheless the gross structural features are still clearly established. For comparison, a perspective view of the unsubstituted anion **1a** is also shown in figure 5.2.

The structure clearly shows that $Fe(CO)_3$ moiety is bonded to the formylcycloheptatrienyl ligand in an η^3-fashion, with the formyl group attached to the central carbon of the allyl fragment. Comparison of the Fe-C_7 ring distances in the formyl-substituted anion **3a** with that of unsubstituted anion **1a** indicates that they are very similar. But interestingly, it is noted that in **3a** the exocyclic C-C bond is rather short (1.38 Å) and shows double bond character. The carbon atom of the formyl moiety is 2.65 Å away from the Fe atom. This distance is long for direct bonding, but probably still indicates secondary interaction between Fe and the formyl group. Thus, in the solid state, the bonding can be best described by the forms shown below, with significant contribution from the trimethylenemethane like resonance form. Finally, the formyl oxygen is bonded to the sodium ion, which is associated to the crown-ether ligand as well.

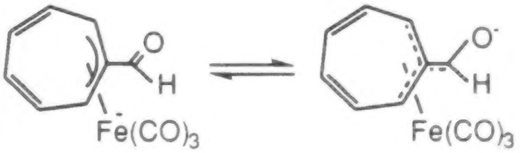

Comparison of this structure with a heptafulvene complex, $(\eta^4\text{-}C_7H_6CH_2)Fe(CO)_3$, which has a typical trimethylenemethane like bonding mode, indicates that even though the exocyclic carbon-carbon distance of **3a** is close to that observed in the heptafulvene Fe complex (1.428 (8) Å) (Figure. 5.3),[9] the Fe distance to the exocyclic carbon in **3a**

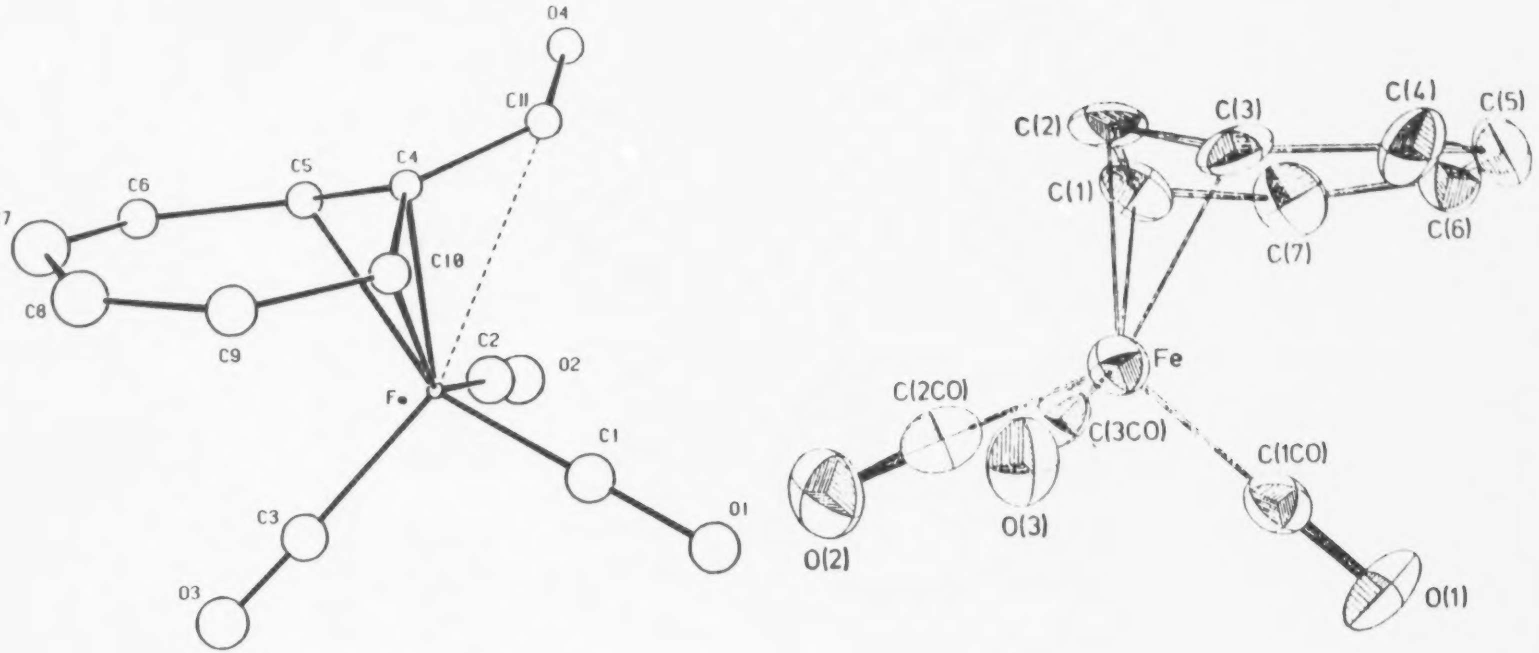
O4
C11
C5
C4
C6
C7
C10
C8
C9
C2
O2
Fe
C1
C3
O1
O3
C(2)
C(3)
C(4)
C(5)
C(1)
C(7)
C(6)
Fe
C(2CO)
C(3CO)
C(1CO)
O(2)
O(3)
O(1)

Selected Bond Distance (Å)*

Fe-C5	2.21(3)	C4-C11	1.38(5)
Fe-C4	1.97(4)	C11-O4	1.32(4)
Fe-C10	2.12(5)	Na-O4	2.27(3)
Fe-C11	2.65(5)		

* The disordered 18-crown-6 is not shown. Atoms are represented by circles drawn at an arbitrary size.

Selected Bond Distance (Å)

Fe-C1	2.113(12)
Fe-C2	1.983(10)
Fe-C3	2.137(11)

Figure 5.2 Perspective views of $(\eta^3\text{-}C_7H_7)Fe(CO)_3^-$ and $(C_7H_6CHO)Fe(CO)_3^-$ (**3a**).

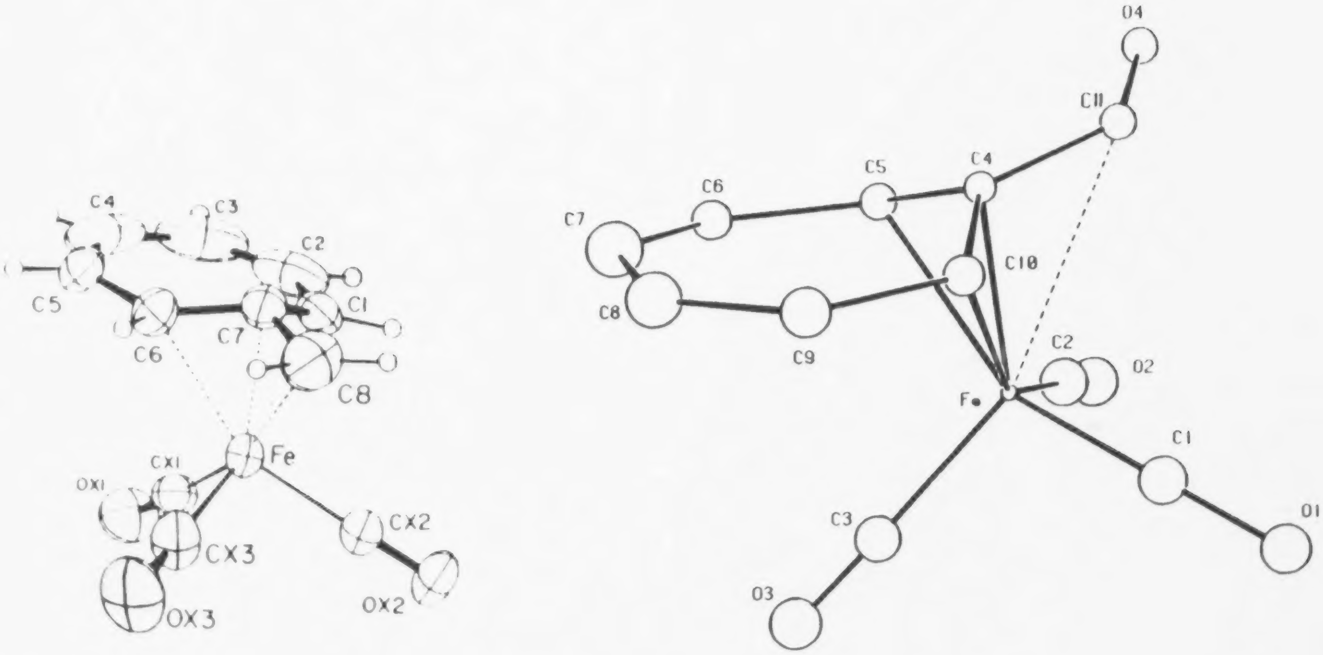
C4
C3
C2
C5
C1
C6
C7
C8
Fe
CX1
OX1
CX3
CX2
OX3
OX2
O4
C11
C5
C4
C6
C7
C10
C8
C9
C2
O2
Fe
C1
C3
O1
O3

Selected Bond Distance (Å)

Fe-C7	1.946(2)	C7-C1	1.412(4)
Fe-C1	2.175(3)	C7-C6	1.405(4)
Fe-C6	2.192(3)	C7-C8	1.428(5)
Fe-C8	2.120(3)		

Selected Bond Distance (Å)*

Fe-C5	2.21(3)	C4-C11	1.38(5)
Fe-C4	1.97(4)	C11-O4	1.32(4)
Fe-C10	2.12(5)	Na-O4	2.27(3)
Fe-C11	2.65(5)		

* The disordered 18-crown-6 is not shown. Atoms are represented by circles drawn at an arbitrary size

Figure 5.3 Perspective views of (η^4-$C_7H_6CH_2$)$Fe(CO)_3$ and (C_7H_6CHO)$Fe(CO)_3^-$ (**3a**)

(2.65 (5) Å) is much longer than that of the heptafulvene complex (2.120 (3) Å). Thus the interaction between Fe and the exocyclic carbon in **3a** is weak and could be a major factor for the facile rearrangement of compounds **3**. The heptafulvene complex is rigid at room temperature.

Although we have obtained some information on the solid structure of **3**, the structures in solution are still difficult to resolve. The major isomer in THF solution could be accommodated by the solid state form. The minor isomer is more problematic as is the appearance of the room temperature ^1H NMR spectrum. More work is needed, but it is clear that rearrangement is not accompanied by the C_7-CHO bond rotation.

Recently Williams et al. reported a detailed study on the isomerization of acylcycloheptatriene Fe complexes. It is believed that in this isomerization the key step also involves an equilibrium between a series of cycloheptatrienide anions (Scheme 5.4),[4c] much like what goes on with anion **3a**.

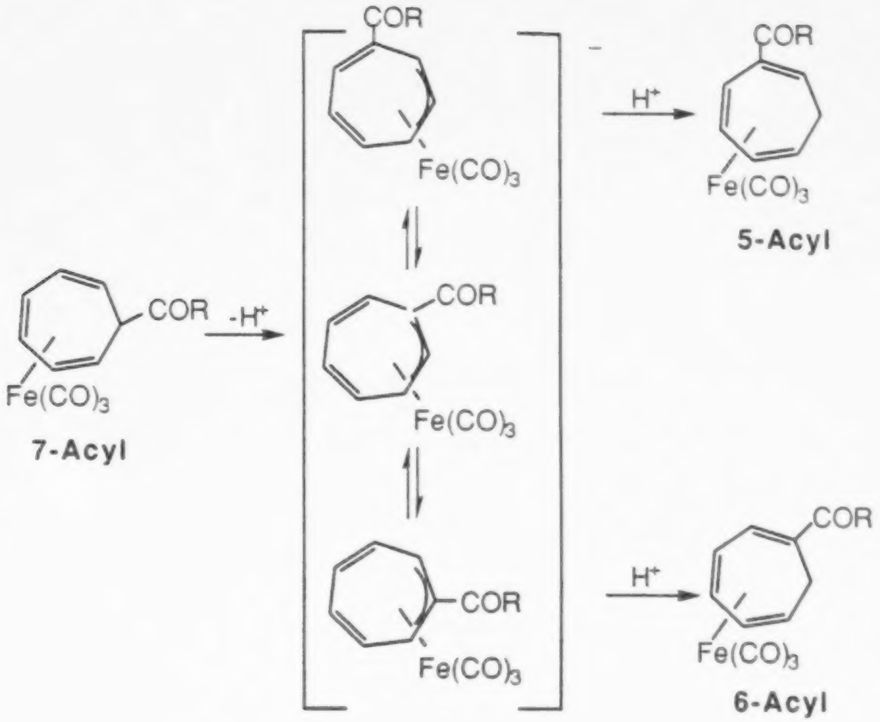
COR
Fe(CO)3
7-Acyl
-H+
COR
Fe(CO)3
COR
Fe(CO)3
COR
Fe(CO)3
H+
COR
Fe(CO)3
5-Acyl
H+
COR
Fe(CO)3
6-Acyl

(Scheme 5.4)

5.2.2. Reaction of $[(CHOC_7H_6)Fe(CO)_3]^-$ with CH_3I.

The reaction of **3a** with CH_3I was carried out in THF at room temperature. Normal work-up and silica gel column chromatography provided two products **5** and **6** as yellow and yellow orange solids (in a ratio of 2:1). Both compounds are fairly stable in the solid states, but their solutions are air sensitive.

Mass spectra and elemental analysis suggested a molecular formula of $[(CH_3)(CHO)C_7H_6]Fe(CO)_3$ for these products. The IR spectrum of both **5** and **6** show three carbonyl bands in the terminal carbonyl region which are typical for (diene)Fe$(CO)_3$ compounds. The major difference between the two compounds is the position of the formyl CO band. In **5** this band appears at 1737 cm^{-1} while the same band in **6** is at 1701 cm^{-1}. The low frequency shift in **6** indicates a greater conjugation of the formyl group with the C_7 ring.

The room temperature ^{1}H NMR spectra (Table 5.1) of **5** and **6** show distinct signals for each proton environment and are typical for substituted (η^4-cycloheptatriene)Fe$(CO)_3$ complexes which are known to be rigid at room temperature.[7] The assignments of the proton signals were based on ^{1}H-^{1}H decoupling experiments and by comparison of their chemical shifts with that of similar benzoyl complexes.[4b] In compound **5** no aliphatic proton peak was observed and the methyl signal was a singlet at 1.13 ppm, which indicate the methyl group and formyl group are at the same carbon atom of the C_7H_7 ring. Based on this the structure of (η^4-7-CH_3-7-CHO-C_7H_6)Fe$(CO)_3$ is assigned to **5**. Thus the low field doublet of doublets at 5.96 ppm was assigned to H_5, and a multiplet at 5.12 ppm to H_6. The two internal diene protons gave two multiplets around 5.34 ppm and the outer diene protons appeared at the higher field (H_1 3.15, H_4 2.98 ppm).

In a similar fashion the structure of compound **6** was assigned to (η^4-5-CHO-7-$CH_3C_7H_6$)Fe$(CO)_3$. The reason is clear. The resonance at 3.00 ppm is in the saturated alkyl proton region and it is coupled to the methyl group, thus it is assigned to H_7. In turn the methyl signal at 1.54 ppm is a doublet ($J_{Me\text{-}H7}$=7 Hz). This clearly indicates that the methyl group is at the C7 atom. The fact that the peak due to H_6 is shifted to lower field (6.15 ppm) suggests that this olefinic proton may be at the end of an α,β-unsaturated aldehyde group, which causes this downfield shift. Although the spectral data between **5** and **6** and the related benzoyl substituted

Table 5.1 ^{1}H and ^{13}C NMR data of [η^4-$C_7H_6(CHO)(CH_3)$]$Fe(CO)_3$ (**5**-**6**) and [η^4-$C_7H_6CHOSi(CH_3)_3$]$Fe(CO)_3$ (**7**).

		assignment^{b,c}										temperature °C
	Solvent	H1	H2	H3	H4	H5	H6	H7	CHO	CH_3		
5	$CDCl_3$	3.15	5.36	5.32	2.98	5.96	5.12		9.35	1.13		r.t
6	CD_2Cl_2	3.70	5.60	5.45	3.34		6.15	3.00	9.18	1.54		r.t
7-E	C_6D_6	3.42	4.67	4.7-4.8	2.80	5.48	6.10		6.21^c			r.t
7-Z	C_6D_6	4.35	4.7-4.8		2.90	5.35	5.24		6.30^c			r.t
		assignment^d										
		C1	C2	C3	C4	C5	C6	C7	C8	CH_3	CO	
5	$CDCl_3$	63.22	95.21	85.33	54.37	131.21	126.03		199.15	22.79	210.11	r.t
6	CD_2Cl_2	66.45	94.95	88.72	48.25	38.31	151.71	142.18	192.28	23.75	210.89	r.t
7-E	C_6D_6	64.53	91.06	85.56	58.31	117.63	122.47	121.12	137.89	-0.72	211.27	r.t
7-Z	C_6D_6	58.09	90.48	86.17	57.01	123.04	124.62	127.44	140.91			r.t

a. Chemical shift (δ) in ppm from Me_4Si. b. Assignment based on homonuclear spin-decoupling experiments. c. Assignment based on a NOE experiment. d. Assignment based on ^{1}H-^{13}C heteronuclear decoupling experiments. e. Assignment based on chemical shift of **5** and APT experiments.

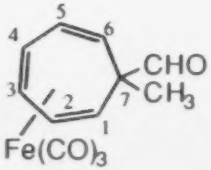

5

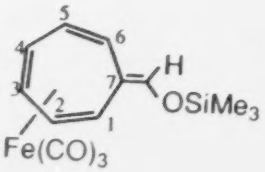

7-Z

complexes are similar, the isomer ratio is not same. In latter reaction a 6:1 preference for (η^4-7-CH_3-7-PhCO-C_7H_6)Fe$(CO)_3$ was observed.

Interestingly, these results are different from reactions of the unsubstituted anion **1a** with CH_3I. In this case attack of the metal was reported, but the compound was not stable and decomposed to (C_7H_8)Fe$(CO)_3$ (**4**) upon attempted chromatography.[3e]

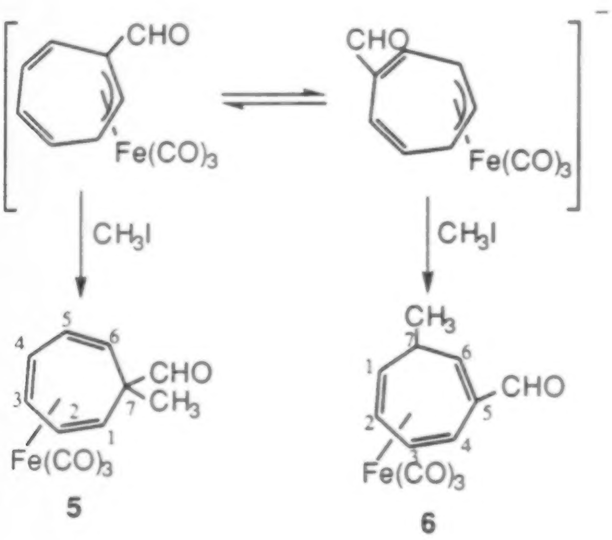

(Scheme 5.5)

The experimental results show that, as far as the CH_3I reaction is concerned, the important reactive forms of anion **3a** appear to be the same as those identified by Williams et al. (Scheme 5.5).

5.2.3. Reaction of [($CHOC_7H_6$)Fe$(CO)_3$]$^-$ with Me_3SiCl.

The reaction of **3a** with Me_3SiCl was carried out at -78°C. Work-up and crystallization from hexane solution afforded the products as a yellow brown solid in an isolated yield of 74%. The solid appeared less stable than the methyl derivatives **5** and **6**. It rapidly decomposed upon silica gel column chromatography and was sensitive to air even in the solid state.

The mass spectrum and elemental analysis suggested a constitution, $(Me_3SiCHOC_7H_6)Fe(CO)_3$ for the product The IR spectra of the product showed only three carbonyl bands at 2047s, 1987s and 1971s cm^{-1} which is typical for an $(\eta^4$-diene$)Fe(CO)_3$ complex. Interestingly, no formyl band was observed. This indicated that the $SiMe_3$ group is most likely bonded to the formyl oxygen with the formation of a heptafulvene derivative. It is noteworthy that similar selectivity was also observed by Williams et al. in reactions of the benzoyl iron anion, $(PhCOC_7H_6)Fe(CO)_3^-$. The reaction with MeI resulted in ring attacked products (see the previous section), whereas silyl chloride gave coordinated heptafulvenes.

The ^1H and ^{13}C NMR data of the compounds are collected in Table 5.1. The ^1H NMR spectrum is displayed in figure 5.4 and shows that the product is actually a mixture of two isomers in an approximate ratio of 2:1. Also shown in the figure is the related phenyl acetoxyheptafulvene derivative obtained by Williams et al..[4b, 10] The similarities are clear. The assignment appearing in the table and figure were determined by homo- and heteronuclear decoupling experiments and are consistent with the (7-trimethylsiloxyheptafulvene)$Fe(CO)_3$ formulation, which exists as two isomers **7**-E and **7**-Z due to the different orientations of the $SiMe_3$ substituent about the exocyclic double bond.

The identity of the isomers was established by NOE experiments. Irradiation of the formyl proton of the major isomer resulted in the intensity change of the H6 ring proton. This suggested that the formyl proton is close

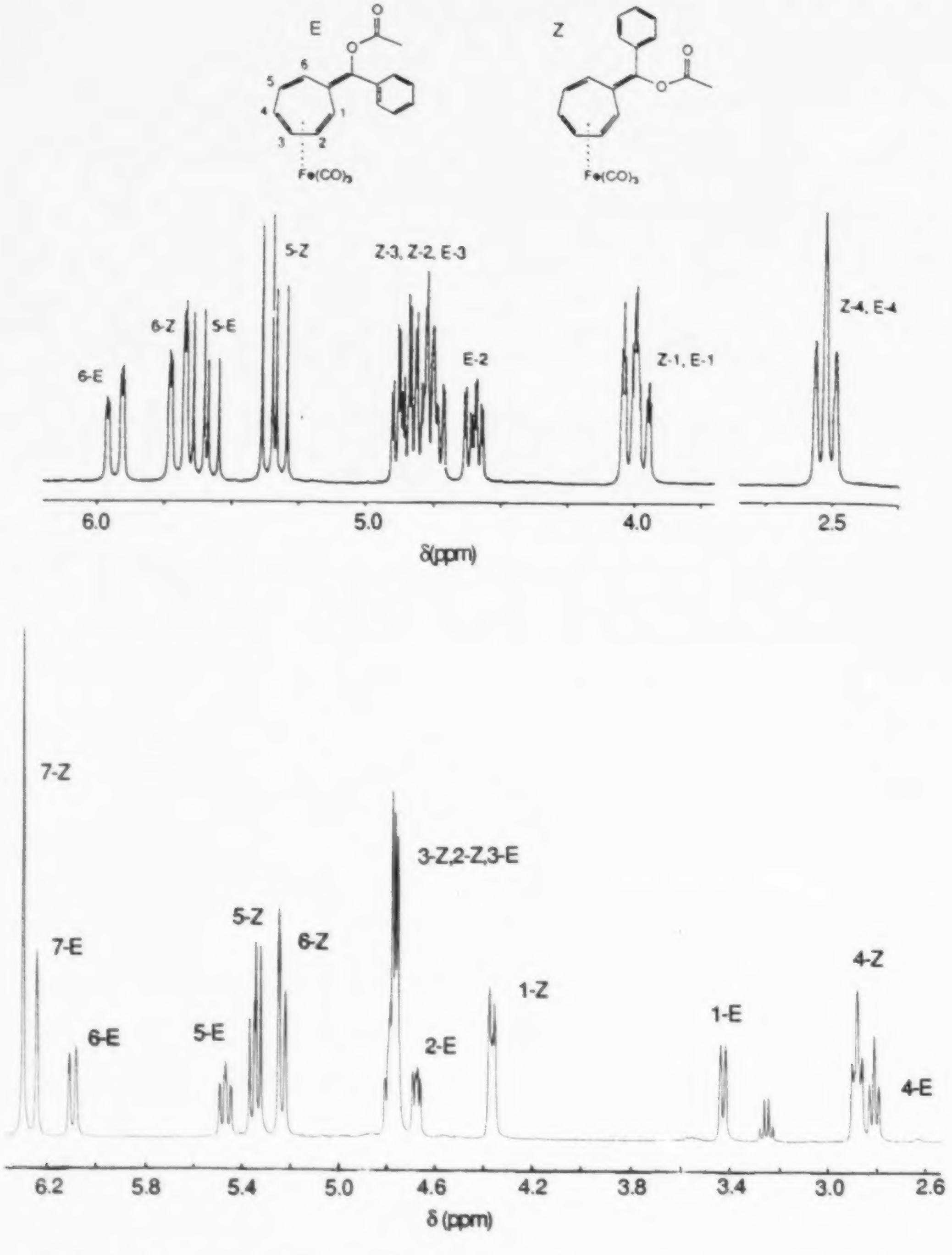

Figure 5.4 ^{1}H NMR spectra (300 MHz) of (8-phenyl-8-acetoxyheptafulvene)Fe(CO)$_3$ and (8-trimethylsiloxyheptafulvene)Fe(CO)$_3$ (**7E**, **7Z**).

to H6 and $SiMe_3$ group is at the same side of $Fe(CO)_3$. Thus we assign the major isomer as **7**-Z.

Thus the Me_3SiCl reaction appears to sample different reactive forms of the anion (Scheme 5.6). This again is different from the reactivity of the unsubstituted anion **1a** where Me_3SiCl gave ring substituted products.[11]

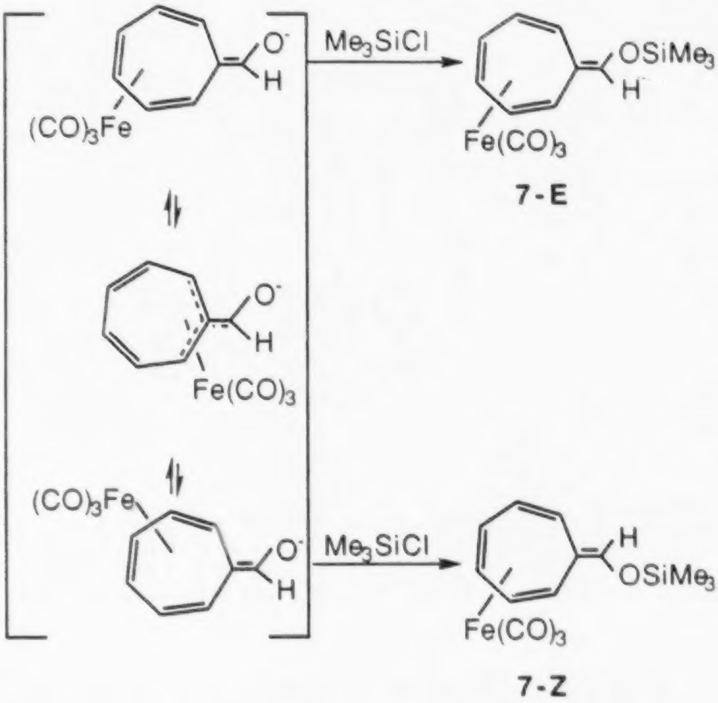

O⁻
H
(CO)₃Fe
Me₃SiCl
OSiMe₃
H
Fe(CO)₃
7-E
O⁻
H
Fe(CO)₃
(CO)₃Fe
O⁻
H
Me₃SiCl
H
OSiMe₃
Fe(CO)₃
7-Z

(Scheme 5.6)

5.3. Conclusion.

The synthesis and characterization of $[(C_7H_6CHO)Fe(CO)_3]^-$ (**3**) and its derivatives have been carried out. In the solid state anion **3**, like the unsubstituted anion, $[(\eta^3\text{-}C_7H_7)Fe(CO)_3]^-$ (**1a**), favors the η^3-bonding mode with secondary interaction with the exocyclic CHO. The same trimethylenemethane like structure may predominate in solution at room temperature, but the nature of the other isomers present and the mechanism of interconversion between isomers is not clear at this stage. Reaction of the anion with MeI and Me_3SiCl resulted in ring substituted and heptafulvene type derivatives, respectively. Thus preliminary results suggest that anion **3** may be useful precursor for substituted $(RC_7H_6CHO)Fe(CO)_3$ and (heptafulvene)$Fe(CO)_3$ derivatives.

5.4. Experimental.

5.4.1. General Techniques and Reagents.

All experimental procedures were performed in standard Schlenk glassware under a static atmosphere of rigorously purified nitrogen. All solvents were dried by refluxing under nitrogen with the appropriate drying agent and distilled just prior to use.

Sodium bis(trimethylsilyl)amide, trimethylsilyl chloride, and methyl iodide were purchased from Aldrich. Tetraphenylarsonium chloride (Ph_4AsCl) was obtained from Aldrich and dried at 180°C under vacuum (1 mmHg) overnight. $(\eta^4\text{-}C_7H_8)Fe(CO)_3$[12] and $(\eta^4\text{-}C_7H_7CHO)Fe(CO)_3$[13] were prepared according to literature methods.

Infrared spectra were obtained with a Nicolet MX-1 Fourier Transform interferometer and a Bomem MB-100 spectrometer. Mass spectra were taken with an A.E.I. MS-12 spectrometer operating at 70eV or 16eV. NMR spectra were recorded on Bruker WH 200, Bruker WH 360, Bruker AM 400 or Bruker AM 300 spectrometers. Elemental analyses were performed by the Micoanalytical Laboratory of this department.

5.4.2. Preparation of Na[(C_7H_6CHO)Fe(CO)$_3$] (3a).

A benzene solution (75ml) of NaN(SiMe$_3$)$_2$ (2.41g, 13mmol) was added dropwise at room temperature to (C_7H_7CHO)Fe(CO)$_3$ (**2**) (2.89g, 11.1mmol) also in benzene (30ml). The reaction mixture rapidly turned deep red and some red precipitate began to form. After addition was completed the suspension was stirred for another hour at room temperature. Hexane (50ml) was added to complete the precipitation of the sodium salt. The precipitate was filtered under nitrogen and washed with pentane (2 x 50ml). The solid anion was dried under vacuum to give an orange red powder (2.8 g, 90%).

IR (THF) : υ_{CO} 1985(s), 1910(vs, br) cm^{-1}.

^{1}H NMR (200 MHz, 20^{o}C, THF-d_8): 7.92 (br, 1H, CHO), 5.48 (br, 2H, C_7H_6), 5.18 (br, 1H, C_7H_6), 4.7 (br, 2H,C_7H_6), 4.5 (br, 1H,C_7H_6). (-100^{o}C): isomer **A**, 7.8 (br, 1H, CHO), 6.42 (br, 2H, C_7H_6), 5.42 (br, 2H, C_7H_6), 4.68 (br, 1H,C_7H_6), 3.42 (br, 1H, C_7H_6); isomer **B**, 8.28 (br, 1H, CHO), 5.75 (br, 2H, C_7H_6), 4.68 (br, 1H,C_7H_6), 4.12 (br, 2H, C_7H_6).

5.4.3. Preparation of [Ph$_4$As][(C_7H_6CHO)Fe(CO)$_3$] (3b).

A THF solution (20ml) of Na[(C_7H_6CHO)Fe(CO)$_3$] (**3a**) (558mg, 1.98mmol) was added dropwise to a slurry of Ph$_4$AsCl (820mg, 1.98mmol) in THF (10ml). The mixture was stirred at room temperature for about an hour. The IR spectrum showed that cation exchange was complete. The mixture was filtered. Addition of heptane (pretreated with K for 6 hr) (30ml) to the filtrate gave some dark-red precipitate. The precipitation of the solid was completed by removing THF under vacuum. The dark red solid was filtered and immediately transfered into a dry box. The solid was redissolved in THF (5ml). Attempts to grow single crystals by slow diffusion of hexane into THF solution failed.

5.4.4. Reaction of 3a with MeI.

Excess MeI (1.5ml) was added dropwise at room temperature to $Na[(C_7H_6CHO)Fe(CO)_3]$ (**3a**) (680mg, 2.4mmol) in THF (20ml). After the addition was completed the mixture was stirred at room temperature for 3 hr. The original dark red solution turned dark brown. The IR spectrum showed complete consumption of **3a**. The solvent was removed under vacuum to afford a dark brown oil. The residue was extracted with hexane (3 x 20ml). The extracts were concentrated and separated by a column chromatography (Silica Gel-hexane) and eluted with hexane-ether (10:1) to give a yellow solution. Removal of solvent afforded yellow solids of **5** (345mg, 52%) which can be crystallized from hexane at -78°C. Further elution with same solvent gave the other product **6** as a yellow-orange solid (83mg, 12%).

Anal. Found: C, 52.33; H, 3.71. $C_{12}H_{10}FeO_4$ calcd.: C, 52.59; H, 3.68%.

For **5**, IR (hexane) : υ_{CO} 2057(s), 1984(s), 1971(s) 1737(m) cm^{-1}.

For **6**, IR (hexane) : υ_{CO} 2056(s), 1994(s), 1984(s) 1701(m) cm^{-1}.

^1H and $^{13}C\{^1H\}$ NMR data are listed in Table 5.1.

5.4.5. Reaction of 3a with Me_3SiCl.

Excess Me_3SiCl (0.8ml) in THF (25ml) was added dropwise at -78°C to Na $[(C_7H_6CHO)Fe(CO)_3]$ (**3a**) (1.0g, 3.5mmol) in THF (30ml). After the addition was completed the mixture was stirred at -78°C for 1 hr. The original dark red solution turned dark brown. The IR spectrum showed complete consumption of **3a**. The solvent was removed under vacuum at -78°C to afford a yellow brown residue. The residue was extracted with pentane (3 x 15ml). The combined extracts were concentrated to 2ml and crystallized at -78°C overnight to afford **7**-E and **7**-Z as a brown yellow solid (863mg, 74%). Attempted further separation of **7** by fractional crystallization was not successful.

For **7**. Anal. Found: C, 50.39; H, 5.03. $C_{13}H_{16}FeO_4Si$ calcd.: C, 50.62; H, 4.86%.

IR (pentane) : υ_{CO} 2047(s), 1987(s), 1971(s) cm^{-1}..

Mass spectrum (16eV, 70°C); M^+, M^+-nCO (n=1-3).

^1H and ^{13}C $\{^1H\}$ NMR data are listed in Table 5.1.

5.5. References.

1. (a). Dauben, H. J.; Rifi, M. R., *J. Am. Chem. Soc.* **1963**, *85*, 3041

   (b). Doering, W. von E.; Gaspar, P. P., *J. Am. Soc. Chem.*, **1963**, *85*, 3043

2. (a). Maltz, H.; Kelly, B. A., *J. Chem. Soc., Chem. Commun.* **1971**, 1390

   (b). Sepp, E.; Purzer, A.; Thiele, G.; Behrens, H., *Z. Naturforsch.*, **1978**, *33b*, 261

   (c). Astley, S. T.; Takats, J., *Organometallics,* **1990,** *9*, 184

3. (a). Bennett, M. J.; Pratt, J. L.; Simpson, K. A.; LishingMan, L. K. K.; Takats, J., *J. Am. Chem. Soc.*, **1976**, *98*, 4810

   (b). LiShingMan, L. K. K.; Reuvers, J. G. A.; Takats, J.; Deganello, G., *Organometallics,* **1983**, *2*, 28

   (c). Moll, M.; Behrens, H.; Kellner, R.; Knochel, H.; Wurstl, P., *Z Naturforsch, B: Anorg. Chem., Org. Chem.* **1976**, *31b*, 1019

   (d). Edelmann, F.; Takats, J., *J. Organomet. Chem.*, **1988**, *344*, 351

   (e). Ball, R. G.; Edelmann, F.; Kiel, G.-Y.; Takats, J.; Drews, R., *Organometallics,* **1986**, *5*, 829

   (f). Deganallo, G.; Boschi, T.; Toniolo, L., *J. Organomet. Chem.,* **1975**, *97*, C46

4. (a). Williams, G. M.; Rudisill, D. E., *Tetrahedron Lett.,* **1986**, *27*, 3465

   (b). Williams, G. M.; Rudisill, D. E., Barnum, B. A., Hardcastle, K., Heyn, R. H., Kozak, C. J., McMillan, J. W., *J. Am. Chem. Soc.,* **1990**, *112*, 205

   (c). Williams, G. M.; Pino, M. J., *Organometallics,* **1992**, *11*, 1345

5. Airoldi, M.; Barbera, G.; Deganello, G.; Gennaro, G., *Organometallics*, **1987**, *6*, 398

6. Nitta, M.; Nishimuna, M.; Miyano, H., *J. Chem. Soc. Perkin Trans. I*, **1989**, 1019

7. Deganello, G., *"Transition Metal Complexes of Cyclic Polyolefins"*, Academic Press, London, **1979**, Chapter *1*, p. 67,

8. Hoffmann, P.; *Z. Naturforsch.*, **1978**, *33b*, 251

9. Churchill, M. R.; DeBoer, B. G., *Inorg. Chem.*, **1973**, *12*, 525

10.(a). Goldschmidt, Z.; Bakal, Y., *J. Organomet. Chem.*, **1979**, *179*, 197

(b). Goldschmidt, Z.; Bakal, Y., *J. Organomet. Chem.*, **1979**, *168*, 215

(c). Goldschmidt, Z.; Hezroni, D.; Gottlieb, H. E.; Antebi, S., *J. Organomet. Chem.*, **1989**, *373*, 235

11. Reuvers, J. G. A.; Takats, J., *Organometallics*, **1990**, *9*. 578

12. Manuel, T. A.; Stone, F. G. A., *J. Am. Chem. Soc.*, **1960**, *82*, 366

13. Johnson, B. F. G.; Lewis, J.; McArdle, P.; Randall, G. L. P., *J. Chem. Soc., Dalton*, **1972**, 456